



UNIVERSITY
OF
JOHANNESBURG

COPYRIGHT AND CITATION CONSIDERATIONS FOR THIS THESIS/ DISSERTATION



- Attribution — You must give appropriate credit, provide a link to the license, and indicate if changes were made. You may do so in any reasonable manner, but not in any way that suggests the licensor endorses you or your use.
- NonCommercial — You may not use the material for commercial purposes.
- ShareAlike — If you remix, transform, or build upon the material, you must distribute your contributions under the same license as the original.

How to cite this thesis

Surname, Initial(s). (2012). Title of the thesis or dissertation (Doctoral Thesis / Master's Dissertation). Johannesburg: University of Johannesburg. Available from:
<http://hdl.handle.net/102000/0002> (Accessed: 22 August 2017).

IMPROVEMENT OF INDOOR ENVIRONMENT SIGNAL RECEPTION USING PLC-RF DIVERSITY TECHNIQUES

by

FRANK NONSO IGBOAMALU

A thesis submitted to the Faculty of Engineering and the Built
Environment in fulfillment of the requirements for the degree of

Doctor of Engineering

in

Electrical and Electronic Engineering Science

at the

University of Johannesburg

Supervisors:

Prof. H.C. Ferreira

Dr. A. R. Ndjiongue

Dr. A. S. De Beer

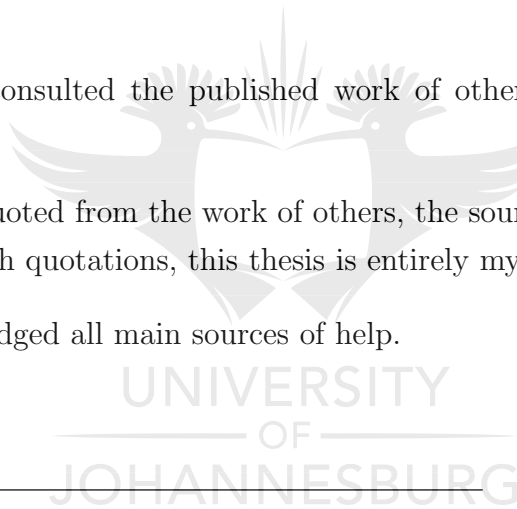
2019

Declaration of Authorship

- This work was done mainly while in candidature for a research degree at this University.
- Where I have consulted the published work of others, this is always clearly attributed.
- Where I have quoted from the work of others, the source is always given. With the exception of such quotations, this thesis is entirely my own work.
- I have acknowledged all main sources of help.

Signed:

Date:



Abstract

The demand for broadband communication has substantially increased over the past decade. Among the applications of broadband is the provision of high data rate communication within structures such as multi-storey buildings. The use of free-space radio-frequency (RF) signals to achieve broadband communication in multi-storey environments faces restrained coverage due to obstruction caused by walls, metals and concrete slabs in such buildings. This challenge necessitates the need to seek alternative communication technologies that will provide the required continuous connectivity in such environments. One such technology is power-line communication (PLC) technology.

PLC technology is regarded as one of the technologies that can be employed to overcome the limited coverage associated with the use of RF technology in multi-storey buildings and mega-structures. PLC is a cost-effective system that uses the pre-existing electrical distribution networks in a building to transmit data.


This thesis focuses on the performance analysis of the combination of PLC and RF technologies to overcome the challenges to communication posed by the obstructions in multi-storey buildings. PLC-RF technology that takes into consideration the mobility of the end-user is proposed, followed by an analysis of the system channel frequency response. The signal is detected and demodulated by an RF receiver. First, the performance of such a system is analysed and the resultant measurements proposed. Second, an overall system concatenation of the PLC and RF systems is proposed.

A combination of PLC and RF technologies is proposed for achieving signal transmission in indoor environments, taking into account the internal characteristics of multi-storey buildings. Diversity combining techniques, namely selection combining (SC) and

maximum ratio combining (MRC), are exploited to recover the retransmitted message. Furthermore, the estimated cost of implementing a hybrid system is analysed, followed by a proposal for the outage probability for both the SC and the MRC.



Dedication



This Thesis is dedicated to my family members, especially to
my father *Chief Francis Chukwudi*, my mother *Lolo*
Christiana Chinenye, son *Frank Chuka*, daughter *Goziem*
Rita and to my wife, *Dr. Ugo Chioma*, for their patience
through out these years.

Acknowledgements

To begin with and preeminent, I would like to return all the glory to God Almighty for giving me the strength, capacity, information, and opportunity to embrace this research study and for his conservation towards the completion of this research. Without him by my side and his gifts, this accomplishment would not have been conceivable.

This journey will not be conceivable to do without the assistance, support and direction that I received from everyone around me at the time where I needed them most.

I would like to appreciate my supervisor Late Prof. Ferreira for his heartfelt and direction at all times. He has given me important direction, motivation, and recommendations in my journey for knowledge. He has given me all the opportunity to seek after my research and instructed me how to stay focus in all through my research. Unfortunately, he passed away a few months to the conclusion of this work. Without his guidance and constant feedback this Ph.D. would not have been achievable. I would like to commit this work to him.

This Ph.D. study would not have been conceivable without the help and full support from my co-supervisors. Dr. Alain Richard Ndjiongue and Dr. Arnold de Beer for their guidance that came at a critical stage of this degree. Their patience during the numerous focus one on one discussions is very much appreciated. I am particularly thankful to them for giving hope to proceed with the research during a period that was incredibly difficult for me, even at the point of almost giving up.

My acknowledgment would be fragmented without saying thanks to the greatest source

of my strength, my family. The favors of my parents Chief F.C Igboamalu and LoLo Christiana Igboamalu for always believing in me and encouraging me to follow my dreams along with their spiritual support. A very special thank you to my elder brother Dr. Igboamalu Chris for his invaluable advice.

I thankfully acknowledge the grant received towards my Ph.D. from the commonwealth.



Dissertation Related Publications

Journal Publications

- 1) F. N. Igboamalu, A. R. Ndjiongue & H. C. Ferreira, "PLC-RF diversity: channel outage analysis", *Telecommun. Syst.*, Accepted October. 2019 Chapter 6.
- 2) F. N. Igboamalu, A. R. Ndjiongue, H. C. Ferreira & A.S.de Beer, "Contactless PLC: Channel analysis and measurements campaign", *SAIEE Africa Research Journal.*, Submitted August. 2019 (Chapters 4, 5).

Conference Publications

- 1) A.S. de Beer, F.N. Igboamalu, A. Sheri, H.C. Ferreira & A.J. Han Vinck, "Contactless power line communications at 2.45 GHz ", in *Proc. 20th IEEE ISPLC Conf.*, Bottrop Germany, Mar. 20-23, 2016, pp. 31-36 (Chapters 5).

Other Publications

- 1) F. N. Igboamalu & M. R. Kamarudin "Indoor body measurement using polarization and space diversity patch antenna," in *Proc. IEEE Int. Conf. Antennas, Propagation Sys., (INAS), Johor, Malaysia. 3-5, Dec. 2009.*
- 2) M. Shaneshin, F. N. Igboamalu & M. R. Kamarudin "Printed loop antenna for medical implanted communication system," in *Proc. IEEE Int. Conf. Antennas, Propagation Sys., (INAS), Johor, Malaysia. 3-5, Dec. 2009.*

agation Sys., (INAS), Johor, Malaysia. 3-5, Dec. 2009.

- 3) U.A.K Chude-Okonkwo, F.N Igboamalu, R. Ngah & T.A Rahman "Mobile radio channel characterization and stationarity issues," in *Proc. IEEE Int. Conf. Antennas, Propagation Sys., (INAS), Johor, Malaysia. 3-5, Dec. 2009.*



Table of Contents

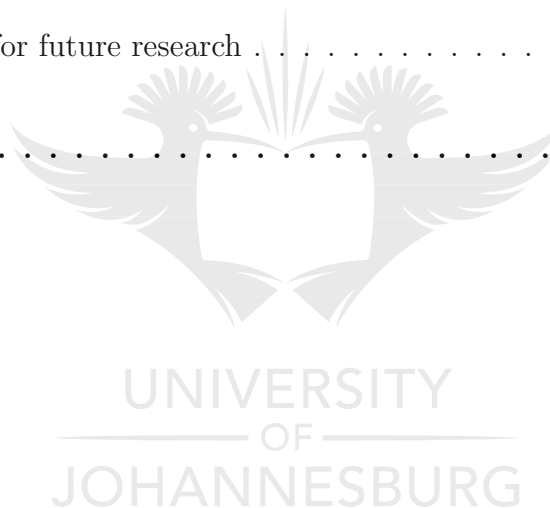
| | |
|---|-------|
| Declaration of Authorship | ii |
| Abstract | iii |
| Dedication | v |
| Acknowledgements | vi |
| Dissertation Related Publications | viii |
| List of Figures | xv |
| List of Tables | xix |
| List of Abbreviations | xx |
| List of Symbols | xxiii |
| 1 Introduction | 1-1 |
| 1.1 Introduction | 1-1 |
| 1.2 Problem statement | 1-2 |

| | | |
|----------|--|------------|
| 1.3 | Research questions | 1-3 |
| 1.4 | Aims and objectives | 1-3 |
| 1.5 | Main contributions | 1-4 |
| 1.6 | Thesis organization | 1-5 |
| 2 | Overview of PLC and RF Communications | 2-1 |
| 2.1 | Introduction | 2-2 |
| 2.2 | PART I: RF technology | 2-2 |
| 2.2.1 | The indoor wireless environment | 2-2 |
| 2.2.2 | Wireless channel modelling | 2-4 |
| 2.2.3 | Wireless channel noise | 2-8 |
| 2.3 | PART II: PLC technology | 2-8 |
| 2.3.1 | PLC technology brief history | 2-8 |
| 2.3.2 | The PLC channel | 2-10 |
| 2.3.3 | Noise and disturbances in PLC | 2-12 |
| 2.4 | PART III: Techniques of modulation | 2-14 |
| 2.5 | PART IV: Other PLC-RF related work | 2-15 |
| 2.6 | PART V: Summary | 2-18 |
| 3 | Modeling Techniques for PLC-RF Systems. | 3-1 |
| 3.1 | Introduction | 3-2 |
| 3.2 | Transmission line effect. | 3-2 |
| 3.3 | Coupling circuit (CC) | 3-3 |
| 3.4 | Long-wire antenna | 3-4 |
| 3.5 | Radiation pattern | 3-5 |

| | | |
|----------|---|------------|
| 3.6 | Diversity technique | 3-9 |
| 3.6.1 | Frequency diversity | 3-10 |
| 3.6.2 | Time diversity | 3-11 |
| 3.6.3 | Space diversity | 3-11 |
| 3.7 | Combining techniques | 3-12 |
| 3.7.1 | Selection diversity | 3-12 |
| 3.7.2 | Maximum ratio combining | 3-15 |
| 3.7.3 | Equal gain combining | 3-18 |
| 3.8 | Summary | 3-20 |
| 4 | Contactless PLC: Channel Analysis | 4-1 |
| 4.1 | Introduction | 4-2 |
| 4.2 | A model for a contactless PLC system | 4-3 |
| 4.2.1 | Modulator-demodulator | 4-3 |
| 4.2.2 | PLC Channel and model | 4-4 |
| 4.2.3 | RF Channel and model | 4-5 |
| 4.3 | Analysis | 4-5 |
| 4.4 | Conclusion | 4-11 |
| 5 | Contactless PLC: Preliminary Measurement | 5-1 |
| 5.1 | Introduction | 5-2 |
| 5.2 | PART I: Setup of the laboratory experiment | 5-3 |
| 5.2.1 | The RF-Link | 5-4 |
| 5.2.2 | Traveling wave contactless PLC | 5-5 |
| 5.2.3 | Throughput measurement | 5-7 |

| | | |
|----------|--|------------|
| 5.3 | Result of the experiments | 5-9 |
| 5.4 | The industrial setting | 5-10 |
| 5.4.1 | Contactless PLC | 5-11 |
| 5.4.2 | RF links | 5-11 |
| 5.5 | Free standing cable | 5-12 |
| 5.5.1 | Contactless PLC | 5-12 |
| 5.5.2 | The RF Link | 5-12 |
| 5.6 | PART II: Setup of the residential experiments | 5-13 |
| 5.6.1 | Data collection | 5-14 |
| 5.6.2 | The laboratory layout | 5-15 |
| 5.6.3 | Results of the power-line cable and wireless data upload | 5-15 |
| 5.6.4 | Results of the power-line cable and wireless data download | 5-18 |
| 5.7 | Discussion | 5-18 |
| 5.8 | Conclusion | 5-19 |
| 6 | PLC-RF Diversity: Channel Outage Analysis | 6-1 |
| 6.1 | Introduction | 6-2 |
| 6.2 | Description of a model for a PLC-RF system | 6-2 |
| 6.3 | Channel analysis of PLC and RF systems | 6-3 |
| 6.3.1 | Effect of the coupling circuit on the PLC channel | 6-3 |
| 6.3.2 | Analysis of the coupling circuit simulation | 6-4 |
| 6.3.3 | Introduction to receiver combining | 6-8 |
| 6.3.4 | PLC and RF signal-to-noise ratios | 6-9 |
| 6.3.5 | Joint PLC-RF | 6-12 |
| 6.3.6 | Selection combining | 6-16 |

| | | |
|-------------------|---|-------------|
| 6.3.7 | Maximum ratio combining | 6-18 |
| 6.4 | Results of the analysis | 6-19 |
| 6.5 | Hybrid technology estimated implementation cost | 6-22 |
| 6.6 | Conclusion | 6-23 |
| 7 | Conclusion | 7-1 |
| 7.1 | Employment of broadband communication technology in indoor environments: problems, procedures, and proposals for their solution | 7-1 |
| 7.2 | Contributions and applications of the study to developments in broadband communication technology | 7-4 |
| 7.3 | Suggestions for future research | 7-5 |
| References | | Rf-1 |



List of Figures

| | | |
|------|---|------|
| 2.1 | Graph representing distance loss, shadowing, and multipath propagation. | 2-6 |
| 3.1 | Transmission line | 3-3 |
| 3.2 | Charge uniformly distributed in a circular cross section cylinder wire. . . | 3-7 |
| 3.3 | Coaxial cable simulation model | 3-7 |
| 3.4 | Radiation pattern for long wire antenna as a function of frequency [1]. . . | 3-9 |
| 3.5 | Frequency diversity | 3-10 |
| 3.6 | Time diversity | 3-11 |
| 3.7 | Selection combining | 3-12 |
| 3.8 | SNR improvement with selection combining. | 3-13 |
| 3.9 | Weight branches for maximum ratio combining. | 3-15 |
| 3.10 | SNR improvement with maximum ratio combining. | 3-16 |
| 3.11 | Weight branches for equal gain combining. | 3-18 |
| 4.1 | System model of the generalized cascaded PLC-RF. | 4-4 |
| 4.2 | Model of the a contact-less PLC using RF to connect the end user. . . . | 4-5 |
| 4.3 | Attenuation vs distance for Set 1 and Set 2 above. | 4-6 |

| | | |
|------|---|------|
| 4.4 | PLC channel for Set 2 characteristics for $a_0 = 0, 0.01$ and 0.0001 , and $a_1 = 20 \times 10^{-10}, 20 \times 10^{-10}$ and 10×10^{-10} | 4-6 |
| 4.5 | PLC channel based on Set 1 characteristics for $a_0 = 0, 0.01$ and 0.0001 , and $a_1 = 20 \times 10^{-10}, 20 \times 10^{-10}$ and 10×10^{-10} | 4-7 |
| 4.6 | RF channels for voltage 1 st path RF = 0.05, 0.25, 0.55 and 0.85. | 4-7 |
| 4.7 | PLC-RF channel based on characteristics OF Set 1 for $a_0 = 0, 0.01$ and 0.0001 , and $a_1 = 20 \times 10^{-10}, 20 \times 10^{-10}$ and 10×10^{-10} | 4-8 |
| 4.8 | PLC-RF channel based on characteristics OF Set 2 for $a_0 = 0, 0.01$ and 0.0001 , and $a_1 = 20 \times 10^{-10}, 20 \times 10^{-10}$ and 10×10^{-10} | 4-9 |
| 4.9 | PLC-RF channel based on characteristics of Set 1 for voltage 1 st path RF = 0.05, 0.25, 0.55 and 0.85. | 4-9 |
| 4.10 | PLC-RF channel based on characteristics of Set 2 for voltage 1 st path RF = 0.05, 0.25, 0.55 and 0.85. | 4-10 |
| 5.1 | Set up for the direct RF-link. | 5-3 |
| 5.2 | Set up for the traveling wave contactless PLC. | 5-4 |
| 5.3 | Detail of the coupling circuit for traveling wave contactless PLC. | 5-5 |
| 5.4 | Top view of a building plan depicting positions for measurements of contactless cable and RF in an industrial setting | 5-6 |
| 5.5 | Isometric view of a building plan and positions for the measurements contactless cable and RF in an industrial setting | 5-7 |
| 5.6 | Data transfer rates to different positions in the building of (Fig. 5.4) using contactless PLC. | 5-8 |
| 5.7 | Data transfer rates to different positions in the building of (Fig. 5.4) using RF links. | 5-8 |
| 5.8 | Data transfer rates to different positions along a free standing cable using contactless PLC. | 5-9 |
| 5.9 | Data transfer rates to different positions along a clear line of sight - using direct RF links. | 5-10 |

| | | |
|------|--|------|
| 5.10 | Measurement set up for antenna and power line cable. Fig. 5.10 a represent the typical RF setting for the experiment and Fig. 5.10 b, represent the contactless PLC connection setup. | 5-14 |
| 5.11 | Overview of building plan. | 5-16 |
| 5.12 | Overview of building plan. | 5-17 |
| 5.13 | Antenna upload 50 Mbps. | 5-17 |
| 5.14 | Antenna download 50 Mbps. | 5-19 |
| 6.1 | A model of a PLC-RF system for a multiple-storey | 6-2 |
| 6.2 | Substrate of microstrip coupling circuit front view | 6-4 |
| 6.3 | Substrate of microstrip coupling circuit side view | 6-4 |
| 6.4 | Power versus frequency CC analysis at 2.45 GHz | 6-5 |
| 6.5 | Impedance versus frequency CC analysis at 2.45 GHz | 6-5 |
| 6.6 | Current versus frequency CC analysis at 2.45 GHz | 6-6 |
| 6.7 | Reflection coefficient versus frequency CC analysis at 2.45 GHz | 6-6 |
| 6.8 | The PLC channel highlighting the two coupling circuits | 6-7 |
| 6.9 | $P_{out} = f(\gamma_{th})$, MRC. Variation of the outage probability for various values of γ_{th} , 3 dB, 9 dB, 15 dB, 19 dB and 25 dB, for Fig. 6.9 MRC and Fig. 6.10 SC, $\gamma_1 = \gamma_2$ | 6-8 |
| 6.10 | $P_{out} = f(\gamma_{th})$, SC. Variation of the outage probability for various values of γ_{th} , 3 dB, 9 dB, 15 dB, 19 dB and 25 dB, for Fig. 6.9 MRC and Fig 6.10 SC, $\gamma_1 = \gamma_2$ | 6-9 |
| 6.11 | Variation of the outage probability (MRC) for various values of g_0 , 0.2, 0.4, 0.6, 0.8 and 1, for $\gamma_{th} = 9$ dB and , $\gamma_1 = \gamma_2$ | 6-10 |
| 6.12 | $P_{out} = f(\gamma_{th})$, $\gamma_1 = 3$ dB. Variation of the outage probability (MRC) for various values of g_0 , 0.2, 0.4, 0.6, 0.8 and 1, for $\gamma_{th} = 9$ dB and variable γ_2 | 6-11 |
| 6.13 | $P_{out} = f(\gamma_{th})$, $\gamma_1 = 15$ dB. Variation of the outage probability (MRC) for various values of g_0 , 0.2, 0.4, 0.6, 0.8 and 1, for $\gamma_{th} = 9$ dB and variable γ_2 | 6-12 |

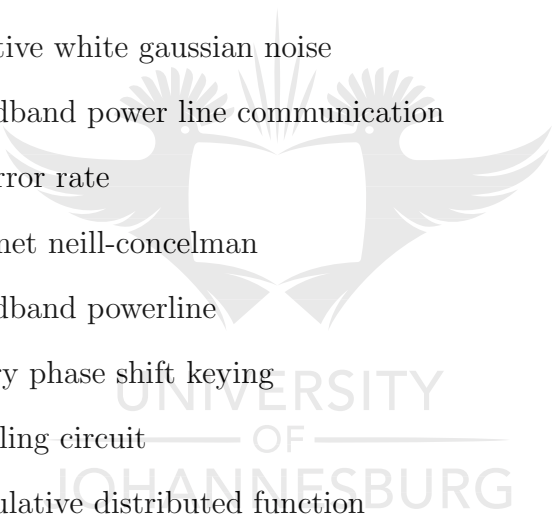
- 6.14 $P_{out} = f(\gamma_{th})$, $\gamma_2 = 3$ dB. Variation of the outage probability (MRC) for various values of g_0 , 0.2, 0.4, 0.6, 0.8 and 1, for $\gamma_{th} = 9$ dB and variable γ_1 . [6-13](#)
- 6.15 $P_{out} = f(\gamma_{th})$, $\gamma_2 = 15$ dB. Variation of the outage probability (MRC) for various values of g_0 , 0.2, 0.4, 0.6, 0.8 and 1, for $\gamma_{th} = 9$ dB and variable γ_1 . [6-14](#)
- 6.16 Variation of the outage probability (SC) for various values of g_0 , 0.2, 0.4, 0.6, 0.8 and 1, for $\gamma_{th} = 9$ dB and , $\gamma_1 = \gamma_2$ [6-15](#)
- 6.17 $P_{out} = f(\gamma_{th})$, $\gamma_2 = 3$ dB. Variation of the outage probability (SC) for various values of g_0 , 0.2, 0.4, 0.6, 0.8 and 1, for $\gamma_{th} = 9$ dB and variable γ_2 . [6-15](#)
- 6.18 $P_{out} = f(\gamma_{th})$, $\gamma_2 = 15$ dB. Variation of the outage probability (SC) for various values of g_0 , 0.2, 0.4, 0.6, 0.8 and 1, for $\gamma_{th} = 9$ dB and variable γ_2 . [6-16](#)
- 6.19 $P_{out} = f(\gamma_{th})$, $\gamma_2 = 3$ dB. Variation of the outage probability (SC) for various values of g_0 , 0.2, 0.4, 0.6, 0.8 and 1, for $\gamma_{th} = 9$ dB and variable γ_1 . [6-17](#)
- 6.20 $P_{out} = f(\gamma_{th})$, $\gamma_2 = 15$ dB. Variation of the outage probability (SC) for various values of g_0 , 0.2, 0.4, 0.6, 0.8 and 1, for $\gamma_{th} = 9$ dB and variable γ_1 . [6-18](#)

List of Tables

| | | |
|-----|--|------|
| 4.1 | Cable characteristics Set 1. | 4-8 |
| 4.2 | Cable characteristics Set 2. | 4-8 |
| 6.1 | Hybrid technology estimated implementation cost. | 6-22 |



List of Abbreviations



| | |
|----------|---|
| APSK: | Amplitude phase shift keying |
| AWGN: | Additive white gaussian noise |
| BBPLC: | Broadband power line communication |
| BER: | Bit error rate |
| BNC: | Bayonet neill-concelman |
| BPL: | Broadband powerline |
| BPSK: | Binary phase shift keying |
| CC: | Coupling circuit |
| CDF: | Cumulative distributed function |
| CENELEC: | European Committee for Electrotechnical Standardization |
| CSI: | Channel state information |
| EGC: | Equal gain combining |
| ESL: | Equivalent series inductance |
| FECO: | FEldeberechnung fr krper mit beliebiger oberffche |
| FSK: | Frequency shift keying |
| HDTV: | High definition television |
| HSRC: | Hybrid power line/wireless a single relay channel |
| IEEE: | Institute of Electrical and Electronics Engineers |

| | |
|----------|--|
| ISI: | Inter-symbol interference |
| ISO: | International organisation for standardisation |
| LAN: | Local area network |
| LOS: | Line-of-sight |
| MRC: | Maximum ratio combining |
| Mbps: | Megabits per second |
| MIMO: | Multiple input-multiple output |
| MISO: | Multiple input-single output |
| NBPLC: | Narrow band power line carrier |
| (N)LOS: | (Non) line-of-sight |
| OFDM: | Orthogonal frequency division multiplexing |
| OWC: | Optical wireless communications |
| OSI: | Open system interconnection |
| PLC: | Power line communications |
| PSK: | Phase shift keying |
| PDF: | Probability density function |
| QAM: | Quadrature amplitude modulation |
| QoS: | Quality of service |
| RF: | Radio frequency |
| SC: | Selection combining |
| SENELEC: | Societe nationale d'electricite du Senegal |
| SISO: | Single input-single output |
| SNR: | Single-input single-output |
| SRC: | Single relay channel |
| SG: | Smart grid |
| SER: | Symbol error rate |
| UWB: | Ultra-wideband |

| | |
|----------|---|
| USB: | Universal serial bus |
| TP-Link: | Twisted pair link |
| TVWA: | TV white space |
| VLC: | Visible light communications |
| VLCC: | Visible light communications consortium |
| WiFi: | Wireless fidelity |
| WBAN: | Wireless body area network |



List of Symbols

| | |
|----------------|--------------------------------|
| G | Average PLC channel gain |
| σ_g | PSD of Gaussian noise |
| h_{rf} | RF channel impulse response |
| H_{RF} | RF channel frequency response |
| h_{plc} | PLC channel impulse response |
| H_{PLC} | PLC channel frequency response |
| \mathbf{r}_i | i^{th} received symbol |
| \mathbf{s}_i | i^{th} sent symbol |
| \mathbf{n}_1 | RF noise |
| \mathbf{n}_2 | PLC noise |
| \mathbf{Y}_i | i^{th} received symbol set |
| \mathbf{S}_i | i^{th} sent symbol set |
| CC_{in} | Input to coupling circuit |
| CC_{out} | Output to coupling circuit |
| P_t | Transmitter power |
| B | Transmission bandwidth |
| \mathbf{g} | Attenuation factor |
| \mathbf{P}_0 | Outage probability |

| | |
|------------------|-----------------------------|
| E_b | Ratio of energy per bit |
| m | Number of tap RF |
| γ_{SC} | Selection combining SNR |
| γ_{MRC} | Maximum ratio combining SNR |
| N_0 | PSD density noise |
| σ_{th} | Thermal noise |
| σ_T | Impulsive noise variance |
| $\bar{\gamma}_i$ | Link average SNR |
| H | Hue parameter of a colour |
| n_i | Additive noise vector |
| d | Distance |
| \mathbf{C}_s | Sent colour set |
| \mathbf{g}_c | Path gain |
| \mathbf{g}_0 | Coupling circuit gain |
| γ_{th} | Average SNR |
| γ_1 | PLC SNR |
| γ_2 | RF SNR |
| P_{outSC} | Outage probability of SC |
| P_{outMRC} | Outage probability of MRC |

Note that this is not a complete list of every symbol used in this thesis. Various symbols are used only once, such as those in the literature overview chapters, and are thus not listed here. Whenever a symbol is used with a different definition in the text, that definition will take precedence over the definition given here.

1

Introduction

1.1 Introduction

Radio frequency (RF) in indoor communication is the most frequently used technology in the telecommunication industry. RF faces severe signal degradation in an indoor environment. This is a result of the scattering of the transmitted signals caused by wall thickness and metal objects inserted between the floors of multi-storey buildings. In most cases, the obstruction is due to the equipment inside the building (tables, wall demarcations, chairs, amongst others) that affects the signal strength. In general, the RF signal suffers from high attenuation when facing thick walls, thick concrete, and many other structural materials [2]. This problem develops when RF is deployed in an indoor environment.

A very popular RF technology for providing broadband connectivity to users in indoor (and outdoor) situations is wireless fidelity (WiFi) technology. WiFi technology standardised by the IEEE 802.11 standard [3] was made available to the public in 1997. It exploits 2.4 GHz for IEEE 802.11b and 5 GHz for IEEE 801.11a [3], and currently facilitates the development of the Internet of Things (IoT) [4, 5]. As the demand for high data rate and transmission speed increased, other WiFi standards were developed, including IEEE 802.11g in 2003 and IEEE 802.11 in 2009. Irrespective of its wide application, WiFi is still challenged by overcrowding at both 2.4 GHz and 5 GHz and by the poor propagation of the retransmitted signal.

Another communication technology that has promising possibilities for application in indoor environments is power-line communication (PLC). By improving link performance, PLC has recently been used as an alternative communication option to combat

fading caused by signal scattering in an indoor wireless communication system. PLC is a cost-effective form of telecommunication technology since it exploits existing electrical wires for data transmission. PLC aims at utilising electrical power cables simultaneously as an electronic communications channel and a power transmission medium. Among the applications of PLC are high definition television (HDTV), and video conferencing and control, amongst others. It has been on trial in home automation and smart grid applications [6, 7] and it has even been envisaged that PLC could perform better than RF in multi-storey buildings (including the basement) [6].

However, a major challenge to a PLC system is how to overcome the issue of non-white and non-Gaussian noises. Indeed, its channel is one of the noisiest among most wired and wireless communication channels. The noise in a PLC system usually comes from the electrical components connected to the power line, such as impulse voltage and electrical arc between the lines. Overcoming the noise challenge will help to improve the quality of service, increase speed, and enhance data transmission. To combat signal degradation due to noise and attenuation, and to improve spectral efficiency and error performance, a diversity technique is often employed. The diversity technique is a well-known tool used to overcome fading. The principle behind diversity is to receive copies of a signal from different signal sources that are independent of each other [8]. The output signals are combined in some optimum manner using different combining techniques. In this thesis, a diversity system using two different channels (PLC, RF) is proposed. The transmission system is analysed, and signal reception is based on both SC and MRC combining technique.

1.2 Problem statement

WiFi technology is widely employed to provide broadband communication services in multi-storey indoor environments. However, it is challenged by several issues including spectrum saturation and as mentioned above, by RF signal attenuation due to structural obstruction such as walls and concrete slabs in the buildings. An alternative communication technology that promises an approach to combating attenuation and scattering in an indoor wireless communication system is the PLC. PLC and RF technologies can be combined to form a diversity system. This technology has been reported in the literature for smart grid applications using frequencies between 3 kHz and 500 kHz. For existing

literature, as in most results proposed for PLC technology, the impact of the coupling circuit on the PLC signal is not taken into consideration. It is well known, as explained in [9], that the coupling circuit has an impact on the transmitted signal. Limitation of RF (signal attenuation due to structural obstructions) and the impact of the coupling circuit on the PLC signal mentioned above, prompted the investigation reported in this study. It should be noted that the work is dedicated to high data rate applications (2.4 GHz).

This thesis attempts to solve the aforementioned communication problems pertaining to indoor multi-storey buildings by proposing a joint PLC-RF transmission system in which the receiver exploits diversity combining techniques to produce the final message.

1.3 Research questions

In order to address the problem stated above, the following research questions will be addressed:

- 1) How can a hybrid PLC-RF system be designed to improve the signal performance and signal strength at a frequency of 2.45 GHz?
- 2) What is the effect of a coupling circuit in PLC-RF diversity at 2.45 GHz, and how does it affect performance of the system?
- 3) What is the best combining technique that will be suitable to use in combining PLC and RF for a parallel transmission at 2.45 GHz?

1.4 Aims and objectives

The aim of this research is to combine PLC and RF technologies using diversity schemes, in an effort to solve the problem of effective communication lack by broadband communication services in indoor environments. This will help to improve signal performance in such environments and support the application of the Internet of Things emerging from the Fourth Industrial Revolution, besides other applications that require high data rates especially in the indoor environment.

The following are the objectives of this thesis:

- 1) To design a PLC-RF diversity system that operates at 2.45 GHz to solve signal penetration of RF technology in multi-storey buildings.
- 2) To develop such a system, a channel model will be proposed and its transmission system analysed, while considering the effects of the couplers used in the PLC link.
- 3) Display the best combining technique for PLC-RF diversity that operates at 2.45 GHz.

1.5 Main contributions

The main contributions are as follows:

- 1) The PLC-RF diversity system that operates at 2.45 GHz is designed. A discussion on a hybrid PLC-RF system, in which such a diversity system is used, is presented (see Chapter 6).
- 2) A channel model for PLC-RF diversity that operates at 2.45 GHz is proposed, and its transmission system analysed with due regard for the effects of the couplers used in the PLC link. The proposed system and the incoming data are coded and modulated (see Chapter 6).
- 3) The best combining method for PLC-RF diversity that operates at 2.45 GHz is proposed. Different combining techniques are studied to identify the most suitable one (see Chapter 6).
- 4) The PLC-RF system in which the end-user is mobile due to the contactless aspect of the system, at 2.45 GHz is proposed. The system was analyzed, and a channel model was proposed along with its frequency response (see Chapter 4).
- 5) The measurement results highlighting the channel capacity and performance is proposed. The transmission medium was analyzed on the PLC side and define the transmission capability with respect to the types of wire used. We implement the system practically and measure the radiated signal strength and the feasible data rate for both RF and PLC, separately. (see Chapter 5).

1.6 Thesis organization

The rest of the thesis is organised as follows:

Chapter 2 is divided into 5 sections, excluding the introduction. Section I describes RF technology and its environment. A description of the indoor wireless environment and wireless channel modeling are presented. This includes a detailed description of basic radio wave propagation, indoor environment propagation, path loss, shadowing, multipath, and Rayleigh. Section II entails a brief history of PLC technology, including indoor/outdoor PLC environments, and the PLC channel. Section III deals with techniques of modulation; Section IV with other PLC-RF related work, and finally, Section V provides a summary of the chapter.

Chapter 3 introduces the first modeling techniques for the PLC-RF system. The PLC channel, such as contactless PLC, is briefly introduced. An overview of transmission line effect, coupling circuit and the radiation pattern of a long-wire antenna is presented. It includes a basic description of different diversity techniques and their application on PLC-RF. Furthermore, combining techniques, which include selection combining, maximum ratio combining and equal gain combining, are presented.

Chapter 4 deals with contactless power-line communication at 2.45 GHz channel analysis, including comprehensive designs. The results of simulations are presented.

Chapter 5 discusses the preliminary measurement method for contactless power-line communication at 2.45 GHz. The results obtained from the measurement are then presented.

Chapter 6 reports a PLC-RF diversity channel analysis for both channels and the results are provided. The simulation measurements are performed, and the results of each channel are compared.

In Chapter 7 concluding remarks for the work reported in this thesis are given. Suggestions for future research are also presented in this chapter.

2

Overview of PLC and RF Communications

This chapter provides an overview of PLC and RF technologies and their applications. It focuses on the resources required for PLC-RF system integration. The RF channel model, which involves both indoor and outdoor environments, and the history of PLC and its channel model are discussed. Various aspects of PLC, including channel characteristics, attenuation, noise, and spectrum, are also discussed. The OFDM techniques that are applicable in PLC technologies are highlighted, and previous studies on hybrid PLC-RF are reviewed.



2.1 Introduction

WiFi is commonly utilised for interfacing devices, such as laptops or desktop computers, to each other in wireless mode and to the wired network. It employs RF technology to transmit and receive data at high speed in both indoor and outdoor environments. It operates within the generic terms of the IEEE 802.11 standard for wide local networks (WLANs). WiFi is used worldwide for Internet access because of its simplicity and because it is a cost-effective way of accessing the Internet without requiring wire.

However, WiFi faces a fundamental challenge, viz. the impact of obstacles that affect signal propagation and spectrum saturation. This has drawn the attention of researchers whose endeavours have produced a variety of solutions to the problem. PLC is one possible way out, but its immobility is one of the most serious barriers there are others - that slows down the mass implementation of PLC technology. This is often due to the fact that end nodes are physically connected to power wires which generally presents a high risk of electrical shock.

An overview of PLC and RF technology is given in this chapter. The details are important since they will facilitate an understanding of the main elements that affect the behaviour of the PLC and RF channel model. The channel model, together with noise, is also presented in this chapter, and modulation techniques that are applicable in PLC technology are highlighted.

2.2 PART I: RF technology

2.2.1 The indoor wireless environment

This thesis focuses more on the indoor than the outdoor environment and involves multi-storey buildings and the effects of building materials on wireless signals. It is necessary to briefly discuss the indoor environment propagation characteristics and the factors that affect radio propagation in order to facilitate a broad understanding of indoor wireless propagation.

2.2.1.1 Basics for radio wave propagation

The propagation of radio waves refers to as the process by which energy travels through a given medium from the transmitting to the receiving antenna. The medium is informed of electromagnetic waves where radio signals use the speed of light as a communication channel. The RF propagation can be determined by how well a signal travels in free space or radiates using other uniform media. Different radio signals have different properties which depend on high and low frequencies. The four major propagation mechanisms are reflection, transmission, scattering, and diffraction [10], all of which have a significant impact on electromagnetic waves and the environment.

2.2.1.2 Propagation in the Indoor environment

Most researchers have worked on radio propagation in the indoor environment. The measurement of the indoor environment, which is based on narrowband and wideband systems, is described in [11–19]. The indoor environment is associated with a short distance between the transmitter and the receiver [20], and the loss in the indoor link is usually caused by free space loss. The signal strength in the indoor environment depends on the height of the antenna, as well as on hardware equipment (tables, types of doors, windows and other reflection shape object) within the environment. Transmission techniques in the indoor environment can be classified as follows: a direct LOS and an indirect LOS. In the direct LOS, the transmitter and receiver normally establish communication by transmitting a signal between transmitter and the receiver, although in indoor environments, most of the receiver locations are obstructed by walls or other in-built obstacles. The effect of the obstruction on the direct path of the signal can be considered dominant with the direct line of sight. In this system, the transmission rate is high, and it maintains low multipath dispersion and low path loss.

Indirect LOS depends on three main propagation mechanisms. As indicated in the previous section, the signal can take many different paths from the transmitter to the receiver as a result of reflection, scattering, and diffraction. In some cases, the signal can reach the receiver directly, but might be phase-shifted, which will produce a distorted signal. Because of reflection, the transmitting signal usually scatters off walls, ceilings, or the doorways of a building. The reflection can thus be induced by some object or it can be energy reflection which includes both the electrical and physical properties of an

object. These will create multiple paths between the transmitter and the receiver. The reflection normally reduces the power of the received signal.

2.2.1.3 Propagation in building environment

A comparison between propagation in indoor and outdoor environments in terms of multipath is given in [21]. It can be observed that the indoor environment has greater multipath as a result of obstruction associated with the constructions materials and building structures used in the building [22]. A similar situation applies to offices and residential houses. In this thesis, the focus is on the office and residential environment, since both have similar propagation patterns. The aim of propagation in every building is to achieve a high data rate together with high capacity. For partitioned apartments, propagation measurement is discussed in [11–19]. These sources show that reflection is a major factor influencing the signal strength. However, measurements [17] have shown that radiating energy along corridors has the most significant propagation at a distance of up to 10m. Another factor that influences indoor propagation is building materials, which include metal, bricks, and glass. Understanding the transmission and reflection characteristics of building material helps to predict the accuracy of data propagation.

2.2.2 Wireless channel modelling

Radio propagation can be grouped into three independent levels based on the electromagnetic (EM) wave propagation mechanism: path loss, shadow fading and multipath fading [23]. The attenuation in the wireless link can be calculated in terms of summation of path loss, shadowing and multipath fading, which represents the total attenuation as follows [23].

$$a(t) = a_{PL}(t)a_{SH}(t)a_{FA}(t), \quad (2.1)$$

where $a(t)$, $a_{PL}(t)$, $a_{SH}(t)$ and $a_{FA}(t)$ are total attenuation, attenuation of the path loss, attenuation shadow fading, and attenuation of multipath fading.

2.2.2.1 Pathloss

Path loss is the type of attenuation that propagates the transmitted signal from the transmitter, which is the source, to the receiver at a given time interval [24]. Absorption due to moisture and radiated power dissipation can be classified as two major causes of path loss. Distance from the transmitter to the receiver is one of the major factors that determines the received power of the path loss, in other words, path loss is a function of distance which is known as free space propagation [25]. Different path loss model descriptions are given in [24, 25]. The channel linear path loss is given by

$$P_L = \frac{P_t}{P_r}, \quad (2.2)$$

where P_t and P_r are the source power, and destination power respectively. In free space propagation, the received power for path loss of a channel in dBs is given by

$$P_L dB = 10 \log_{10} \frac{P_t}{P_r}, \quad (2.3)$$

where P_L is the channel linear pathloss.

2.2.2.2 Shadowing

Shadowing is a result of objects obstructing the path of a transmitting signal, thereby causing loss of signal from the transmitter. This results in fluctuation in the power of the received signal. The signal is lost because of absorption, reflection, scattering, and diffraction. The path loss in dB can be expressed according to Log-Normal fading as

$$\begin{aligned} P_L(d)dB &= \overline{P_L}(d) + X_\sigma \\ &= \overline{P_L}(d_0) + 10\gamma \log \left(\frac{d}{d_0} \right) + X_\sigma, \end{aligned} \quad (2.4)$$

where X_σ is the random shadowing effect. The Log-Normal distribution, which is the probability distribution of a random variable whose logarithm is normally distributed, is given by

$$f_X(x; \mu, \sigma^2) = \frac{1}{x\sigma\sqrt{2\pi}} \exp \left(-\frac{(\log x - \mu)^2}{2\sigma^2} \right), \quad (2.5)$$

where x is the random variable, μ , and σ^2 mean and variance of the distribution (in dB), respectively.

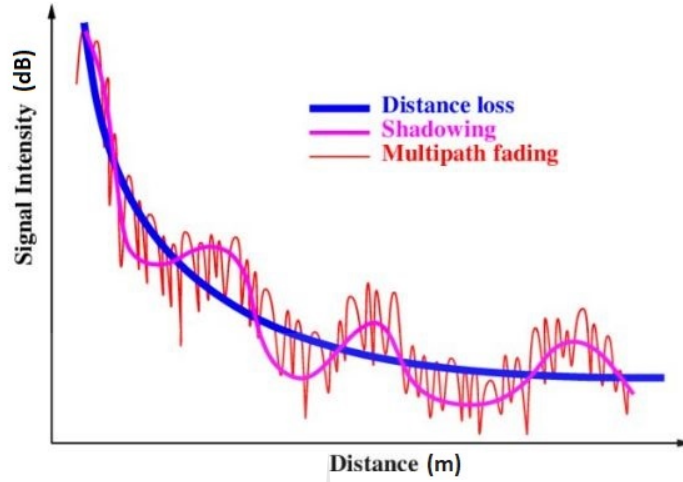


Figure 2.1: Graph representing distance loss, shadowing, and multipath propagation.

2.2.2.3 Multipath

The application of multipath propagation in both channels (PLC, RF) are the same, the only difference is that in the RF channel, the fading phenomenon depends on the physical nature of the channel. In general, fading in the wireless channel is caused by an additional signal as a result of the multipath phenomenon. The multipath fading in wireless communication is cloned by the Ricean and Rayleigh models which have been adopted in [26], to analyze the characterisation of wireless channels [26]. The Ricean model is used in situations where LOS is applicable, while Rayleigh concentrates more on NLOS. Here the focus is more on the Rayleigh distribution because in the PLC-RF system there is NLOS. The graphical representation of the intensity for signal behaviour over a distance for three components of the channel response is shown in Fig. 2.1 [26].

Ricean fading: Ricean fading is essentially part of radio propagation and is a stochastic model for interpreting the partial cancellation of a radio signal. In such a situation, the signal arrives at its destination via different paths. At any point when one signal path within LOS is stronger than the others, Ricean fading occurs. Once the Ricean occurred,

the envelope obeys a Ricean distribution. Its probability density function is given by

$$p(\alpha) = \frac{2\alpha}{\Omega} \exp\left(-\frac{\alpha^2 + A^2}{\Omega}\right) I_0\left(\frac{A\alpha}{\Omega}\right), \quad (2.6)$$

where A represents the peak amplitude of the dominant path and I_0 is the modified Bessel function of the first kind and zero-order. The random variable for the signal amplitude is represented by α , while Ω represents the average power of the random variable.

Rayleigh fading: Rayleigh fading is a statistical model for predicting or calculating the effect of the environment on a radio signal. It is more effective when there is NLOS between the transmitter and the receiver. The multipath fading associated with wireless communication systems is commonly modeled by Rayleigh and Ricean distributions. This study focuses on the modeling and simulation of Rayleigh fading. However, where there is an issue of NLOS, the issue of attenuation as regards multipath fading in a wireless channel.

Rayleigh distribution can also be described as two orthogonal components that have complex number values. Such values include magnitude of both imaginary and real parts which is for a zero mean Gaussian random variable. The two random process for the orthogonal components of the imaginary and real parts respectively, are given as R_s and R_c , it can be defined as

$$R_c = E_0 \sum_{n=0}^N C_n \cos(\omega_c t + \phi_n) \quad (2.7)$$

and

$$R_s = E_0 \sum_{n=0}^N C_n \sin(\omega_c t + \phi_n), \quad (2.8)$$

we can express Tz as

$$R_c = R_c(t) \cos(\omega_c t + \phi_n) - R_s(t) \sin(\omega_c t + \phi_n), \quad (2.9)$$

where R_c and R_s are gaussian random processes for a large value of N with due regard for the central limit theorem and Tz is the complex number of gaussian random process. The envelope of Tz is given by

$$\alpha = \sqrt{R_c^2 + R_s^2}. \quad (2.10)$$

The channel response is modeled in a wireless channel to have a Rayleigh distribution. The PDF expression is given by [27],

$$p(\alpha) = \frac{2\alpha}{\Omega} \exp\left(-\frac{\alpha^2}{\Omega}\right), \quad (2.11)$$

where α represents the random variable for the signal amplitude and Ω represents the average power of the random variable. The channel fading parameter and spectral density of noise power in terms of the instantaneous SNR value per bit is given by [27]

$$p(\gamma) = \frac{1}{E_b N_0} \exp\left(-\frac{\gamma}{E_b N_0}\right), \quad (2.12)$$

where γ is the SNR per bit, E_b is the ratio of energy per bit, N_0 is the spectral density of noise power.

2.2.3 Wireless channel noise

The wireless channel noise is mostly caused by the thermal performance of the receiver and it associated with additive white Gaussian noise (AWGN).

2.3 PART II: PLC technology

2.3.1 PLC technology brief history

PLC uses an electrical power delivery network to transfer a signal from the source to the receiver, and it carries both electric power and data simultaneously. PLC operation is carried out by a signal modulating carrier on the electrical power network and utilises an electrical cable for data transmission [28–30]. There are three stages of electrical power classification: transmission over high, medium and low-voltage which is 44-132 kV; 1-44 kV, and 0-1000 V over transmission lines [31] respectively. PLC is applicable in all three

stages. Its advantage over other techniques is that in every building and home, there are existing power lines which are normally linked to a power grid. There is therefore, no need to install additional infrastructure because the existing electrical power supply can be used as the signal transfer medium.

In 1922, narrowband PLC was mainly used for the delivery of low-speed communication [32]. The first carrier frequency operating system started its operation over a high-voltage line with a 15 to 500 kHz frequency range [33] for telemetry applications. The first industrial system was developed in France in 1960 and made use of kVA of power. It is generally known as Pulsadis. Thereafter, the CENELEC band PLC systems, which operate between 3 kHz and 145.8 kHz frequency range [34], came into existence. The low data transmission works perfectly over a power line and it allows bi-directional operation over low voltage, for example in remote meter readings. Power-line technologies have a wide frequency band which allows the speed of both high and low data transmission over power lines. Frequency bands are grouped into three main sets: ultra narrowband (UNBPLC) technologies which are very low data rate, less than 100 bps; lower band frequency between 0.3 and 3 kHz, and upper band frequency between 30 and 300 Hz. According to European standards, narrowband BPLC technologies operate within the range of 3-500 kHz frequency, and broadband BPLC technologies operate within the band 1.5-250 MHz.

Over time, research also introduced medium voltage and low voltage networks. In time research involving PLC technology has gained in popularity, and there is an increase in demand for networking in various areas such as offices and in industrial organisations amongst others, where power lines utilise high-speed data transmission that is greater than 2 Mbps [35, 36]. In general, current PLC technologies have gained in popularity and look very promising for energy providers and their users. Moreover, such technology has been improved from the energy distribution network to the data transmission medium, and many other applications have emerged from PLC technology such as Internet access broadband and the wide area of the Smart Grid. Broadband uses PLC technology to improve Internet access broadband through a normal power line. It is also regarded to as power-band or power-line internet. A device such as a computer or laptop can be connected to the electrical outlet of a building and it will get access to the internet at high speed. Moreover, a broadband power line (BPL) has some advantage over a DSL connection. The cost of developing another Ethernet infrastructure in an existing building will be saved. BPL uses existing electrical wiring to give users access to the internet in remote areas using existing infrastructure. Beside the efficiency of low power devices, security

is a major problem facing the wireless framework and its limited maximum throughput. Some studies on broadband power-line communication modeling have shown that there is a significant improvement in power-line technology to compare with wireless, and good results have been obtained on the actual behaviour of power-line usage [37–39].

2.3.2 The PLC channel

The multipath reflections normally occur in an electrical power network within a multipath propagation environment. However, this type of reflections is normally regarded as discontinuities and unmatched loads. The periodic change of loads which is synchronised is determined by cyclic time variation of the PLC channel in terms of its frequency selective fading. A PLC channel modeling experiment can be performed using a top-down or bottom-up approach [40]. Both modeling approaches have advantages and disadvantages: the top-down modeling approach is easy to implement, and its computation is simple and straight-forward. The top-down approach is performed by finding a suitable model that uses either impulse responses or frequency responses. The parameters of the transfer function of a PLC network are extracted from the actual measurement of the signal in the channel. One of its disadvantages is the inability to replicate the character of the channel in a different PLC network, and furthermore, it is also prone to error as regards to the measurement.

The bottom-up modeling approach uses theoretical details to extract all parameters of the transfer function, that is, it makes use of transmission theory to derive its channel model. The bottom-up type of approach is used in this study, although, a channel model approach is adopted, for modelling of an indoor power-line channels behaviour in terms of periodic time-varying. The factors that determine the multipath propagation model that defines the PLC channel can be referred to as the effects of reflection; the effects of the cable (attenuation), and phase-shift propagation effects [41].

The PLC channel transfer function modeling techniques can be achieved by using a time or frequency domain, although it depends on the algorithms being used. However, the time domain channel is regarded as a multipath model in which the channel is classified as a multipath environment. The frequency-domain algorithms, on the other hand, use the fragmented network which is often regarded as elements in cascade and are referred to as either transmission or scattering matrices [42]. In the following sections, the two

main modeling approaches are reviewed.

The indoor PLC environment: The network for an indoor PLC system consists of branching. The loads are connected through AC outlets to various points, which as a result, experience different types of noise, conditions for frequency channel selection, and attenuation that is on the high side [43]. The impedance mismatches heavily influence performance of indoor PLC environment because various terminal points are connected to the network.

The indoor environment provides an alternative to broadband networking by using power-line communication [44], and without the need for installing a new infrastructure network [44]. Indoor PLC includes various environments, such as offices, houses and public environments, which all exhibit similar characteristics. The channel capacity of the indoor environment is analysed in [45], and the result of the study show that there is a variation in voltage, depending on the environment. Indoor power-line distribution typically utilises two-wire transmission lines one of which is red (hot) and the other black (neutral), the ground is normal the unsheathed copper wire.

The outdoor PLC environment: The network outdoor PLC environment consists of a few long branches. It consists of two voltage levels: low voltage and medium voltage which normally vary between countries, depending on the local voltage regulation body. The power distribution network determines the voltage level that is used in the transmission network for signal propagation coverage. The outdoor PLC environment requires low fading and high attenuation in comparison with that of indoor PLC environments [46].

2.3.2.1 Top-down PLC channel model

The PLC top-down channel model is generally an echo-based channel with an impulse response. The echoes, which are the reception of multiple delays, occur due to the reflections from the appliances that are connected at the branch endpoints of the transmitted signal. The top-down channel uses data fitting to develop statistical channel models that produce low complexity. This is one of its advantages, although there is an issue of low flexibility which is a major disadvantage. The model, as well as the derived parameters, differ from one frequency band to another. Generation of the channel realisation can be

achieved with a short interval once the model and parameters are provided. The impulse response of an echo-based framework can be defined as [43].

$$H_p(f) = \sum_{i=1}^N g_i e^{\beta - (f)} l_i e^{-j2\pi f \tau_i}, \quad (2.13)$$

where t , k_i and τ_i are the number of taps, attenuation and the delay of individual echo, respectively. The attenuation coefficients, k_i , of echoes is expressed using the effective cable length, l_i . The weighting factor g_i of the i^{th} path represents the link topology [43, 47]. The skin effects and dielectric loss are determined by the factor f . The Fourier transform of the channel model statistic is expressed [43, 47] and also the channel frequency response for spectral analysis.

2.3.2.2 Bottom-up PLC channel model

The transmission line effects model and the voltage ratio model are used to model the PLC bottom-up approach [48]. The voltage ratio approach describes the relationship between an input voltage and an output voltage in a network. A detailed description of the bottom-up approach model with its transmission-line theory was explained in [49], and the theory behind the bottom-up is highlighted in [40, 50]. The elements of the network are generally modeled mathematically in such a way that they can be incorporated to generate channel realisations. The channel model of a bottom-up approach can be summarized as the product of the channel transfer function and the units of the various electrical power sources in the network topology. The formula for the bottom-up approach is presented in [40, 50] and it is given by

$$\mathbf{H}_p(f) = \prod_{j=0}^{I_p-1} \frac{V_{Rx_i}(f)}{V_{Tx_i}(f)}, \quad (2.14)$$

where V_{Rx_i} and V_{Tx_i} are the voltages measured at the receiver and the transmitter input ports, respectively, and I_p the number of input ports.

2.3.3 Noise and disturbances in PLC

The noise in PLC differs from that in the classic AWGN. In this study both noise types are emphasised. In the following section, PLC noise and interference are discussed.

PLC channel noise The PLC noise scenario basically depends on the environment which involves several parameters such as magnitude and graphical representation that will determine the sources of the noise [47, 51]. The PLC noise is typified as background noise and impulse noise [52–55]. There are two types of background noise, viz. coloured background noise and narrowband noise [52]. Impulse noise in turn, consists of impulse periodic noise and synchronous and asynchronous impulse noise [52].

Back ground noise: This is the result of low power noise emanating from various sources. It is the noise that is normally caused by household devices, e.g. an electrical cooker and an iron, among others [52]. Background noise can be disregarded because of its relatively low power spectral density (PSD) [56, 57]. The PSD, P_{backg} , of background noise can be calculated as [58].

$$P_{backg}(f) = \rho + \alpha|f|^\gamma, \quad (2.15)$$

where ρ , α and γ vary with time and location. The power levels of coloured noise, which is associated with background noise, vary with time, from one second, minute or hour to the next, and thus change over time.

Narrowband noise: Narrowband noise is caused by signal spectrum interference or coupling of a RF signal, e.g. Wi-Fi and broadcasting station, amongst others. The amplitude of narrowband noise depends on time, and normally dominates part of the spectrum [56, 57]. The noise originates from television vertical scanning frequency are connected to the same transmitter harmonics. The television scanning frequency noise has been presented in [52, 59].

Impulse noise: The main cause of impulse noise is the switching on of the power supply from the transients network. The power supply which varies within a few seconds depending on the load connected to it. In [52, 56], a comparison of PSD for impulse noise and background noise is given. In conclusion, the PSD of impulse noise is estimated to exceed the range of 10-15 dB in comparison with the background noise, which at times can reach 50 dB.

Asynchronous impulsive noise: This kind of noise is the most dominant type, besides being the most difficult to predict. Asynchronous impulsive noises usually originate from transients. It has the ability to connect or disconnect from an electrical appliance on the power-line network depending on the load connected in the network. Such noise is sometimes known as sporadic impulsive noise. Asynchronous impulsive noise modeling is based on periodic function that represents an additive white Gaussian noise with zero mean. It is detailed in [52], and is given by

$$\sigma_n^2(t) = \sum_{l=0}^{L-1} A_l |\sin(2\pi t/T_{AC} + \theta_l)|^{n_l}, \quad (2.16)$$

where n_l , θ_l and A_l are the main characteristics of the noise. Note that T_{AC} is the mains period and L represents the number of noise classes.

2.4 PART III: Techniques of modulation

OFDM has been adopted as the modulation scheme for wireless and PLC channels [60]. In [61, 62], the authors consider NBPLC/wireless diversity combining, for which they propose OFDM as the transmission modulation scheme. In this case, the same information is sent through both channels at the same time. In the solution provided by OFDM-PLC, the 78.6 kbps data rate can utilize 48 data sub-carriers at its maximum capacity and in the frequency range of 24 to 93 kHz [63]. Based on these frequencies, there will be an increase in the transmission filters which will help to reduce unwanted signal. The problem with this solution is that it does not align with the CENELEC A principle. For CENELEC to work, the data rate speed of 78.6kbps will be utilised with the 48 data sub-carriers which must match the 16-PSK modulation. Moreover, the PLC channel is a low SNR environment. In addition, OFDM depends on the carrier frequency offset. Consequently, other solutions should be investigated.

To combat signal degradation due to noise and attenuation, to reduce error rates, and to improve spectral efficiency, it is necessary to employ some form of signal modulation technique. Solutions such as MIMO-OFDM for the PLC channel have been proposed [64–66]. Most of the solutions (PSK-QAM) are based on full channel state information (CSI) [67]. Solutions based on CSI are preferable, but are not the best, which means that there is a need for more research for an optimal solution to PLC channel because of

the unpredictability of CSI. Differential code shift keying (DCSK) and spread frequency shift keying (S-FSK) were proposed for SENELEC A [68, 69]. The ideal solution will accommodate low-power and low-cost constraints. Energy detection of the chosen scheme must attain a minimum BER on the AWGN channel.

Different modulation techniques are highlighted in [70]. Here a suggestion is made that a better performance can be achieved using BPSK modulation when compared with other modulation techniques such as QPSK, 8-PSK, or 4-QAM and 16-QAM [70]. For purposes of simplicity, the modulation technique used in this study is BPSK, and outage probability is used to calculate the numerical performance.

2.5 PART IV: Other PLC-RF related work

The hybrid system is gaining more popularity recently for indoor communication, which is likely to be considered as a future possible solution for wireless communication systems. A more flexible solution, which could considerably impact on the communication industry, is the use of a radio frequency (RF) antenna [71–75], which will detect the radiation signal provided by the power wire and converts it into an electrical signal. The signal received will be detected definitely by the PLC receiver. It is also regarded as an excellent approach to achieving service quality required. In [76], the hybrid RF-VLC system was proposed, which was more vitality productive and more versatile to the brightening conditions than the individual VLC or RF frameworks. A similar hybrid system was shown in [77], which involves a hybrid system that considered RF as well as optical wireless-based communication technologies. All the results demonstrate that the hybrid system performed better than single RF, PLC, and VLC. Using the wireless and PLC channel simultaneously to improve indoor network performance has been proposed by Lai et al. [78]. In this approach, the analysis of a narrowband model was presented using OFDM subcarriers, in which various diversity combining (DC) scheme was used to receive the signals. In their research, bit error rate (BER) for binary phase shift keying (BPSK) is performed which help to analyze the saturated AWGN metric for diversity. Solutions have been proposed for employing selection combining in correlated with log-normal channel noise, in this case, the PLC channel is considered to be log-normal [79]. By using BER for BPSK for analysis, it can be seen that multiple channels employing selection combining is better than the single channel in terms of unwavering quality [79]. The two technologies were

combines together using a hybrid system which are TV white space (TVWS) and broadband power line communication (BBPLC). The two technologies were proposed for a smart grid multimedia network in [61], where the same signal is sent through both TVWS and BBPLC channels.

A similar hybrid wireless-PLC systems experiment was performed in [60], in comparison to not hybrid systems. From the computational simulations that were based on the physical layer of the IEEE P1901.2 standard, it was concluded that the hybrid PLC-wireless system offers a gain of the signal-to-noise ratio (SNR) when compared to only a wireless or PLC system. The hybrid PLC/wireless channel was analyzed for data communication purposes, using statistical modeling, which was presented in [80]. A practical hybrid wireless-PLC systems scheme based on single relay channel (SRC) [72] is introduced. The hybrid power line/wireless a single relay channel (HSRC) significant performance was exhibited which outperforms both power line and wireless SRCs in all considered scenarios.

This provides the possibility of using the PLC as an access technology. To the best of our knowledge, a joint PLC-RF framework in which the transfer function of the coupler is considered has not yet been investigated. In such a system, the coupling circuit ought to be considered as one of the major components that will impact the performance of a PLC channel. With this in mind, in this thesis, a diversity system using two different channels (PLC, RF) is proposed. The transmission system is analyzed, and signal reception is based on both SC and MRC. The outage probability analysis is proposed, and resultant signals are obtained by both SC and MRC combining technique.

In [81], the measurement campaign of hybrid PLC/wireless channels are analyzed. The results of the analysis indicate that the communication of portable devices over the electric distribution grid is viable. A previous study on PLC/wireless diversity combining can be found in [62], which summed the received signals for both NBPLC and wireless link along with the diversity combining techniques and then add them to the conventional combining techniques using closed-form expressions for average BER. In [82], a solution for combining a received signal using diversity-combining techniques for hybrid NBPLC and unlicensed wireless transmission is proposed. It makes use of differential modulation schemes. In [83], the research introduced an approach, which is amplify-and-forward relaying was used for in-home PLC and wireless systems. The capacity of the system for both PLC and wireless channel were analyzed using the exploited statistical properties. It

was concluded that the performance of the hybrid system is better to compare with single wireless or PLC system. In [5], the researcher discusses the advantages of a hybrid system when compared to a non-hybrid one using a hybrid power-line/wireless data communication system. Numerical results show that hybrid power-line/wireless data transmission is more stable in comparison with data transmission via an individual power-line or wireless system. The scheme described in [82] helps improve the performance robustness in the communication link by reducing interference and noise. Selection diversity was proposed for the analysis of a closed-form expression for an average BER performance. In [84], the authors introduce another narrowband PLC and an unlicensed wireless communication system in which the output signal is combined, but in this case, the two channels carry the same information. The channel performance is analysed using the average BER. A solution using wireless and power-line communication channels to increase the coverage and throughput of an indoor network is proposed in [85]. For the channel model, OFDM was used for transmission over different media.

It should be noted, first, that in all the sources referred to above, the authors analysed the performance diversity for a PLC-wireless channel using the average BER and a few tools. This is an interesting channel analysis in terms of the noise factor. Further investigation on issues such as the channel outage probability is needed. This will receive attention later in this study. Second, in most of the sources the coupling circuit is not considered in the analyses reported by the authors. Furthermore, they consider the transfer function of the coupler as one unit which is not usually the case.

Combining RF and PLC technologies are proposed in the literature for various applications [3, 61, 62, 79, 81, 84–87]. In most of the sources consulted, PLC is proposed as a fundamental aspect of RF, and signals to be transmitted by the WiFi router come from the PLC channel.

Over view of contactless PLC: In [81] hybrid PLC-wireless channels are presented. The discussion demonstrates how physical portable devices can communicate with each other through an electric distribution grid. The frequency band used for the analysis is in the range of 1.7 to 100 MHz. The magnitude for the channel frequency response is also discussed in this source. The study concludes that the channel frequency response of a hybrid PLC-wireless for a portable device is better when compared with an individual portable PLC or wireless. Similar to the work in [81], the authors of [4] report an experiment involving characterisation of a hybrid PLC-wireless channel. In their work, the

authors give measurement of the hybrid channel in the PLC and its performance. The researchers characterise the hybrid PLC-wireless channels. The study reveals that the hybrid channel measurement offers lower attenuation than a non-hybrid channel offers [4].

The authors of [88] performed an experiment involving a power-line cable and its propagation characteristics. In their work, they demonstrate that application of radio wave on an existing power-line network for a large building will help to enhance signal penetration when a WiFi wireless network is used. This was also confirmed in a similar exercise reported in [89] where the authors performed the experiment using wireless communications at 2.4 GHz frequency over a power-line network inside a multi-storey building. In their work, RF LOS for outdoors can go up to 100 m, which is not the case in an indoor multi-storey building, where the signal will be obstructed by the floors or ceilings, leading to a signal drop by 10 m, or might even be blocked completely. The power-line network in the building acts as a guide to the weak signals from their source to their final destination.

Similar to work reported in [87], the author of [87] performed a measurement analysis of a contactless PLC system. This study shows that electromagnetic interference (EMI) is produced from a power line that carries a communication signal and it can be transmitted to a receiver by means of a contactless off-the-shelf power line connected to an antenna. Power lines that carry communication signals tend to produce radiation through the principle of EMI. Signal can be transmitted via a wireless medium and received through the power line. This can be achieved by using off-the-shelf power lines and a modem connection to an antenna. The limitation here is the 2 m radiating distance that operates within the frequency band range from 150 kHz to 30 MHz. Advanced work needs to be carried out in which a longer radiating distance is considered.

2.6 PART V: Summary

In this chapter, the background of RF and PLC technology as regards communication systems in general is discussed. An overview is provided of the transmission of RF, using radio waves, and the behaviour of the channel model in indoor and outdoor environments received attention. Furthermore, PLC transmission that uses a power-line cable for its delivery is dealt with. RF and PLC design were considered and fundamental principles for both technologies were highlighted. Emphasis was placed on the modulation methods, and the PSK technique was mentioned. A brief description of PLC noise was given and finally,

relevant aspects from published studies on hybrid PLC-RF systems by other researchers were highlighted.

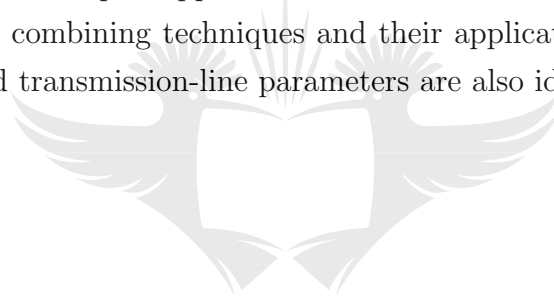
This background, in which the basics of the proposed technologies together with the benefit of integrating the systems have been highlighted, sets the scene for the next chapter. In it the necessary statistical tools as well as the different diversity techniques for the PLC-RF channel will be analysed.



3

Modeling Techniques for PLC-RF Systems.

In this chapter the statistical tools required to demonstrate a PLC-RF channel are presented. The diversity techniques applicable to PLC-RF technology are emphasised, and an analysis of various combining techniques and their applications are highlighted. The long-wire antenna and transmission-line parameters are also identified.



UNIVERSITY
OF
JOHANNESBURG

3.1 Introduction

The demand for wireless communications technology in the next-generation network and beyond is moving towards contactless PLC technology, especially for indoor communication applications. This is because it offers better performance, coverage, and reliability through the provision of Internet access for both wireless and power-line mediums. PLC aims to simultaneously use existing electrical power cables as electronic communication channels, besides its regular use as an electrical cable. The main challenge, viz. how to improve signal transmission in terms of a megabits per second (Mbps) rate in indoor communication by using a power line, persists. Although some work has been done in this field [86, 87], it is still a new area of research, and much remains to be done.

3.2 Transmission line effect.

Figure. 3.1 shows the transmission line of a common PLC channel, where L , R , G and C are inductance, resistance, conductance and capacitance respectively. The electrical parameter for the power line that determines the channel frequency response is described in [90], and the calculation for the circuit is given in [90, 91]. The single phase, which consists of parallel L – C circuits with parameters of variable inductances and capacitances, resonate at a specific frequency.

The impedance calculation of the series RLC resonant circuit, which is frequency dependent in Fig. 3.1 (see 2.6 above), is given by

$$Z_s = R + j2\pi fL + \frac{1}{j2\pi fC}. \quad (3.1)$$

The capacitive and inductive reactants may be equal to the resonance. They lead to the circuit being resistive. The resonant frequency is given by

$$f_{res} = \frac{1}{2\pi\sqrt{LC}}, \quad (3.2)$$

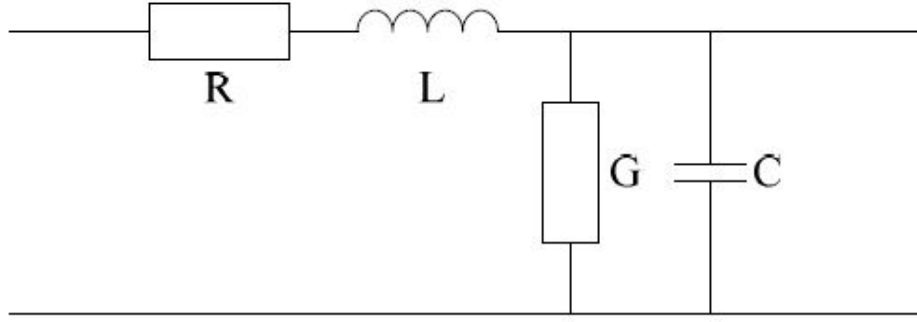


Figure 3.1: Transmission line

and the channel frequency response (f) is

$$H(f) = \frac{1}{1 + \frac{Z}{Z_s(f)}}. \quad (3.3)$$

The long-wire antenna for RF radiation acts as a transmission line, which is a standing wave or traveling-wave antenna, or possibly a guided surface-wave system. The coupling circuit will couple the signal into the transmission line.

3.3 Coupling circuit (CC)

The PLC utilises a CC as part of its major component for transmission. It is simply the interface between the PLC modem and power-distribution network. The CC is used to couple the communication signals in/out of the power line. The coupling of the communication signal can be achieved by using several closed current paths [92]. The closed current paths are discussed in [93]. In their experiment, the authors of [93] show that the CC, which was a RG-58 coaxial cable, was stripped in proximity to the power line to act as coupling circuit which is clearly described in [86].

Input-output coupler: The indoor environment uses three wires lines, such as life wire (L_e), neutral (N_e), and the protection wire (P_e). A maximum of four inputs can be realised including the common-mode (CM) input (L_e-N_e , L_e-P_e , N_e-P_e , CM). However, only one MIMO/SISO combination of two inputs is advised because of the imbalance that

will be created by the others [94]. If the receiving couplers at the receiver do not inject any signal into the channel, it will create an unbalance signal situation in the PLC system. The four ports can be used consequently, a maximum of 2×4 MIMO is feasible ($Q=2$, $N=4 \Rightarrow \Gamma=2$). The different single SISO streams included in the decomposition of the channel matrix H are all affected by a correlated noise vector \vec{n} . It has been shown that for low-level noise, the Le port is less sensitive than the ports situated on the protection and the neutral wires. A coefficient $C^{q,n}$ ($0 \leq C^{q,n} \leq 1$) characterises the correlation between noise types affecting the different wires.

3.4 Long-wire antenna

The radiation pattern of a long-wire antenna depends on its electrical length and can be unpredictable. The wave lengths (λ) in radio wave are used for measuring its length. A wire antenna is a three-dimensional solid electrical conductor of any cross-sectional geometry, although normally it is round or square, with a specific spatial shape and orientation [95]. The simplest wire antenna topology is a $\frac{1}{4}\lambda$ antenna. The $\frac{1}{2}\lambda$ dipole is normally easy to construct. The combination of two of $\frac{1}{4}\lambda$ antennas is $\frac{1}{2}\lambda$. The long-wire antenna normally has different lobes which are usually located at an angle to the axis of the antenna [96,97]. This is caused by drop-off zone radiation that is on the axis. At 0.6 a normal wire antenna will have a single lobe at its right angle axis. The lobe will split into two lobes usually at equal angles to the wire, depending upon an increase in the length of the wire. An increase in the length of the wire in wavelengths is directly proportionate to an increase in the number of the lobes and is difficult to predict.

The length of the wire antenna depends upon three variables such as operating frequency, dielectric value and the material of the conductor. The operating frequency of an antenna operates only in a vacuum environment (free space). The dielectric value (effective relative permittivity) of the material surrounding the conductor, and the material that exists between the conductor that comprises the antenna and the nearest earth plane. This is described in [98,99]. Long-wire antennas are usually created by using a number of dipoles [100]. The length of the wire for long-wire antenna [101] is given by

$$L_a = n \frac{\lambda}{2L}, \quad (3.4)$$

where L_a , n and λ are length of the antenna, number of elements and wavelength respec-

tively. The combination of long wires to form antennas of different shapes will help to increase the gain and directivity over a single wire. The length of long-wire operation depends upon the wavelengths. Moreover, the characteristics of the antenna change slowly with the length of the wire, except in situations where short wires are used; here the change will not be noticed. The lengths of the antenna system for harmonic wires can be determined with the following formula [101],

$$Length = 984 \frac{(N_a - 0.025)}{f}, \quad (3.5)$$

where N_a is the antenna length in wavelengths and f is the frequency. The long-wire antenna operates to give satisfactory gain and directivity over a frequency range that is twice the value for which it was prepared. It receives power and radiates effectively on any frequency for which the whole length is not less than approximately $\frac{\lambda}{2}$. A long-wire antenna has directional patterns that are shaped into horizontal and vertical planes [102]. The radiation concentrates more on the low vertical angles.

3.5 Radiation pattern

The characteristic of radiation pattern for an antenna in the directional function, for the far-field region can be defined as a 3D plot of the radiation [96, 103]. The distance of the far-field is given by [104]

$$R_F = \frac{2(D)^2}{\lambda}, \quad (3.6)$$

while

$$\lambda = \frac{c}{f}. \quad (3.7)$$

The near field distance is given by [104]

$$N_f = \frac{(D)^2}{4\lambda}, \quad (3.8)$$

where D , f , λ and C are the largest dimension of antenna, operating frequency, wavelength and speed of light in free space.

The radiation pattern can be expressed as a graphical representation of radio properties, classified in two-dimensional plots and consisting of an elevation pattern and an azimuth. The radiation of an antenna is a transducer between a radiated wave and a guided wave. Antenna patterns can be grouped into four categories: omni-directional, directional, isotropic and principal plane patterns. For purposes of simplicity, omni-directional and directional antenna patterns will be discussed and analysed in this study. The omni-directional pattern is uniform in a given plane; the antennas that are associated with it are mostly micro-strip patch and dipole antennas. Their reception has the same transmission because of the reciprocity characteristic of the radiation patterns of the antenna. The calculation for directivity of an antenna is given in [96] as

$$D(\theta, \Phi) = 4\pi \frac{F(\theta, \Phi)}{\int_0^{2\pi} \int_0^\pi F(\theta, \Phi) \sin \theta d\theta d\theta}, \quad (3.9)$$

where $F(\theta, \Phi)$ is the function for radiation intensity. In some cases directive antennas perform better than omni-directional antennas in terms of gain. Antenna directivity gain depends on directional properties and antenna efficiency [101, 105]. The gain measurement is discussed in [105]. Moreover, the gain measurement depends on the angle where the maximum radiation occurs [105, 106]. The gain can be calculated as [105]

$$Gain = 4\pi \frac{F(\theta, \Phi)}{P_{in}}, \quad (3.10)$$

where the input power is P_{in}

Long-wire radiation pattern: The electrical field model radiation for an electrical cable of the long electrical antenna depends on two distinct modes, viz. radiated and coupled modes. The radiation is made up of slots where each acts as a magnetic dipole antenna. The slots radiate as a result of the interruption from the currents lines that run along the outer conductor of the coaxial cable.

The fundamental electromagnetic radiation principle depends on the basic relation between current and charges as explained in [107, 108] and shown in Eq. 3.11. The movement of charges in a time-motion results in the creation of a current which activates the radiation. The cross-sectional area of a circular conducting wire in which electrical charges and current are uniformly distributed in terms of the wire area, A , and volume, V , is demonstrated in [109] and shown in Fig. 3.2. The current density J_z (A/m^2) cross-

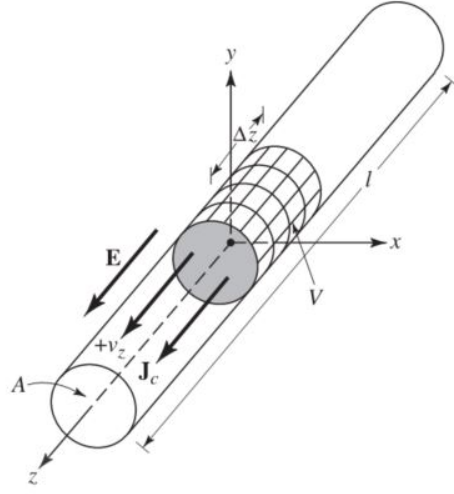


Figure 3.2: Charge uniformly distributed in a circular cross section cylinder wire.



Figure 3.3: Coaxial cable simulation model

section of the wires depends on the uniform velocity and electric volume charge density. v_z (m/s) and q_v (C/m^3) respectively is given by [110] as

$$J_z = q_v v_z. \quad (3.11)$$

The total current Q is inducted on the outer conductor which radiates in the cable. $x, y, \text{ and } z$ are the directions of the radiating field, which operate at half wavelength of a long electrical cable, and act as an antenna over a distance. The power-line simulation software used for the analysis was a long cable wire which functioned as an antenna at high frequency. The frequency and power selected were 2.45 GHz and 5 watts respectively. This helped to indicate a minimal EME/EMF around the cable, as shown in Fig. 3.3. A power cable will have a different EME/EMF emittance, depending on the cable isolation, length and cable type. However, the cable used in this work was non-energised. The characteristics of non-energised cables are mentioned in [86].

A RG-58 coaxial cable was used for the analysis. Based on the characteristics of a RG-58 coaxial cable, it can be assumed to have the same EME/EMF emittance. The radiation in the power cable at high frequency depends on the power and cable distance as shown in Fig. 3.3. As was expected, the simulation result radiated through the cable according to EMF. As the frequency increased, the distance and power were reduced as explained in [86]. Although this matter falls outside the scope of this study, it can be said that further experimentation is needed to establish a perfect finding. The results obtained are preliminary which will be justify in the future work.

The radiation E-field strength of a long-wire antenna in the directional function is given by

$$E_{E-Field} = \frac{\sqrt{30 * P_T * G_T}}{d}, \quad (3.12)$$

where E is the radiation $E_{E-Field}$, the strength, P_T and G_T are transmission power and total gain respectively. The distance d , is the link from the source to the receiver. At higher frequency, the transmission line of a long-wire cable acts as an antenna and the antenna gain is part of radiation lobe as described in [1].

The radiation pattern of a long-wire antenna produces two different lobes viz. the symmetrical and unsymmetrical lobes. In the symmetrical lobe system, the radiation pattern of a long-wire antenna depends on the frequency. A standing-wave antenna depicted in Fig. 3.4 gives a good example of a symmetrical lobe, producing radiation at the center of a long-wire antenna. Alternatively, the unsymmetrical lobes produce more lobes in the current flow direction, and fewer lobes in the opposite direction.

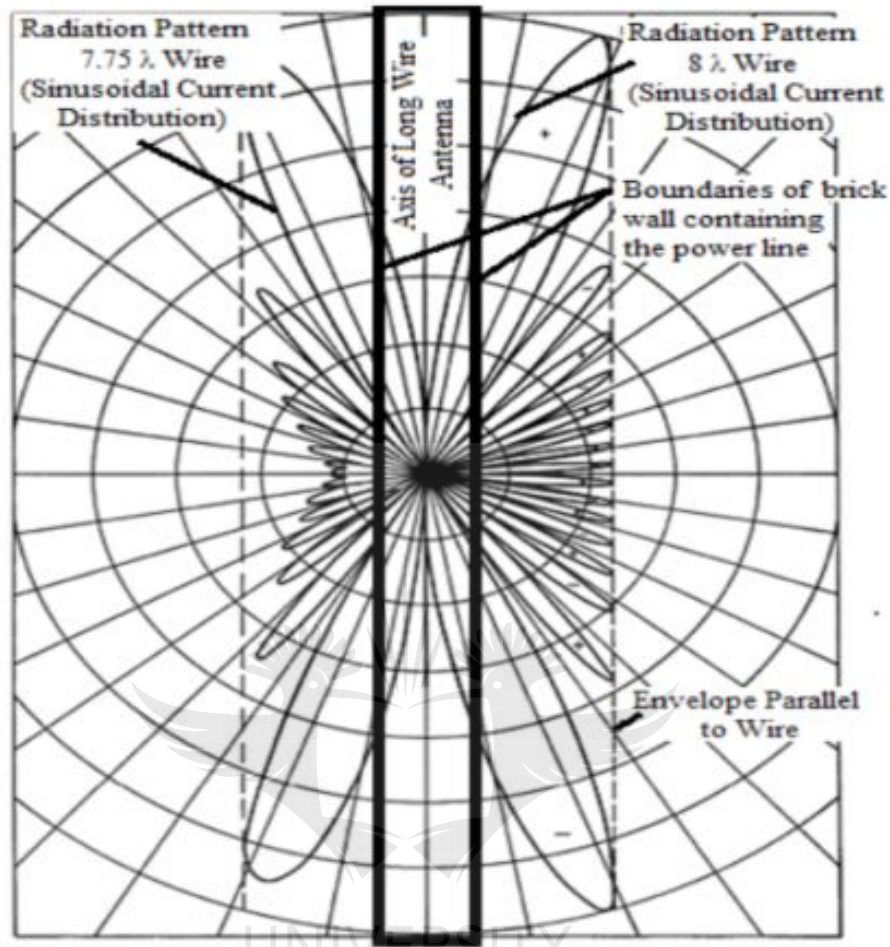


Figure 3.4: Radiation pattern for long wire antenna as a function of frequency [1].

3.6 Diversity technique

Diversity, which leads to better link performance, has been used as a very powerful tool to combat fading in wireless communication systems. Diversity techniques are used in the fading channel to improve the performance of a system by reducing the depth and duration of the fading signal from the receiver. The principle underlying diversity is the reception of the signal on two or more independent, and hence uncorrelated, branches, and then combining the output in some optimum manner so that various branch signals (channels) are significantly uncorrelated. The idea is that at any given point, the receiving antenna will receive a strong signal from one or both channels. In this method, the same signal is transmitted over two different channels at the same frequency and time.

The RF channel is affected by indoor RF obstacles, and likewise the PLC is affected by PLC noise and various physical phenomena. The target is to develop a channel that will help to produce the best channel with the strongest signal at any point in time. Diversity techniques can also be used to overcome noise issues, for example impulse noise as a result of multipath effects. Diversity can be classified in various ways such as frequency, space, time, and polarisation diversity. This study is intended to propose the application of the diversity concept to approach the indoor channel fading by examining the channel reception performance in terms of time and frequency diversity. At the communication channel receiver, coupler diversity is introduced. This will help to combine the coupling outlet to one terminal in time and frequency domain.

3.6.1 Frequency diversity

Frequency diversity can be achieved by using two antennas transmitting simultaneously with different carrier frequencies in a frequency domain, with the assumption that fading will be independent. The process is described in [111]. Coherence bandwidth separates a carrier from others. The only problem with frequency diversity is that it requires large bandwidth, which normally slows down the systems performance. It requires one antenna only, and the total transmitted power is shared among the carriers.

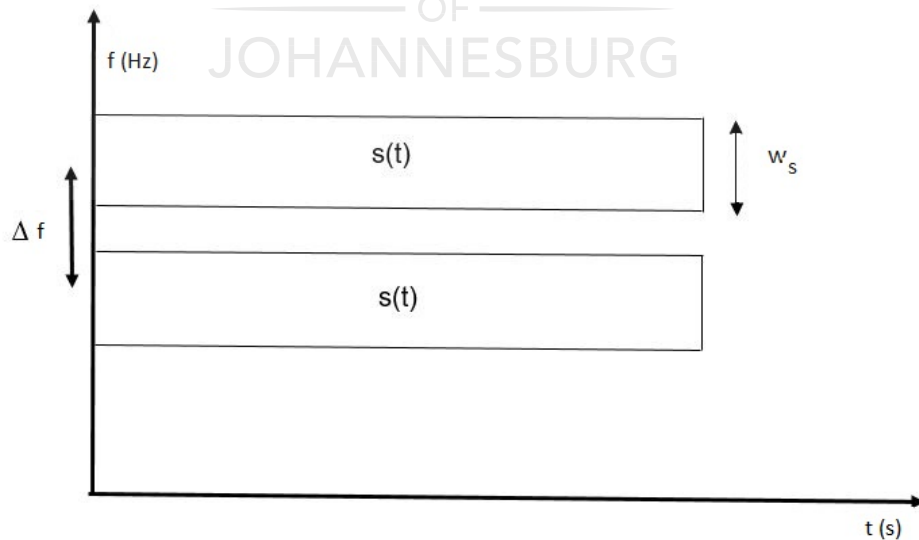


Figure 3.5: Frequency diversity

3.6.2 Time diversity

Time diversity can be achieved by transmitting the signal with the same information more than once at different time intervals and in a way that each signal symbol will be transmitted M times. The interval between symbol transmissions of the same signal is referred to as coherence time. It becomes an issue once the time interval for a time slot exceeds the coherence time. However, the challenge with time diversity is that it requires extra transmission time.

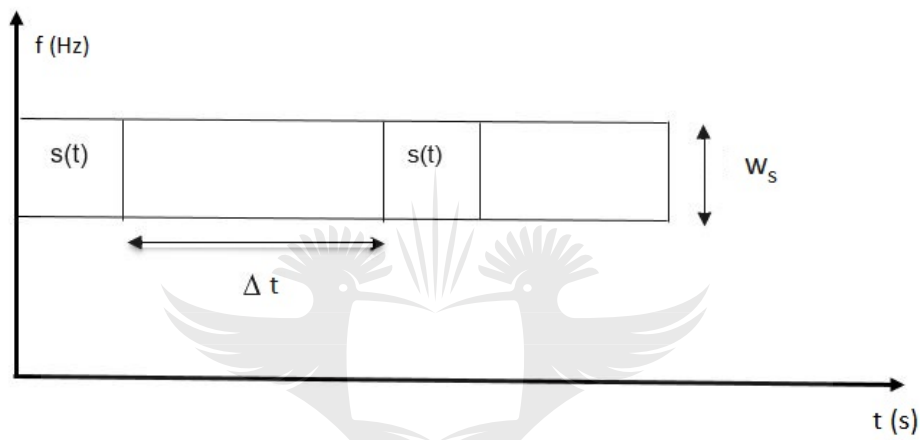


Figure 3.6: Time diversity

3.6.3 Space diversity

Space diversity differs somewhat from frequency diversity and time diversity as regards bandwidth usage and transmission time. It can be obtained by using two or more antennas from the transmitting side and using two or more antennas to receive the signal at the receiver side. The aim is to improve the quality and reliability of the link. The antennas are separated from each other and are placed several wavelengths apart, with a minimum spacing being 0.5 wavelength. The spacing should be adequate to provide spatial decorrelation between the receiving antennas. On the receiving signal side, received signals are combined by means of different combining methods to achieve the best SNR.

The two main types of spatial diversity are macroscopic and microscopic diversity. Macroscopic diversity prevents large-scale fading and it is a log-normally distributed sig-

nal. Shadowing is the major cause of large-scale fading in wireless communication situations because of major variations between transmitter and receiver resulting from the terrain profile and the nature of the surrounding environment. Macroscopic diversity prevents small-scale fading which is caused by multiple reflections from either transmitting or receiving antennas. This can be avoided by choosing an antenna with a strong signal that mitigates the small-signal fading effect.

3.7 Combining techniques

3.7.1 Selection diversity

Selection diversity proves to be the simplest technique when compared with the other techniques. The diversity branch with the strongest signal level should be selected for signal transmission which have already described in [112]. However, the principle behind SC is to select the best signal in terms of its signal strength at any point in time from the transmitted signals. In a situation where there is signal obstruction due to the fading environment, a strong signal can still be achieved. Moreover, SC is mostly used in the area of wireless communication because of its simplicity when compared with other diversity techniques. Since the selection method depends on the SNR performance, it is difficult to measure SNR in a short period of time. However, selection is done by selecting the branch that has the largest received signal with the same average noise power on each branch, as shown in Fig. 3.7. A typical example of SNR improvement with selection combining is

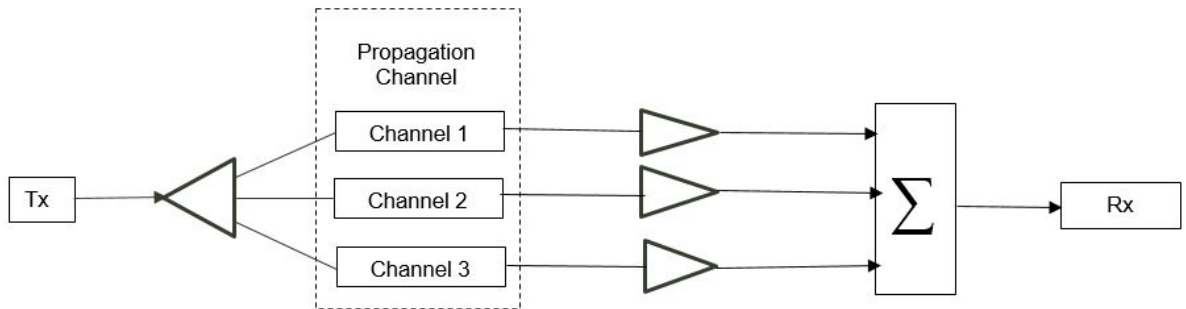


Figure 3.7: Selection combining

shown in (see Fig. 3.8) which was presented in [113]. For, (see Fig. 3.8), it clearly showed

that the SNR performance depends on the number of antennas being used, the more the number of antennas, the better the SNR performance. The selection combining output is

$$y(t) = A_i e^{j\theta_i} s(t) + z_i(t), \quad (3.13)$$

where $A = \max(A_0, A_1, \dots, A_{N-1})$, the received SNR for selection combining is given by

$$\begin{aligned} \gamma &= \frac{A^2 E_b}{N_0} \\ &= \max(\gamma_0, \gamma_1, \dots, \gamma_{N-1}). \end{aligned} \quad (3.14)$$

The CDF equation for independent and identically distributed branch with uncorrelated branches is give by

$$P_\gamma(\gamma) = N_r P_{\gamma_0}(\gamma) [P_{\gamma_0}(\gamma)]^{N-1}, \quad (3.15)$$

where $P_\gamma(\gamma)$ is the CDF and N_r is the number of branches.

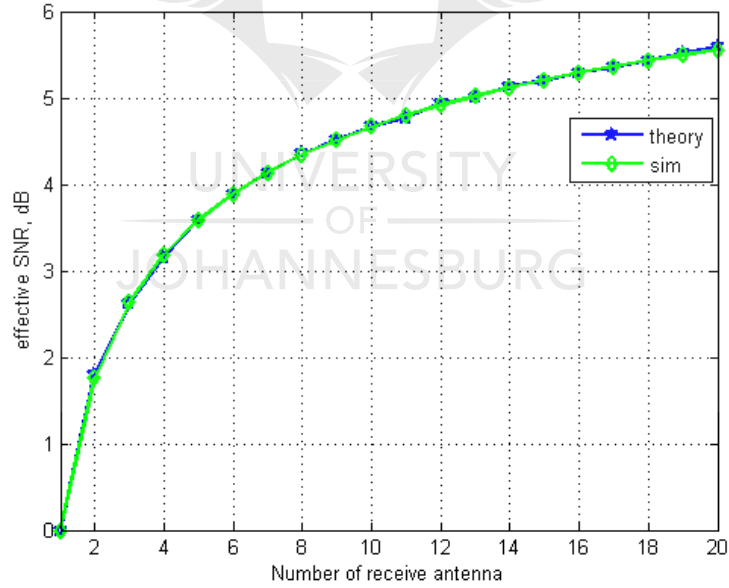


Figure 3.8: SNR improvement with selection combining.

Outage probability for selection combining: The probability of BER depends on the probability of failure for the i^{th} on the receiving antenna [114]. The PDF of the instan-

taneous SNR, in which the ratio of bit energy to noise drops in exponential distribution format, for chi-square with two degrees of freedom is given by

$$f_{\gamma}(\gamma_i) = \frac{1}{\gamma_{av}} \exp\left\{-\frac{\gamma_i}{\gamma_{av}}\right\}. \quad (3.16)$$

The associated CDF is given by

$$\begin{aligned} P_{out, \gamma_1} &= P_r[\gamma_1 < \gamma] = \int_0^{\gamma} f_{\gamma}(\gamma_i) d\gamma_i \\ &= 1 - \exp\left\{-\frac{\gamma}{\gamma_{av}}\right\}, \gamma_{av} \\ &= \frac{E_b}{N_0}, \end{aligned} \quad (3.17)$$

where γ is the threshold for the ratio of bit energy to noise. The total probability for the instantaneous SNR is the product of individual probability which is the actual PDF and is given by

$$\begin{aligned} f_{\gamma}(\gamma_{SC}) &= P_{out}(\gamma_i < \gamma_{SC}, i = \dots, N) \\ &= \prod_{i=0}^N P(\gamma_i < \gamma_{SC}) \\ &= \left(1 - \exp\left\{-\frac{\gamma_{SC}}{\gamma_{av}}\right\}\right)^N, \gamma_{SC} \geq 0. \end{aligned} \quad (3.18)$$

The PDF is derive from the CDF and is calculate as

$$\begin{aligned} f_{\gamma}(\gamma_{SC}) &= \frac{dP_{out}(\gamma_{SC})}{d\gamma_{SC}} \\ &= \frac{N}{\gamma_{SC}} \exp\left\{-\frac{\gamma_{SC}}{\gamma_{av}}\right\} \left[1 - \exp\left\{-\frac{\gamma_{SC}}{\gamma_{av}}\right\}\right]^{N-1}. \end{aligned} \quad (3.19)$$

Bit Error Rate for selection combining: The calculation of BER with AWGN for BPSK [115, 116] is given by:

$$P_e = \frac{1}{2} \operatorname{erfc} \sqrt{\frac{E_b}{N_0}}. \quad (3.20)$$

The total BER for all possible values of SNR is the integral of conditional BER and is given by:

$$\begin{aligned}
 P_e &= \int_0^\gamma \frac{1}{2} \text{erfc}(\sqrt{\gamma_{av}}) P\gamma d\gamma \\
 &= \int_0^\gamma \frac{1}{2} \text{erfc}(\sqrt{\gamma_{av}}) \frac{N}{\gamma_{SC}} \exp\left\{-\frac{\gamma_{SC}}{\gamma_{av}}\right\} \left[1 - \exp\left\{-\frac{\gamma_{SC}}{\gamma_{av}}\right\}\right]^{N-1} d\gamma.
 \end{aligned} \tag{3.21}$$

3.7.2 Maximum ratio combining

Among all the combining techniques, maximum ratio combining (MRC) is the most complex. It uses a coherent technique in which all branches are optimally combined at the receiver. The co-phased and weighted factors for MRC on SNR scaling is discussed in [112, 117]. The most ideal form of diversity combining, which requires a complex design at the receiver circuit to adjust gain in every branch, is the MRC. This is demonstrated in Fig. 3.9, where the individual receiver signal of each branch is weighted according to its voltage to noise power ratio. The best performance of SNR can be achieved by the sum of the individual SNRs. One of the interesting part of MRC is that it may accept the

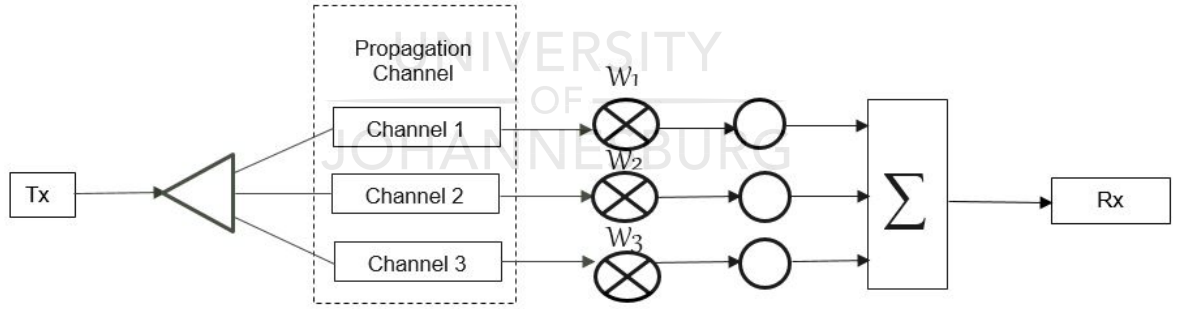


Figure 3.9: Weight branches for maximum ratio combining.

output even if the input was unacceptable, although it requires proper tracking of complex fading, which in practice, is difficult to achieve. Some work has already shown that the SNR can be improved by using maximum ratio combining [113]. Various antennas are used to achieve the improvement of the SNR up to 10 dB, as shown in Fig. 3.10 [113]. The SNR performance for MRC can be slight when compared with that of equal gain combining (EGC) [112], but the difference is that MRC uses co-phased. In MRC, each branch weights have equal magnitude which is used to analyse the received signals from

the source, however, the process gives more details analyses of the received signals. This results in MRC being able to produce acceptable output signals from different unacceptable inputs. MRC still performs better in terms of SNR improvement, followed by EGC which is better than SC [113]. The linear combiner output for MRC is expressed by

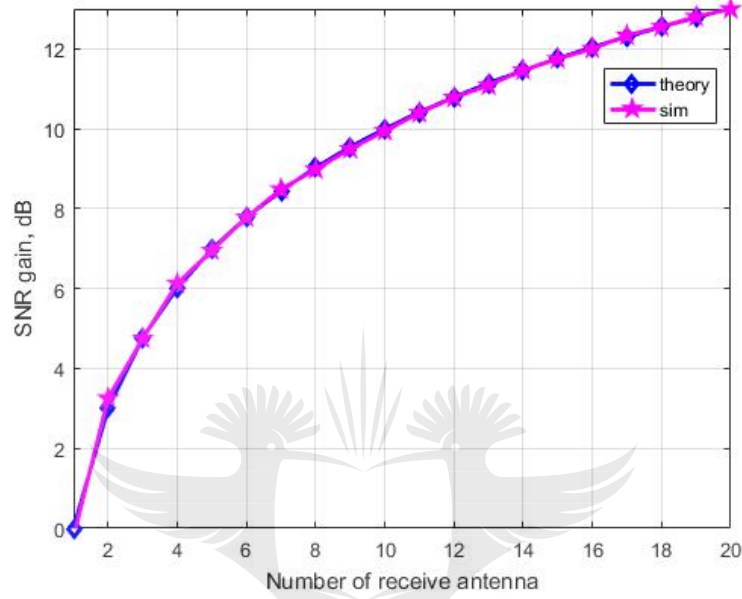


Figure 3.10: SNR improvement with maximum ratio combining.

$$Y(t) = \sum_{i=1}^{N=1} W_i r_t(t). \quad (3.22)$$

The instantaneous signal and noise power of the combined signal is

$$\begin{aligned} \gamma_{MRC}(\Gamma) &= \frac{\sum_{i=1}^{N=1} A_i^2 E_b}{N_0} \\ &= \sum_{i=1}^{N=1} \Gamma_i \cdot \gamma_i. \end{aligned} \quad (3.23)$$

The probability distribution of the SNR at the combiner output, taking into account

the chi-square distribution with two degrees of freedom, is given by [111, 118]

$$f_{\Gamma} = \frac{1}{(N-1)!} \exp\left\{-\frac{\gamma_{MRC}^{N-1}}{\gamma_{av}^N}\right\} \exp\left\{-\frac{\gamma_{MRC}}{\gamma_{av}}\right\}. \quad (3.24)$$

Outage Probability for MRC: A failure due to partially packet lost in transmission of an SNR that will result in a small packet detection is known as outage. In a channel with Rayleigh fading, the outage probability can be obtained from the CDF. This is given in [114] as

$$\begin{aligned} P_r(\gamma_{MRC} < \gamma) &= \int_0^{\gamma} f_{\Gamma}(\gamma_{MRC}) d\gamma_{MRC} \\ &= 1 - \int_0^{\gamma} f_{\Gamma}(\gamma_{MRC}) d\gamma_{MRC} \\ &= 1 - \exp\left\{-\frac{\gamma_{MRC}}{\gamma_{av}}\right\} \sum_{i=1}^{N-1} \frac{(\gamma_{MRC}/\gamma_{av})^{i-1}}{(i-1)!} \end{aligned} \quad (3.25)$$

Bit Error rate for MRC: The Rayleigh distribution of a random variable channel can be related to the chi square variable in a mathematical expression. The square root of the random variable channel of Rayleigh distribution is equivalent to the chi square variable with two degrees of freedom. The PDF of SNR of the Rayleigh distribution is given by

$$P\gamma_i = \frac{1}{\gamma_{av}} \exp\left\{-\frac{\gamma_i}{\gamma_{av}}\right\}. \quad (3.26)$$

The PDF of chi-square random variable with 2N degrees of freedom is given by:

$$P\gamma_i = \frac{1}{(N-1)! (\gamma_{av})^N} \gamma^{N-1} \exp\left\{-\frac{\gamma_i}{\gamma_{av}}\right\}, \gamma_i \geq 0. \quad (3.27)$$

The calculation of BER with AWGN for BPSK [8] is given by

$$P_e = \frac{1}{2} \operatorname{erfc} \sqrt{\frac{E_b}{N_0}}. \quad (3.28)$$

For all possible value of SNR, the total BER is integral of conditional BER and its

given by

$$\begin{aligned}
 P_e &= \int_0^\gamma \frac{1}{2} \text{erfc}(\sqrt{\gamma_{av}}) P \gamma d\gamma \\
 &= \int_0^\gamma \frac{1}{2} \text{erfc}(\sqrt{\gamma_{av}}) \frac{1}{(N-1)! (\gamma_{av})^N} \gamma^{N-1} \exp\left\{-\frac{\gamma_i}{\gamma_{av}}\right\} d\gamma.
 \end{aligned} \tag{3.29}$$

3.7.3 Equal gain combining

Equal gain combining is a relatively complex technique that requires co-phasing. The slight different between EGC and MRC is that MRC offer different levels of complexity while EGC is simpler to implement. The individual branch signals in EGC are normally dependent on each other and will enhance the performance. EGC is the same as MRC, the only measure that is different being the weighting circuit which EGC lacks. EGC uses co-phasing to combine the high quality receiving signals, interference and noise as described in [119]. The signal improvement in EGC is slightly lower when compared with MRC.

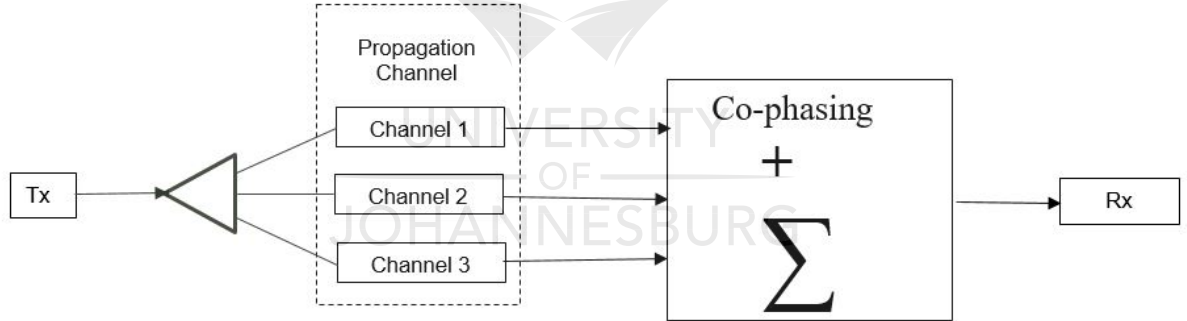


Figure 3.11: Weight branches for equal gain combining.

Figure 3.11 shows the individual signal branch of the coherent and non-coherent noises. It combined using co-phasing and the summation of simple phase circuit. Equal gain combining uses simple phase summing for simplicity. For each branch weighted with the same factor, there is no need for signal amplitude or channel amplitude to gain an accurate estimate [120]. However, there is a need for the signal cancellation for co-phasing of all the signals. This is described in [120].

Other diversity techniques commonly used in wireless communication are mentioned

in [27, 120–124]. For simplicity purposes, SC and MRC will be used as a combine technique for the signal reception in this study.

The linear combiner output of EGC is expressed by

$$y(t) = \sum_{i=1}^N e^{-j\theta_i} r_t(t). \quad (3.30)$$

The instantaneous signal and noise power of the combined signal is

$$\gamma_{EGC}\Gamma = \left[\sum_{i=1}^{N-1} A_i \right]^2 \gamma_{av} N. \quad (3.31)$$

Equal gain combining Eb/No As discussed in [125], the ratio of bit energy to noise at the receiving antenna in terms of its channel is given as

$$\begin{aligned} \gamma_i &= \frac{|h_1|^2 E_b}{N_0}, \gamma_{av} \\ &= E_b / N_0. \end{aligned} \quad (3.32)$$

The calculation of BER with AWGN for BPSK of EGC is described in [125–127]. The EGC technique for two branches of all possible values of SNR per bit is described in [128, 129] and the equation is given by:

$$\begin{aligned} P_e &= \frac{\exp\left\{-\frac{2\gamma_i}{\gamma_{av}}\right\}}{\gamma_{av}} + (\sqrt{\pi})\exp\left\{-\frac{2\gamma_i}{\gamma_{av}}\right\} \\ &= \left[\frac{1}{\sqrt{4\gamma\gamma_{av}}} - \frac{1}{\gamma_{av}} \sqrt{\frac{\gamma}{\gamma_{av}}} \right] \\ &= \left[1 + 2Q\left[\sqrt{\frac{2\gamma}{\gamma_{av}}}\right] \right], \end{aligned} \quad (3.33)$$

where $Q(\cdot)$ is error the function [130, 131].

3.8 Summary

In this chapter, the discussion covered different techniques and tools used to model the hybrid PLC-RF channel receive. The demand for accuracy and long-wire antennas, as well as transmission-line parameters were also presented. Various diversity technique approaches were studied, and their complexities examined. Finally, different combination techniques and their applications received attention.



4

Contactless PLC: Channel Analysis

The demand for broadband has advanced substantially over the past decade, and it has become one of the best ways of achieving high data rate wireless communication. The restrained coverage provided by existing wireless hotspots indicates that there is a need for implementing a low-power system by other technological approaches. Such a system will help to provide the continuous connectivity technology that will be required in future.

This chapter focuses on the performance analysis of the frequency response of both the PLC and RF channels at 2.45 GHz in an attempt to overcome obstructions that WiFi has difficulty penetrating due to LOS issues. These channels denote the concatenation of the PLC and RF channels. In the discussion that follows, PLC and RF technology, with a detection system motivated by the mobility of the end user, is first provided, followed by an analysis of such a system, and then a proposal for its frequency response. Finally, the channel frequency response and its performance are proposed for both channels. Results emerging from the proposed channel model will be discussed.

4.1 Introduction

Immobility is one of the most serious barriers among others, that slows down the mass implementation of PLC technology. This is due to the facts that end nodes are physically connected to the power wires. To solve this dilemma, solutions have been proposed, which allow the end user to be connected to the PLC channel via a secondary communication technology, which allows the node to be mobile and physically separated from the dangerous power network. This solution restricts the end user to be in the same room or to absolutely be located under the beam of the VLC transmitter, which, still, reduces the end user mobility. A more flexible solution, which could considerably impact on the communication industry, is the use of an RF antenna [71–75], which will detect the radiation signal provided by the power wire and converts it into an electrical signal. This signal will be detected definitely by the PLC receiver.

The second solution, which exploits the unwanted electromagnetic radiation, is fundamentally based on the use of the power wires as a RF antenna. The effectiveness of a contactless PLC system is influenced by the transmission frequency range and faces many signal attenuations due to channel parameters. Such systems are introduced in [86, 87], where the PLC end user is contactlessly connected to the PLC channel in such a way that a transmission link is established at frequencies between 150 kHz and 30 MHz as explained in [87], and at 2.5 GHz in [86]. In both articles ([87] and [86]), data transfer was made possible between two computers, one directly connected to the main (original PLC network) via a coupling circuit, and the other connected via a loop antenna to another PLC network totally isolated from the first network.

In this new version of the research involving the contact-less PLC reported in ([87] and [86]) further insight into contactless PLC is provided. The proposed communication system and various portions of the channel are analysed, taking into account the two main PLC frequency bands, viz. the narrow-band PLC (NBPLC) and broad-band PLC (BBPLC). First, the communication channel, which is PLC-RF, is defined, then its frequency response receives attention and a proposal for a channel model is given. Second, the transmission medium on the PLC side is analysed and thereafter, the transmission capability of the types of wire used is analysed. Third, the system is implemented in practice, and the radiated signal strength, the feasible data rate and BER are measured. With the help of RF radiation characteristics, long-wire antennas act as transmission lines and as traveling-wave antennas for signal propagation. The radiation in the transmission

can be energised (with a load on the long-wire) or non-energised (without a load on the long-wire). This process of non-energised can be referred to as a control contactless power-line cable. Here use is made of radiated electromagnetic interference (EMI) generated by power-line cables as presented by Ferreira et al. in [132]. The result of the EMI which is used for contactless transfer is presented in [86, 87]. In these channels a 50 m cable with three wires at 1mm diameter was used. The connection of the link is from the transmitter to the receiver through the power grid in an existing power-line network on the same floor of an indoor environment. The application of an existing power-line network in an indoor environment for signal communication transmitter and the receiver on the same floor is explained in [133, 134]. In this chapter, control contactless is proposed, which means that the power cable was not energised. The control contactless wire consists of the wires; live, neutral and earth. The live and neutral are connectors, while the earth is floating at both side because there is no connection on it. The connection of the earth was not considered in the experiment that's why it was disconnected to be floating. However, since the line and the neutral are in the same or different phases, there could be losses in the channel, thereby increasing the attenuation.

4.2 A model for a contactless PLC system

A model for a contactless PLC where RF technology is used to connect the end node is shown in Fig. 4.1. It includes the data source, a modulator, coupling circuit, a PLC channel, an RF channel characterised by their transfer functions \mathbf{H}_{plc} and \mathbf{H}_{rf} and a demodulator for transmitting the message to the data recipient. The channel consists of the two main components (\mathbf{H}_{plc} and \mathbf{H}_{rf}) and represents a pure cascaded system that may face reflections from each of its components.

4.2.1 Modulator-demodulator

The modulator and the demodulator are fundamental components of this PLC-RF system. The modulator is responsible for producing the signal to be transmitted according to the message from the data source. The demodulator recovers the message from the signal which is detected by the antenna over the channel. Both modulator and demodulator must be based on the same scheme with the same constellation size.

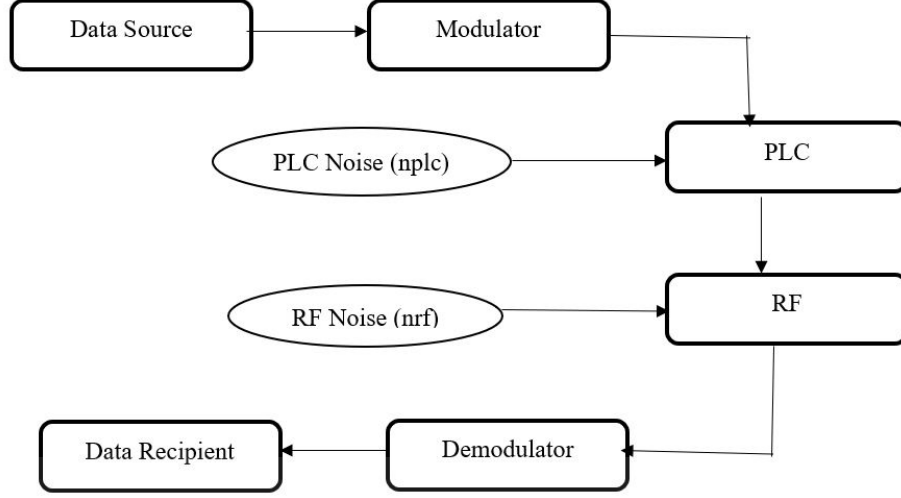


Figure 4.1: System model of the generalized cascaded PLC-RF.

4.2.2 PLC Channel and model

The PLC channel represents the main medium exploited in a contactless PLC system. It consists of wires and has a double-function, including carrying electrical energy and carrying over the communication signal. The PLC channel varies with time and frequency with regard to the multiple power activities occurring on the network. Its model in the time domain is given in [6, 38, 135] as

$$h_{plc}(t) = \sum_{i=0}^M I_i \delta(t - \tau_i) e^{j\tau_i}, \quad (4.1)$$

where M , I and τ are the number of taps, attenuation and echo delay respectively. The frequency domain expression for the PLC channel, which is in the Fourier transform format as discussed in [6, 38, 47, 135] and is given by

$$h_{plc}(f) = \sum_{i=1}^N g_i e^{-(a_0 + a_1 f^k) d_i} e^{-j2\pi f \frac{d_i}{v_p}}. \quad (4.2)$$

The model as given in equation (4.2) is the combination of three parameters (multi-path propagation, attenuation and frequency) that are normally present in the power-line network, where a_0 , a_1 and k are attenuation coefficients, g_i and d_i are the weighting factor



Figure 4.2: Model of the a contact-less PLC using RF to connect the end user.

and the path length respectively, and v_p is the propagation speed of light in the cable.

4.2.3 RF Channel and model

The RF channel uses air as communication medium, the medium of the main technology used to connect mobile nodes. It is characterised by its transfer function \mathbf{H}_{rf} . The model of the RF channel for the proposed experiment is the multipath channel and impulse response. It is given in [136, 137] as

$$H_{RF}(t, \tau) = \sum_{l=1}^L a_l(t) \delta(t - \tau_l(t)), \quad (4.3)$$

where a_l and τ are the complex gain of the l^{th} path and propagation delay for the l^{th} path respectively.

4.3 Analysis

The model proposed in Fig. 4.2 consists of two blocks in cascade. Here it is assumed that the radiated signal does not bounce back to the PLC channel. This is due to the weakness of the signal as discussed in [6, 138] and its given by

$$H(s) = H_{plc} H_{rf}. \quad (4.4)$$

In this study, two sets of attenuation versus distance were used as given in Tables 1 and 2. The attenuation values of Set 1 range from -0.038 to 0.029, while the values of

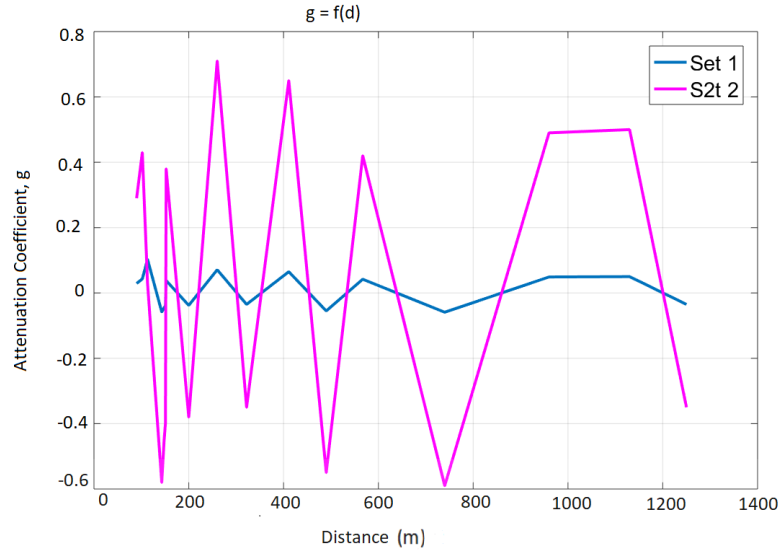


Figure 4.3: Attenuation vs distance for Set 1 and Set 2 above.

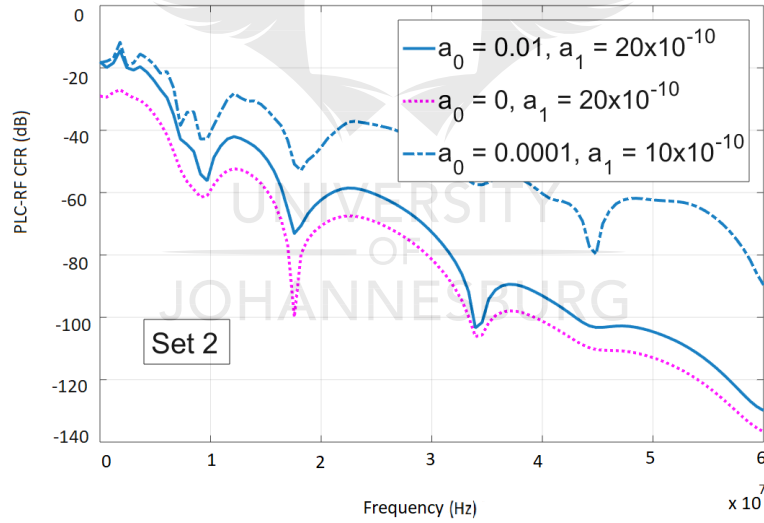


Figure 4.4: PLC channel for Set 2 characteristics for $a_0 = 0, 0.01$ and 0.0001 , and $a_1 = 20 \times 10^{-10}$, 20×10^{-10} and 10×10^{-10} .

Set 2 attenuation range from -0.38 to 0.29. The distance for Set 1 and Set 2 is the same. This is because the changes in the attenuation depend on the environment, and as the environment changes, the channel attenuation is affected. The distance remains constant. Fig. 4.3 shows how the attenuation coefficient, g , relates to the distance, d , for Set 1 and

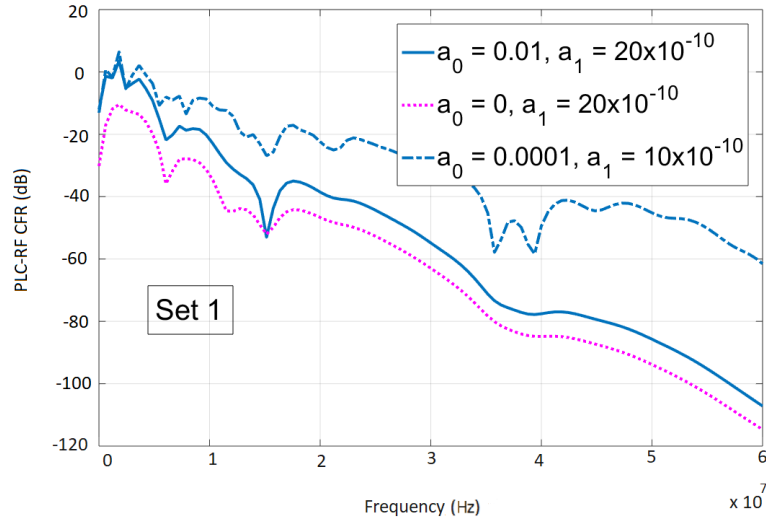


Figure 4.5: PLC channel based on Set 1 characteristics for $a_0 = 0, 0.01$ and 0.0001 , and $a_1 = 20 \times 10^{-10}, 20 \times 10^{-10}$ and 10×10^{-10} .

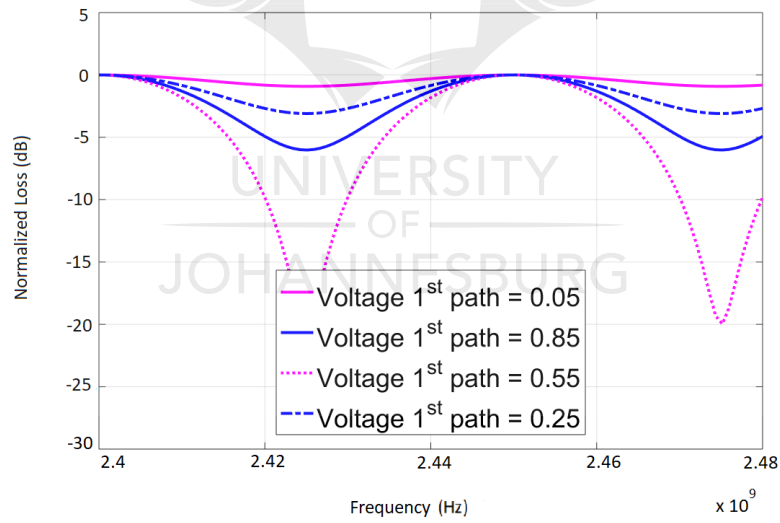


Figure 4.6: RF channels for voltage 1st path RF = 0.05, 0.25, 0.55 and 0.85.

Set 2 respectively.

Figures. 4.4 and 4.5 depict the PLC channel with Set 1 and Set 2 respectively. Each figure includes plot for various values of attenuation and distance for Set 1 and Set 2

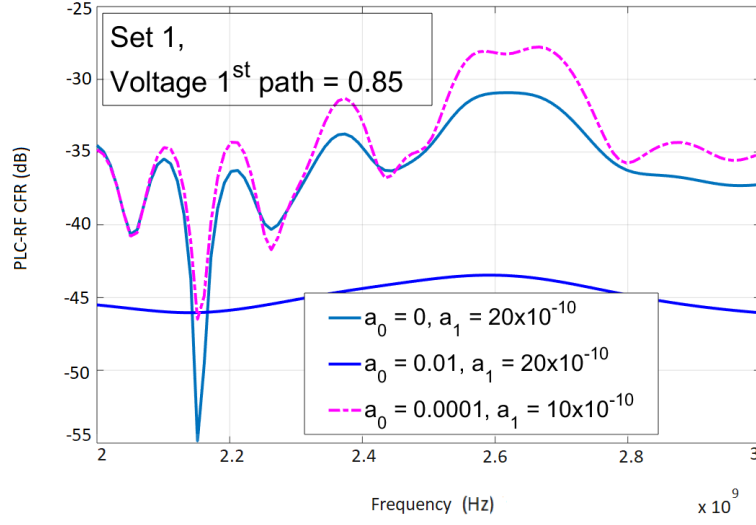


Figure 4.7: PLC-RF channel based on characteristics OF Set 1 for $a_0 = 0, 0.01$ and 0.0001 , and $a_1 = 20 \times 10^{-10}, 20 \times 10^{-10}$ and 10×10^{-10} .

TABLE 4.1: CABLE CHARACTERISTICS SET 1.

| | | | | | | | | | |
|-----------------------|--------|-------|--------|--------|--------|--------|-------|--------|-------|
| Attenuation factor(g) | 0.029 | 0.043 | 0.103 | -0.058 | -0.045 | -0.040 | 0.038 | -0.038 | 0.071 |
| Distance (d) | 90 | 102 | 113 | 143 | 148 | 150.8 | 152.3 | 200 | 260 |
| Attenuation factor(g) | -0.035 | 0.065 | -0.055 | 0.042 | -0.059 | 0.049 | 0.05 | -0.035 | 0 |
| Distance (d) | 322 | 411 | 490 | 567 | 740 | 960 | 1130 | 1250 | 0 |

TABLE 4.2: CABLE CHARACTERISTICS SET 2.

| | | | | | | | | | |
|-----------------------|-------|------|-------|-------|-------|-------|-------|-------|------|
| Attenuation factor(g) | 0.29 | 0.43 | 0.03 | -0.58 | -0.45 | -0.40 | 0.38 | -0.38 | 0.71 |
| Distance (d) | 90 | 102 | 113 | 143 | 148 | 150.8 | 152.3 | 200 | 260 |
| Attenuation factor(g) | -0.35 | 0.65 | -0.55 | 0.42 | -0.59 | 0.49 | 0.5 | -0.35 | 0 |
| Distance (d) | 322 | 411 | 490 | 567 | 740 | 960 | 1130 | 1250 | 0 |

respectively. The selected values of a_0 and a_1 are $0.01, 0, 0001$ and $20 \times 10^{-10}, 10 \times 10^{-10}$ respectively. Fig. 4.3 shows the RF channel frequency responses (CFR) with different values of voltage path, ranging from $0.05, 0.85, 0.55$ to 0.25 . Figs. 4.7, 4.8, 4.9 and 4.10 depict channel frequency response of the indoor wireless radiated RF channel; of the PLC channel exploited as backbone channel, and that of the cascaded system comprising PLC and RF. Figs. 4.7 and 4.8 show the relation between PLC-RF CFR versus the frequency for Set 1 and Set 2 respectively, where the RF radiation radius is fixed for

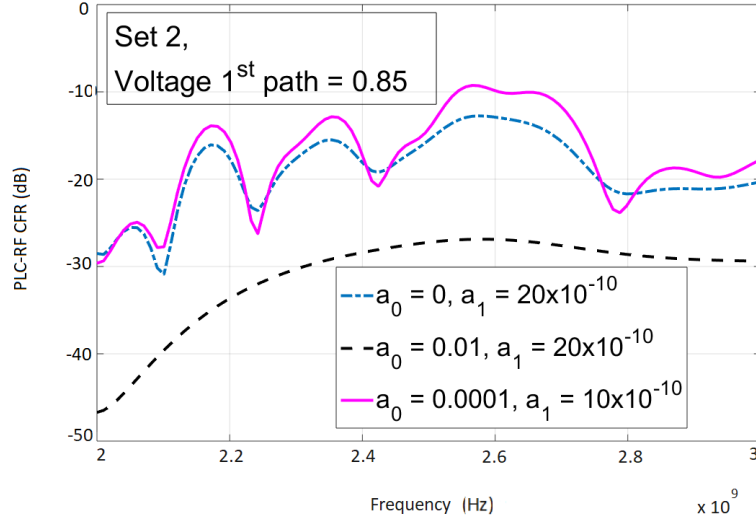


Figure 4.8: PLC-RF channel based on characteristics OF Set 2 for $a_0 = 0, 0.01$ and 0.0001 , and $a_1 = 20 \times 10^{-10}, 20 \times 10^{-10}$ and 10×10^{-10} .

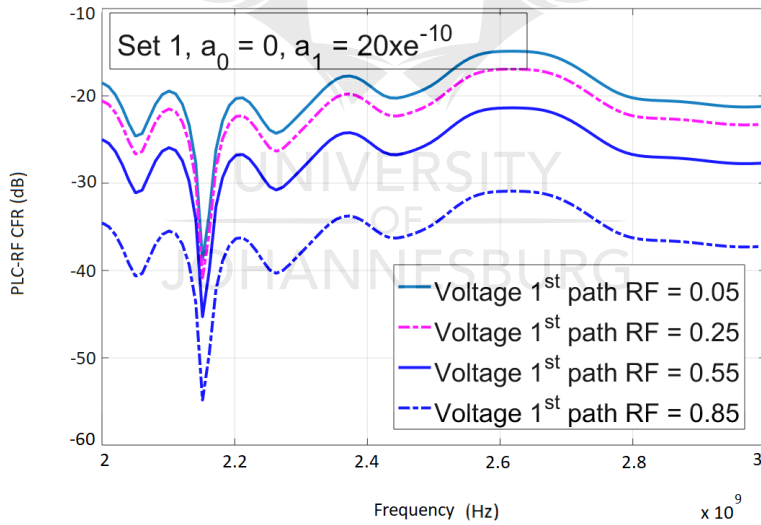


Figure 4.9: PLC-RF channel based on characteristics of Set 1 for voltage 1st path RF = 0.05, 0.25, 0.55 and 0.85.

voltage path at 0.85. The values of the coefficient for a_0 and a_1 of the PLC channel model were selected randomly and record the influence on the cascaded PLC-RF channel. These values respectively correspond to $a_0 = 0, 0.01$ and 0.0001 , and $a_1 = 20 \times 10^{-10}, 20 \times 10^{-10}$ and 10×10^{-10} over frequencies up to 3 GHz. The results show that the

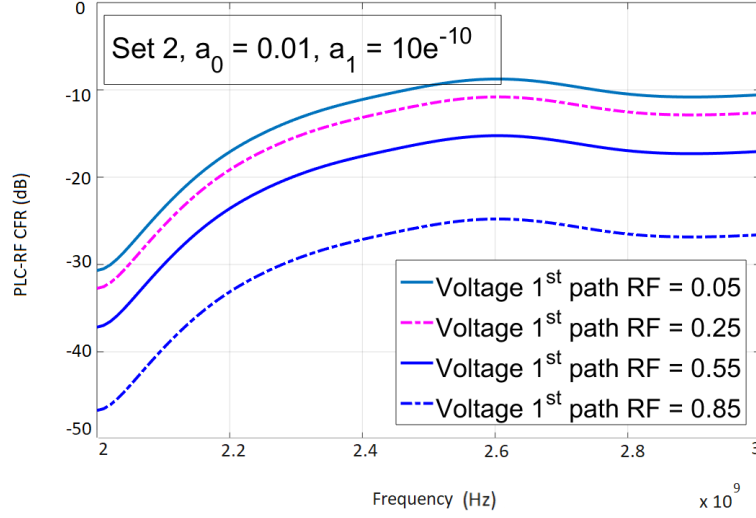


Figure 4.10: PLC-RF channel based on characteristics of Set 2 for voltage 1st path RF = 0.05, 0.25, 0.55 and 0.85.

selected values of a_0 and a_1 are characterised by notches that vary throughout the entire frequency band. It is clear that the RF channel is less attenuated than the transmitted message when compared to the PLC channel. However, the effect of the RF channel as regards to the PLC channel frequency response are observed. This is due to the multiple factors influencing the PLC channel, of which the most significant factor is low impedance of the PLC link. The increase in high value of a_0 for both Set 1 and Set 2 leads to the high values of PLC channel gain, and automatically to the hybrid PLC-RF channel gain.

Figures. 4.9 and 4.10 show the relation between PLC-RF CFR and frequency. The fixed values a_0 and a_1 are given as, $a_0 = (0 \text{ and } 0.01)$ and $a_1 = (20 \ 1010 \text{ and } 10 \ 1010)$, for Set 1 and Set 2 respectively. Various values of voltage path RF at 0.05, 0.25, 0.55 and 0.85 were selected randomly for the experiment. The PLC-RF channel was estimated, using different values of voltage path RF, which provides various results for the system behavior of channel frequency response. There is an increase in the number of PLC-RF taps in the network which also increase with the channel gain. Fig. 4.9 shows that the voltage path RF at 0.85 provides low resolution when compared to Figs. 4.8 and 4.10. The voltage path RF at 0.05 provides less frequency resolution and better precision. It can be seen that each one of the voltage path values has its own attenuation value and the same frequency values. However, the voltage path RF at 0.05 maintains high attenuation in comparison with other values.

4.4 Conclusion

In this chapter cascaded PLC-RF channels were investigated. The measurements of the proposed model and the frequency response of the channel were presented. An overview was given of both the PLC and the RF channels.

The three channels for the cascade system, together with the values of coefficient a_0 , a_1 and voltage 1st path Rf, were studied in an attempt to predict the behaviour of the system. The imposed coefficient of a_0 , a_1 and voltage 1st path RF for the PLC channel model influence the system performance and are recorded on the cascaded PLC-RF channel with t (see Figures. 4.3 to 4.10 above). The corresponding values of a_0 , = 0.01, 0, 0001, a_1 , = a_1 20×10^{-10} and 10×10^{-10} , and voltage 1st path Rf = 0.05, 0.25, 0.55 and 0.85, over frequencies of up to 3 GHz.



5

Contactless PLC: Preliminary Measurement

In this chapter important aspects of this research, viz. measurements to determine the performance of a contactless PLC signal strength and its comparison with that of a RF signal, are dealt with. The chapter is divided into two parts. The first part deals with measurement in an industrial setting (typical South African laboratory standard). Commercial WiFi modems are used for transferring data through a power line for 65m (non-energised) and 20m in a typical industrial energised situation. The signal speed for uploading files and downloading files through the PLC and RF channels in a cable were recorded. The measurement was done using different distances and locations.

The second part of the chapter presents the radiation of WiFi signal at 2.45 GHz over a distance. This is helpful in a situation where RF links LOS is obstructed by indoor equipment, making WiFi penetration difficult. The link performance between a pure 2.45 GHz link and contactless PLC link, which aims to use a power line as traveling-wave antenna to transmit 2.45 GHz radio signal, is discussed. Data throughput was measured in physical settings typical of multiple-storey buildings and with a real power network.

5.1 Introduction

There is a need to expand home Internet network services. The current internet network (usually WiFi) is facing the problem of signal degradation, which recently developed into an issue in communication technology. In addition to degradation, output signal strength is weak. In order to expand a network so that it can accommodate recent home network developments such as remote home sensors, PLC-RF is used. The combination of PLC and RF to resolve the issue of signal degradation in the home network will be a matter for the IoT in future. This will help to integrate services through a reliable and robust system in an Open System Interconnection (OSI). The introduction of the IoT and its comparison with computers and the Internet is one of the innovations in digital technology of the Third Industrial Revolution.

It is envisaged that with the IoT [71, 139] and the Smart Grid [140] connectivity between electrical products and systems will increase rapidly. Power-line communications aim to utilise electrical power cables to supply power and at the same time use as an electronic communication channel. This has several advantages when compared to the situation where power and communication between products and systems are supplied separately, a situation that leads to additional complexity and cost. Conventionally, PLC is used between two fixed systems such as two computers connected via a grid or a sensor connected to a controller [42]. This is in contrast with systems where a RF link supplies the means for communication. With RF link systems (such as WiFi), freedom of movement is ensured.

In this thesis a configuration that uses a power line as a traveling-wave antenna [130, 131, 141] for communications at 2.45 GHz (IEEE 802.11g protocol) is described. For this purpose, two commercial Wi-Fi modems were used to establish communication between two personal computers. One modem was coupled to the power line (fixed), while the other was used in RF mode (mobile) to connect to the line now acting as an antenna. This configuration can be very useful in situations where line of sight is obscured, and direct link RF communication is impaired, for example, inside buildings or between floors of buildings.

The contactless PLC described in this study is similar to previous work by de Beer et al. [87], but in this case, 2.45 GHz was used, which is a frequency far higher than 30 MHz. Although 2.45 GHz has been investigated before for PLC usage and was conceptually

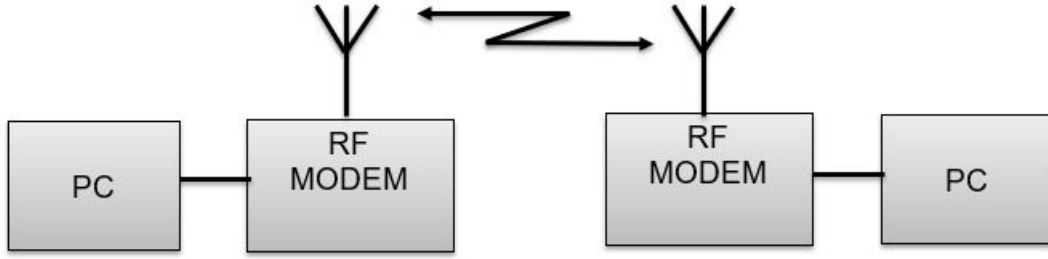


Figure 5.1: Set up for the direct RF-link.

proven in [88, 130, 131], this study gives actual transfer rate performance measurements in an industrial setting. In this study too, traveling-wave contactless PLC is compared to direct link RF communications. It is shown that at long distances, direct RF links perform better than contactless PLC, but at shorter distances (typically up to 40 m), contactless PLC is comparable in performance to the direct RF link.

In this Chapter, two experimental setups are described. One involves a typical industrial setting inside a building, and the other is a best-case free-standing power-line configuration. In both cases, experimental results are given for a direct RF link shown in Fig. 5.1, as opposed to a traveling-wave contactless PLC setup depicted in Fig. 5.2. Since the contactless PLC set-up needs a connection between the power line and RF modem, a coupling circuit was used. Although not a focus of this paper, some detail of the coupling circuit is given.

5.2 PART I: Setup of the laboratory experiment

Two configurations were used for the experiments conducted as part of this study, viz. the RF-link and the traveling-wave contactless PLC. Both configurations were applied in two different environmental settings; namely industrial building (offices in the industrial building was also considered) and open area that has corridor of approximately 60 m long (free-standing power-line configuration was also considered)

The 2.5 mm flat-twin earth cable used for the contactless PLC is the most common type used for indoor power distribution in South Africa. The cable consists of three conductors, viz. live, neutral and ground, but because the cable used in this experiment

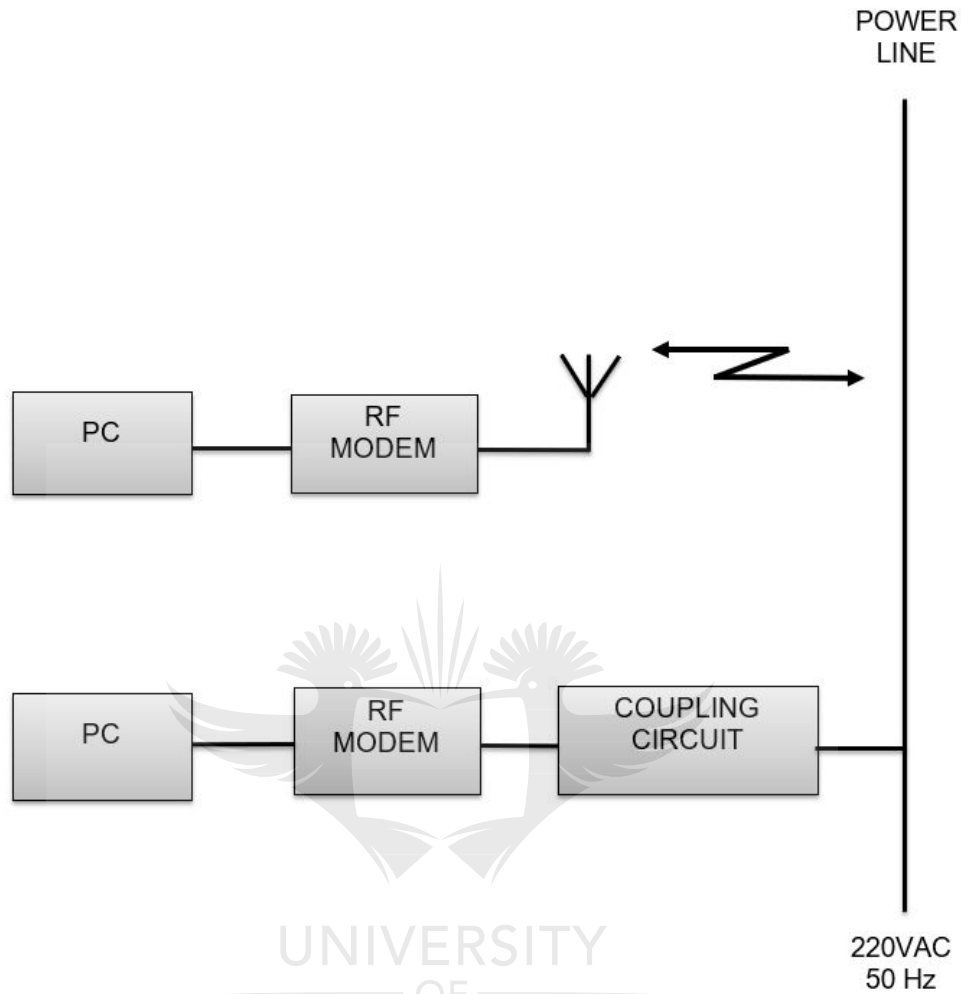


Figure 5.2: Set up for the traveling wave contactless PLC.

was not energised, the ground was not used.

5.2.1 The RF-Link

The RF-link consists of two identical systems, each comprising a personal computer and a commercial Wi-Fi RF modem as shown in Fig. 5.1. The modems were equipped with an antenna tuned at 2.45 GHz. A coupling circuit was used to couple the power-line network to the modem by means of a long-wire antenna. Since the experiments focus on RF transmission of the PLC contactless network, absolute measurements in the actual settings will be considered in the next chapter. The transmitting device Tx consists of

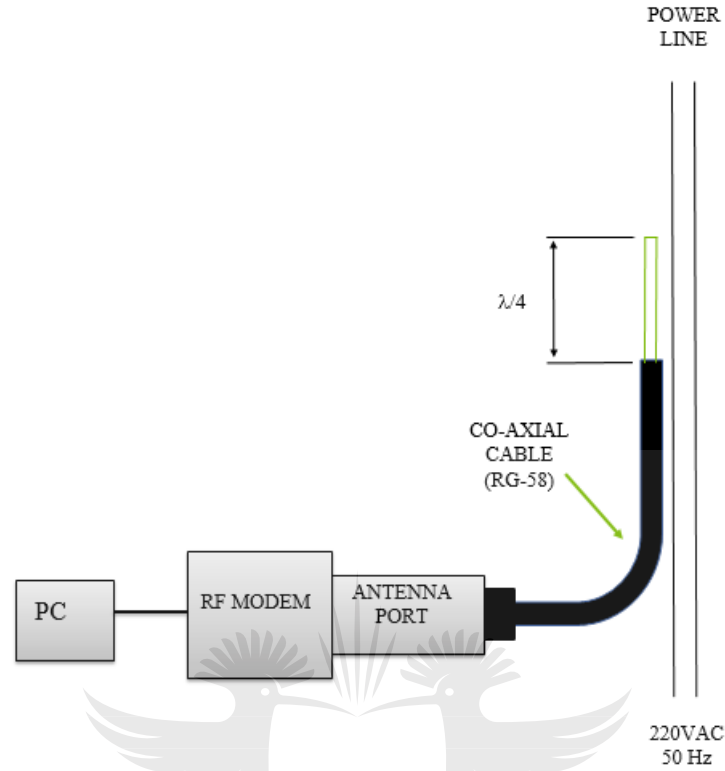


Figure 5.3: Detail of the coupling circuit for traveling wave contactless PLC.

a combination of one of the personal computers, LAN software installed on it and the coupler connecting the PLC. The receiving device Rx comprises a personal computer, LAN software installed on it and a RF modem with a dedicated antenna.

5.2.2 Traveling wave contactless PLC

The traveling-wave contactless PLC configuration is shown in Fig. 5.2. A free-standing personal computer and a RF modem with a dedicated antenna constitute the first and mobile part of the system. This is the same as one part of the RF-link configuration shown in Fig. 5.1. Of importance here is the distance between the modem antenna and the power line. For this study, a distance of 0.5 m was used between the power line and the modem antenna.

The second part of the traveling-wave contactless PLC configuration shown in Fig. 5.2 is a personal computer, modem and coupling circuit. Instead of an antenna, the RF port

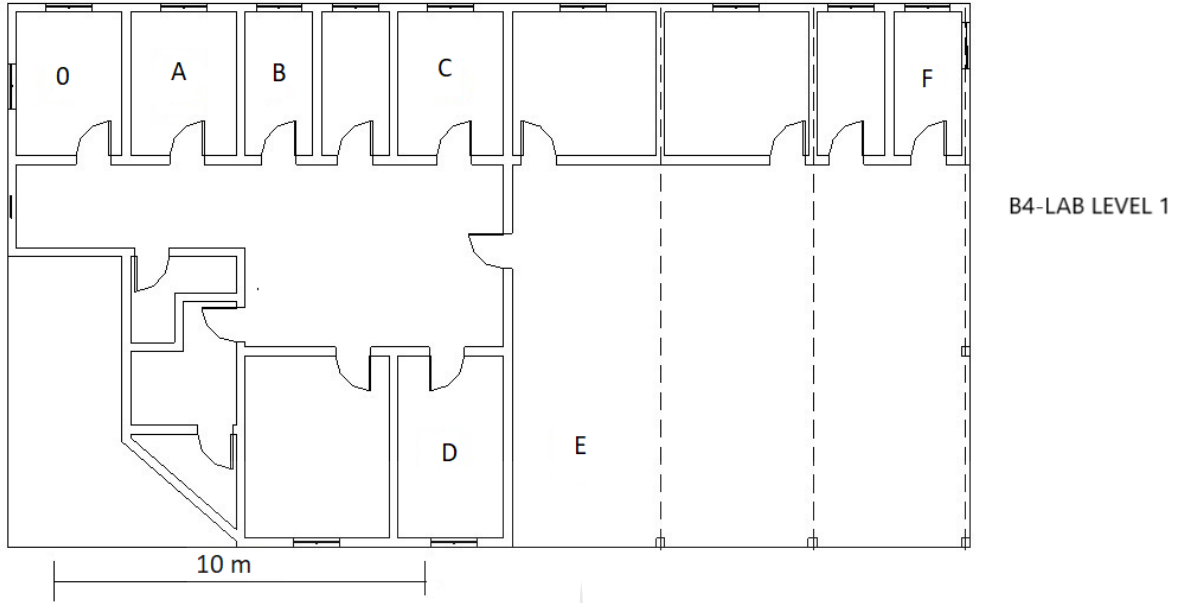


Figure 5.4: Top view of a building plan depicting positions for measurements of contactless cable and RF in an industrial setting

of the modem is connected via a coupling circuit to the power line. This part of the system is fixed.

Details of the coupling circuit are given in Fig. 5.3. Instead of a conventional coupling circuit that uses capacitors and transformers, a microwave configuration was used. This was done because capacitors and transformers have parasitic components, rendering them ineffective at 2.45 GHz. Capacitors, for example, have equivalent series inductance (ESL) effectively blocking microwave frequencies. Transformers, on the other hand, have interwinding capacitance, short-circuiting microwave frequencies, rendering the isolation properties of transformers ineffective.

The coupling circuit used was a stripped piece of RG-58 co-axial cable. The stripped section of the co-axial cable exposed a quarter of a wavelength of the inner conductor. The length of the quarter section was calculated to be

$$\frac{\lambda}{4} = \frac{1}{4} \frac{0.65 c}{2.45 \text{ GHz}} = 20 \text{ mm}, \quad (5.1)$$

where c the speed of light. The relative speed of propagation in an RG-58 coaxial cable was taken at 65 m. The exposed coaxial cable acts as a resonating quarter-wave antenna radiating maximum power onto the power line. Although this configuration might

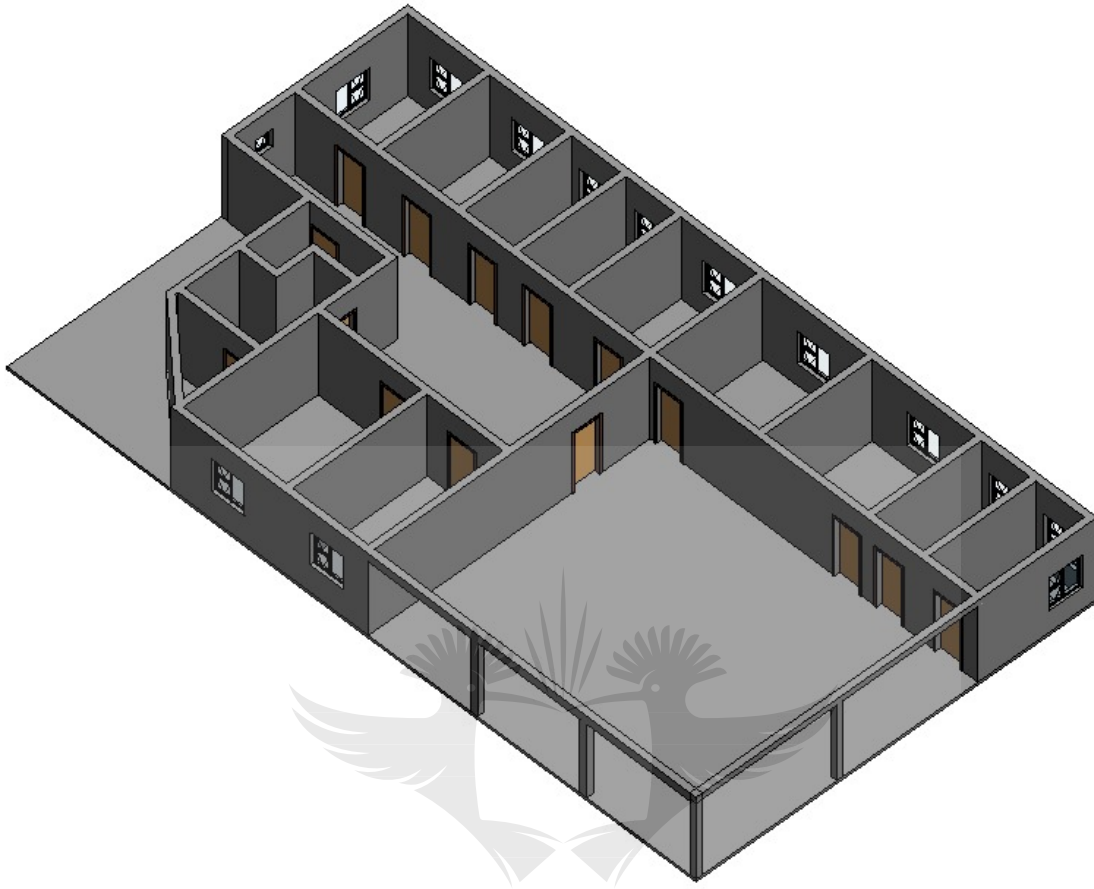


Figure 5.5: Isometric view of a building plan and positions for the measurements contactless cable and RF in an industrial setting

not be optimal, it yielded good results and can be investigated in future research.

5.2.3 Throughput measurement

In order to gauge the effectiveness of the communication link, the data transfer rate, or throughput, was measured between the two personal computers. LAN software was installed on each computer. The purpose of this software was to upload or download a file to or from a personal computer and to measure the transfer time. The time it took to transfer a file of random data was logged, and taking into account the file size, a throughput rate in Mbps was calculated.

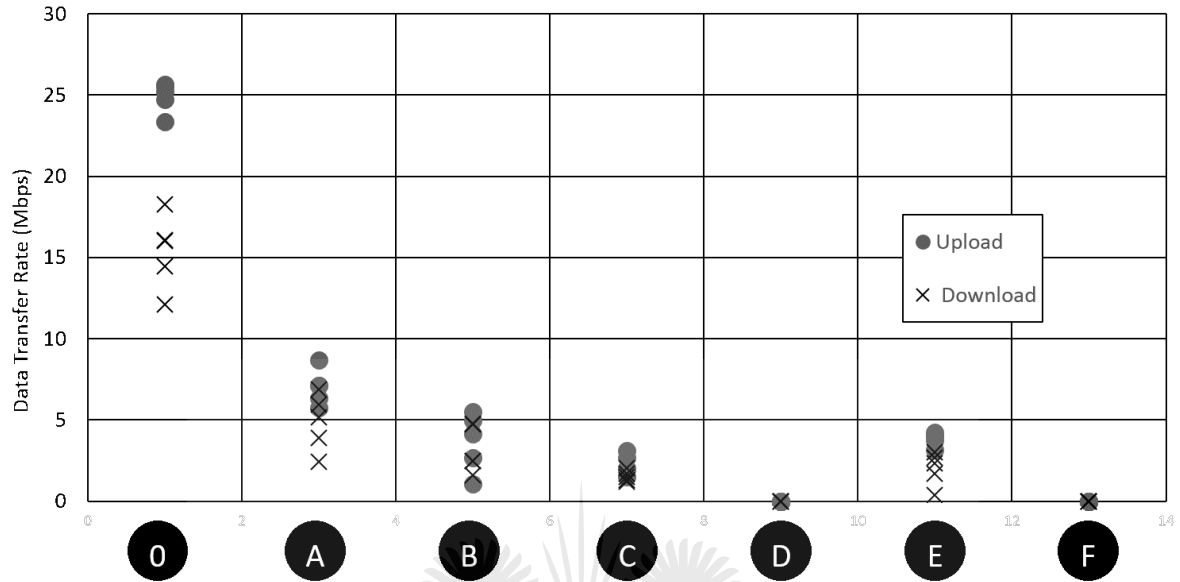


Figure 5.6: Data transfer rates to different positions in the building of (Fig. 5.4) using contactless PLC.

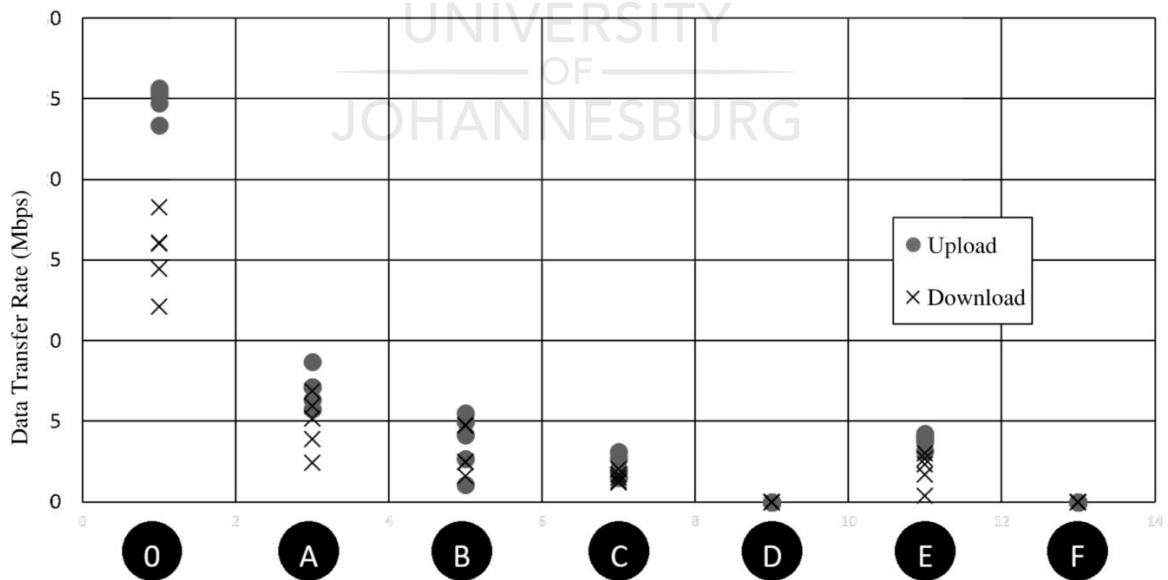


Figure 5.7: Data transfer rates to different positions in the building of (Fig. 5.4) using RF links.

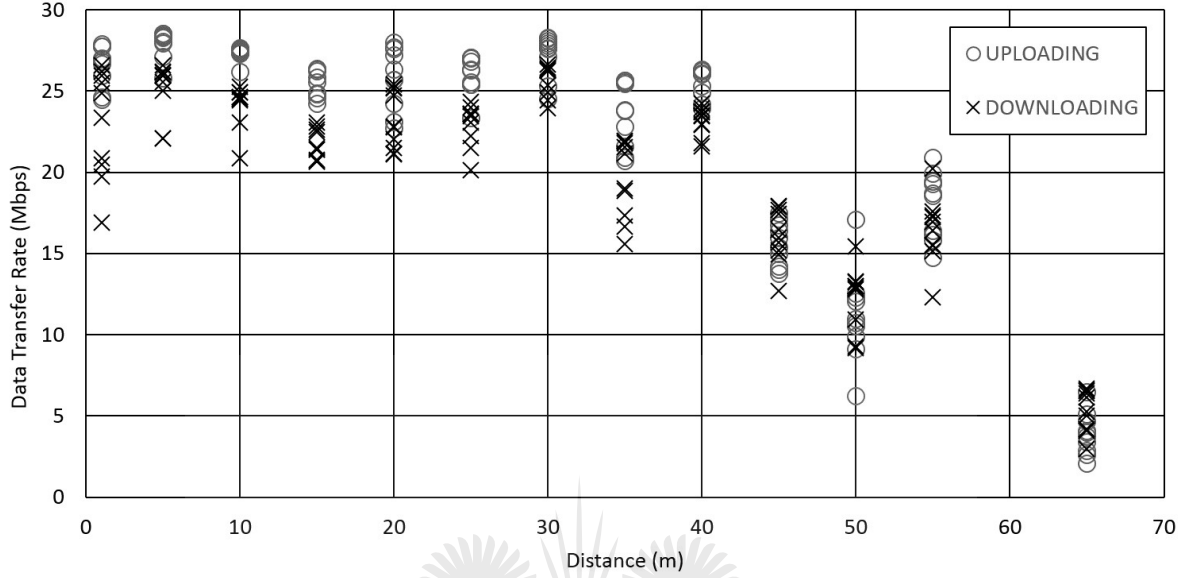


Figure 5.8: Data transfer rates to different positions along a free standing cable using contactless PLC.

During the experiments, a file size of 20 MB was used. Data were transferred in two directions: from a main personal computer to another (downloading) one, and from this computer to the main or uploading computer. These directions will be clarified later.

Measurement of the transfer rate did not give consistent results. Because of this, each transfer rate was measured several times and consequently, the results show a spread of throughput rates.

5.3 Result of the experiments

As mentioned previously (see 5.2 above), in this study measurements were taken in two physical settings. The first was a typical industrial building where the transfer rate of an RF link as compared to a contactless PLC set-up on the live installed power grid was measured. The second setting was performed in a three-storey building. In this setting,

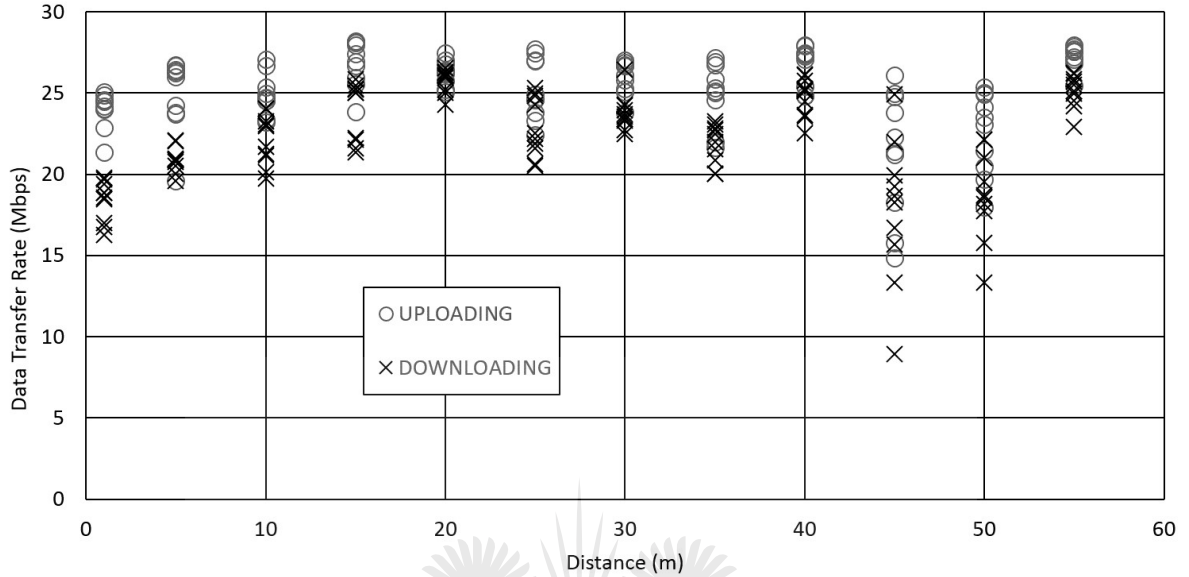


Figure 5.9: Data transfer rates to different positions along a clear line of sight - using direct RF links.

an off-line control cable was used, which is known as contactless PLC. The contactless PLC cable was connected to a non-energised free-standing cable in which the experiment was carried out. The performance of contactless PLC was compared with an RF link.

5.4 The industrial setting

Fig. 5.4 shows the floor plan for B4 LAB Level 1, a building at the University of Johannesburg that was used to measure contactless PLC which was then compared with an RF link. A 10 m section is indicated for scale. For the contactless PLC measurements, a personal computer was used to inject signal through a modem at 0 in Figs. 5.6 and 5.7. This was done with the method shown in Fig. 5.10.

For direct link RF measurements, the personal computer at 0 was stationary and communicated in normal wireless fashion (WiFi) to positions A to F. The computer at

0 was deemed to be the main one and data were downloaded to a second computer at positions A to F. Data were also uploaded from the secondary A to F positions to the main computer at 0.

5.4.1 Contactless PLC

Figure. 5.6 shows data transfer rates to different positions in the building depicted in Fig. 5.4, using contactless PLC across the live installed power-line wiring. At each position the secondary computer, modem, and antenna were positioned roughly in the middle of a room (except for E). Position E was in an open laboratory space (see Fig. 5.4.)

The first set of data points at 0 show transfer rates for the secondary computer in the same room as the main one. A difference in the upload and download rates was observed. It was thought that this might be due to direct interaction between the coupling circuit and the modem antenna of the second computer in the same room. However, at this stage, the power line was not yet active as an antenna.

At positions D and F, the signal was too low to initiate communication. Fig. 5.6 should be compared with Fig. 5.7, which applies to the same building but with RF links.

5.4.2 RF links

Figure. 5.7 shows data transfer rates to different positions in the building in Fig. 5.4 using RF links. At position 0 the results in Fig. 5.7 are comparable to that of Fig. 5.6. Position F was out of range, but communication was established for positions A to E. The data transfer rates for positions A to E were generally higher for the RF link than for the contactless PLC.

The setting above, represents an idealised situation with only soft board partitioning as obstacle. It should be kept in mind that many buildings have concrete or brick and mortar walls. In fact, it is well known [88] that WiFi frequencies have difficulty penetrating walls or between different floors in multistorey buildings and that PLC can offer a solution to this problem. (Also see Chapter 2 above.)

5.5 Free standing cable

From the previous section it is clear that 2.45 GHz WiFi can be conducted on power lines inside a building. To further study this effect, a best-case control was set-up and measured. This comprised a free-standing (non-energised) power cable with a signal directly injected from the RF modem and a free-standing RF modem with an antenna, positioned 0.5 m from the cable. Again, this was compared to a line of sight direct link RF configuration (see Fig. 5.1). In this case, the power lines in the building was depicted as suspected. This is because, in Fig. 5.4, The signal was transmitted through power line that run in metal conduits of the building, which are closely bundled and do not necessarily connect directly between all the points. Furthermore, it is also unclear how different phases of the three-phase supply are distributed. Screening effects and capacitive loading can, therefore, attenuate the signal. The maximum transfer capability of a power line can therefore only be gauged by testing a free-standing uninterrupted length of cable.

5.5.1 Contactless PLC

In Fig. 5.8 data transfer rate results are given for a 2.45 GHz WiFi communication via a contactless PLC set-up (a free-standing, uninterrupted and non-energised cable). Up to 40 m, the results compare well with that of the direct RF link, as described in the next section and shown in Fig. 5.9. After 40 m, the transfer rate drops when compared to the direct RF link. A transfer rate of around 5 Mbps is obtained with 65 m of cable.

5.5.2 The RF Link

In Fig. 5.9 measurements of the data transfer rate are shown for different positions along a clear line of sight using direct RF links. Up to 40 m, data rates are similar to the contactless PLC configuration, but increase after 40 m. At 55 m the direct RF link does not show a decline in data transfer rates.

5.6 PART II: Setup of the residential experiments

The experiments in the residential environment were performed at 2.45 GHz, using a controlled contactless power-line cable as a twisted pair link (TP-Link) router that was connected to a laptop computer. The cables were attached to a male BNC connector in which the earth was soldered to a conductor of a Bayonet Neill-Concelman (BNC) sleeve and a second conductor to the centre terminal of the BNC. The cable was then connected to the second TP-Link BNC output port, from the BNC output port to the universal serial bus (USB) connector, then from the USB output to the laptop, as shown in Fig. 5.10. The transmitting power-line cable was placed on a wooden chair on the ground floor at a height of 0.5 m above the floor, and it remained in the same position for each set of measurements. This height was chosen in order to avoid interference from the floor when the cable came into contact with it. On the receiver side, the transmitting power-line cable was laid from the ground floor to the 3rd floor of the apartment building. The experiment was repeated on every floor. The position of the receiver was not fixed because it was moved from one floor to another. The data were captured and recorded in the receiving laptop, using LAN speed software, which facilitated easy practical application (Fig. 6.1). This is a normal set up for such an experiment, i.e. the position on the ground floor is established, and various measurements are calculated at different points and in different positions, taking two samples at each position. The experiments were performed in a standard two-bedroomed apartment in a residential area in South Africa. They were performed in an open area of a physical layout within an estate complex. Obstruction was posed by the walls and the furniture. One of the reasons for using this area for the experiments was to study the behaviour of the LOS and NLOS condition as regards distance.

In this study, the experimental and measured results were correlated and used to describe the accuracy of the power-line cable and the antenna.

The measurements given in the Figs. 5.13 and 5.14 are estimated from the measured results by using a graphical approach. Figures 5.13 and 5.14 shows the data transfer speed in Mbps versus the floor levels.

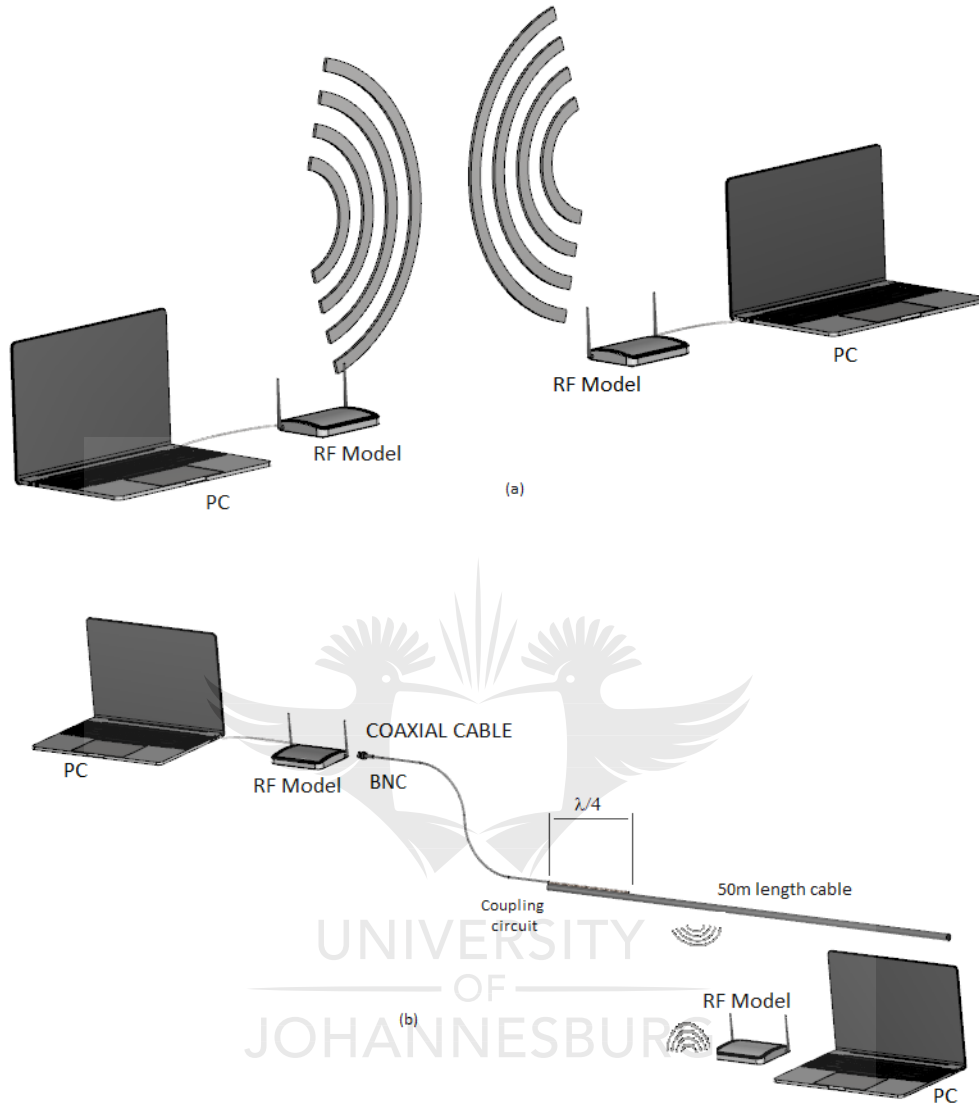


Figure 5.10: Measurement set up for antenna and power line cable. Fig. 5.10 a represent the typical RF setting for the experiment and Fig. 5.10 b, represent the contactless PLC connection setup.

5.6.1 Data collection

As mentioned above (see section 5.2.1 above), LAN speed software was installed on the two laptop computers. The transfer rate in Mbps values (which depends on distance) was measured using the procedure described in the software guide. In a few cases, the result from the LAN speed fluctuated at some distance. The results were exported to

Microsoft Excel, where the data transfer rate was plotted in relation to the floor levels, using matrix laboratory (MATLab) software as shown in Figs. 5.13 and 5.14. TP-Link Wi-Fi was used to measure the speed of the data transfer rate in Mbps. A file with the capacity of 50 Mbps was transferred between the two laptops and the rate of the data transfer was measured for both the power-line cable and the wireless. The transmitter and the receiver were placed in a residential building and the measurements were taken at different positions on the ground floor which has low performance in the RF side. This differed from measurements taken on the 3rd which has low performance in the RF side. All the measurements were captured and plotted in a graph using MATLAB software for purposes of comparison.

5.6.2 The laboratory layout

Fig. 5.11 shows a building layout in a residential area to scale. The positions for the measurements were taken on each floor as shown in Fig 5.11. During the measuring process, all the connecting doors between the rooms were opened for easy radiation from the cable. The cable was dropped from the 3rd floor to the ground floor. At the starting point, the transmitter and the receiver were in contact with each other, but no signal was received because of non-line of sight issues from the wireless. Five meters separated the receiver laptop with a modem and the transmitting laptop. The first measurement was taken in the ground floor and signals were received from both wireless and contactless cables. In the 5 m area, the transmitter was placed at line of sight with the receiving antenna for the wireless. This 5 m space was also placed on the contactless cable so that results could be compared.

5.6.3 Results of the power-line cable and wireless data upload

As shown in Fig. 5.13, indoor measurements were taken three times in different positions in the same room, which meant that data of three positions were collected for the uploading at 50 Mbps data transfer on each floor. However, the best data transfer rate was selected to plot the graph in Fig. 5.13. On the ground floor the speed of the data transfer rate increased at the same rate for both the PLC and the wireless as shown in Fig. 5.13, although the measurement for the wireless was higher than for the PLC. This is understandable because of LOS between the Tx and Rx of the wireless. There was a drop in

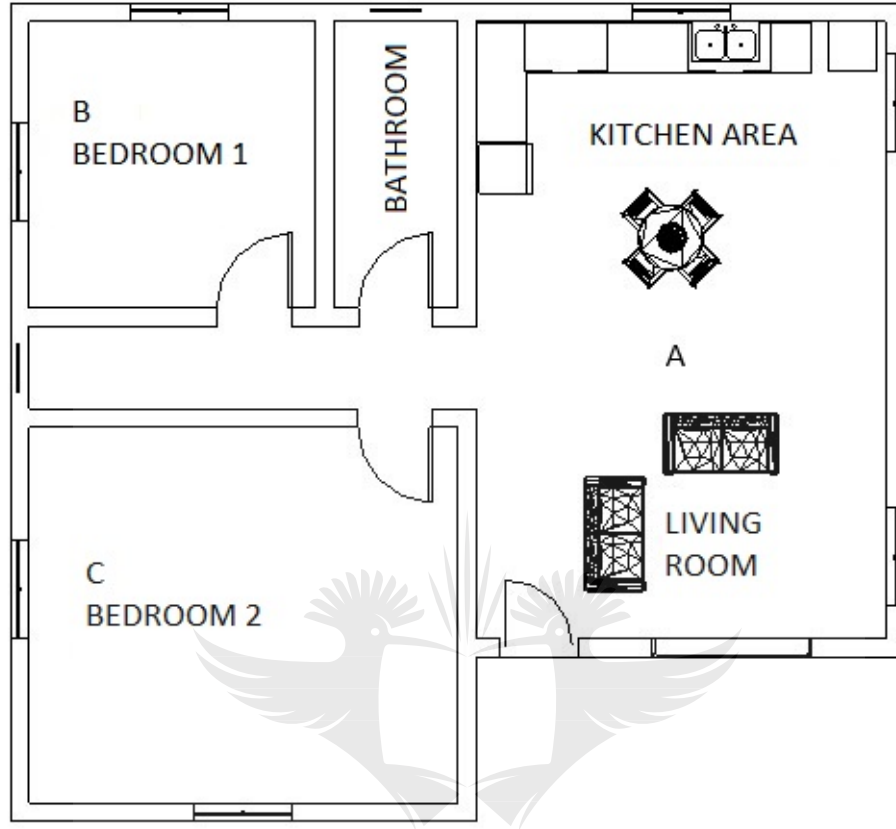


Figure 5.11: Overview of building plan.

the data transfer at c_1 , c_2 and c_3 . This is because of position of the second bedroom which is directly behind the first bedroom. It was observed the walls in between the rooms are blocking the signal. Moreover, the Tx was transmitting from a_0 and c_0 , thus indicating that there was a blockage between the rooms. At a_2 , the PLC speed of data rate transfer outperformed that of the wireless, but this was expected because of the variance between the floors. The same result applied between b_2 and c_2 . In general, as was expected, the received transfer speed decreased from a_0 to c_3 for both the PLC and wireless. Again, as would normally be expected, the variance of the received transfer speed would be more varying at a far distance, since the receivers at a_3 , b_3 and c_3 have greater variance than the receivers at a_0 , b_0 and a_0 (see Fig. 5.13).



Figure 5.12: Overview of building plan.

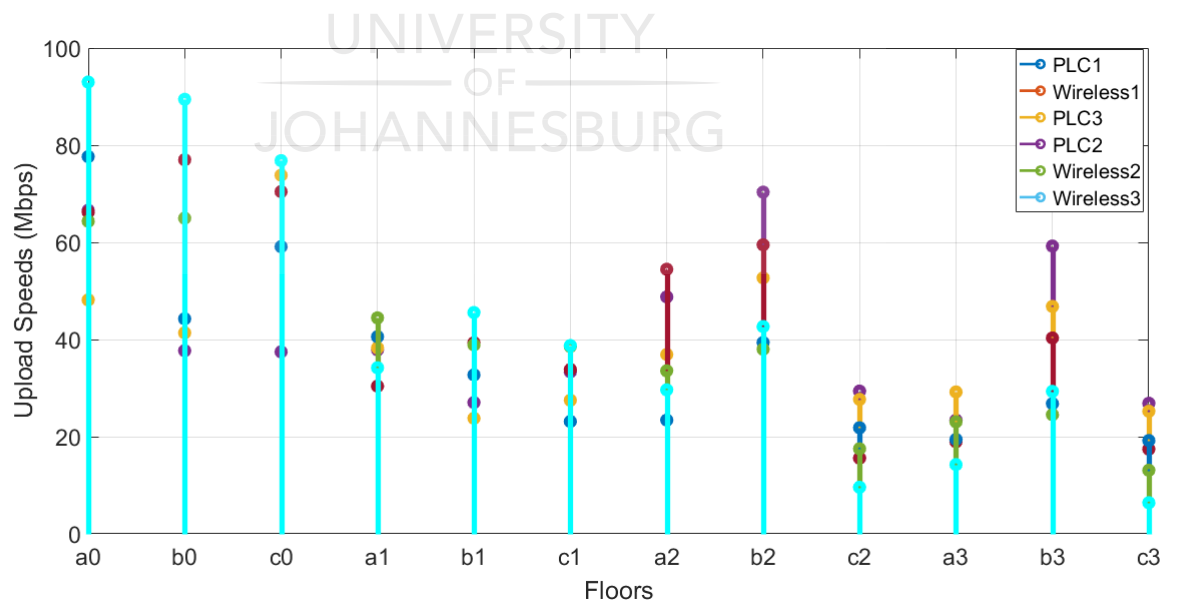


Figure 5.13: Antenna upload 50 Mbps.

5.6.4 Results of the power-line cable and wireless data download

The download experiment was performed alongside the upload experiment, but the results were slightly different. The transfer rate samples were collected when the receiver antenna was moved from one floor level to another. On each floor level, which consisted of a living room and two bedrooms, a_0 , b_0 and c_0 represent the living room, bedroom 1 and bedroom 2 respectively. Samples were collected in each room at three different positions. Fig. 5.14 gives an indoor radiation measurement for the power-line cable and wireless when the receiver antenna was moved from one floor level to another. The results of data downloading at a 50 Mbps transfer rate were plotted. The samples were collected on each floor for the data downloading. In Fig. 5.14 the results show that the speed of the transfer rate decreased as it moved from one level to a higher one. This was to be expected. The receiver antenna, together with the laptop, were positioned at different heights during the testing. There was a gradual increase at a_0 , b_0 and c_0 for both measurements. The results of the transfer rate for the wireless were better than those for the PLC from a_0 to c_1 (the ground floor and first floor) shown in Fig. 5.14. It can also be seen that the results of the PLC start increasing as the process moved from a_2 to c_3 . This meant that, as was expected, the received transfer speed decreased between the floors from a_2 to a_0 as shown in Fig. 5.14

5.7 Discussion

All the results of data transfer speed in Mbps obtained for the power-line cable and wireless at floor-level positions are shown in Figs. 5.13 and 5.14. The results of the power-line cable upload at 50 MB were compared to the wireless results. It was observed that at a_0 , b_0 and c_0 , the wireless speed of transfer was slightly higher in comparison with that of the power-line cable with a high initial LOS, although, as indicated in Fig. 5.13, for the downloading, a decrease was observed after a_1 , b_1 and c_1 , but the difference in the data transfer rate was limited. Figs. 5.13 and 5.14 indicate the transfer rate for the power-line cable and wireless, respectively. For the power-line cable, the transfer rate at a_1 , b_1 and c_1 was slightly higher than that of the wireless transfer rate for upload. This was a result of severe obstruction within the buildings. For the wireless measurement, the speed increased during the transfer rate up to the first level where the direct signal was

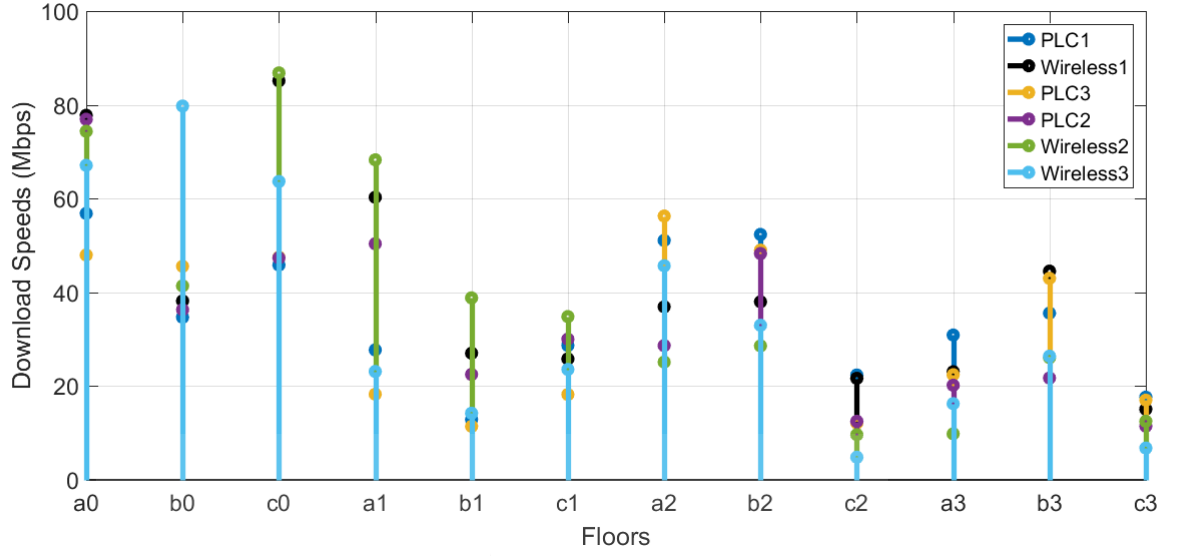


Figure 5.14: Antenna download 50 Mbps.

received by the receiver at LOS. The signal drop shown in Figs. 5.13 and 5.14 indicate the rapid signal drop. When the data transfer rate was plotted against different positions on different floor levels, it was shown that for the wireless measurement, the transfer rate decreased as a result of severe obstruction and the resultant lack of wireless penetration in multiple-storey buildings. Thus, as the floor level increased, the transfer rate decreased, confirming the expected good results.

5.8 Conclusion

In this Chapter preliminary measurements for a contactless PLC and RF link were analysed in two sections. In Section I, the link performance between a pure direct RF link and a contactless PLC link in 2.45 GHz were compared. The aim was to use a power line as a traveling-wave antenna to transmit 2.45 GHz radio signals. This means that one of the two connected modems was coupled to the power line, while the other received data in normal RF mode. Data throughput was measured for two setups using power cables, one in an office environment with a real power network and in an open area laboratory environment, allowing free movement of people, with a free-standing power cable.

The idea of using a ubiquitous power line as a traveling-wave antenna to bridge indoor distances where pure radio links may be compromised, is very interesting. The clear description of the measurement and the results make this study unique. However, the two examples do not cover the situation where contact-less PLC is supposed to outperform a pure wireless link. This is because more of a LOS situation was considered, and the overall performance of WiFi will definitely be better than that of the contactless PLC as seen in the figures Figs. 5.13 and 5.14.

In Section II, a practical approach to hybrid PLC-RF systems at 2.45 GHz was presented. The influence of a long-wire antenna in a building was considered for both a PLC and a RF channel. It was shown that the long-wire acted as an antenna in the hybrid system. The measurement campaign of a hybrid PLC-RF was also presented. The measurements were performed in a three-storey building in South Africa and the results were then discussed.



6

PLC-RF Diversity: Channel Outage Analysis

As discussed in Chapter 2, when signals from indoor access points of a RF network system are deployed in a multi-storey building, they suffer from high attenuation as a result of the thick walls and metal structures of the building. This is caused by scattering of the retransmitted signals by the walls and structures. PLC technology is considered to be a method of overcoming this challenge. In this study, a combination of RF and PLC technologies for achieving signal transmission in indoor environments is proposed, taking into account the characteristics of multi-storey buildings. Diversity combining techniques, viz. SC and MRC are used to recover the retransmitted message. The outage probability for both SC and MRC are also proposed.

UNIVERSITY
OF
JOHANNESBURG

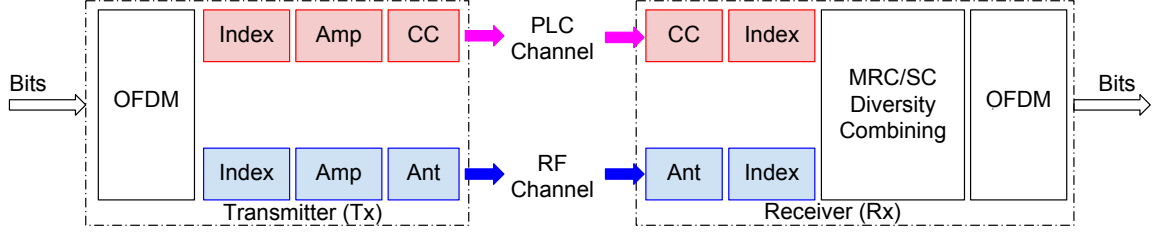


Figure 6.1: A model of a PLC-RF system for a multiple-storey

6.1 Introduction

As discussed in Chapter 2, when signals from indoor access points of a RF network system are deployed in a multi-storey building, they suffer from high attenuation as a result of the thick walls and metal structures of the building. This is caused by scattering of the retransmitted signals by the walls and structures. PLC technology is considered to be a method of overcoming this challenge. In this study, a combination of RF and PLC technologies for achieving signal transmission in indoor environments is proposed, taking into account the characteristics of multi-storey buildings. Diversity combining techniques, viz. SC and MRC are used to recover the retransmitted message. The outage probability for both SC and MRC are also proposed. [142].

This Chapter aims to analyse the outage probability of PLC-RF diversity combining. Two techniques are exploited to analyse this probability of failure, viz. selection combining and maximum ratio combining. In each case, the behaviour of system SNR in the PLC-RF is proposed. The outage probability of the system is analysed using PDF and CDF from the SNR. In particular, the effect of a coupling circuit in the PLC analysis is considered.

6.2 Description of a model for a PLC-RF system

Notation: For better legibility, the parameters related to the PLC channel are indexed with "1" while those related to the WiFi channel are indexed with "2".

A model of a diverse PLC-RF system is proposed in Fig. 6.1. The incoming data is coded and modulated using PSK, APSK, or QAM. The principle of OFDM scheme

was used to obtain the modulated signal which is coded into the channel, and then it is sent to both the PLC and RF links for cyclic prefix indexation. Two different signals are obtained, $s_1(t)$ and $s_2(t)$. These signals are transmitted using the PLC and RF channel.

As far as the PLC is concerned, a CC is exploited to couple the message signal to the channel. The channel consists of multiple types of noise. A current amplifier helps boost the current that is transmitted over a long distance. On its receiver side, the PLC detected signal, $\bar{s}_1(t)$ is transmitted to the combining module after the cyclic prefix index has been removed.

The RF signal, $s_2(t)$, from the OFDM module is treated by adding its own prefix which differs from that of the PLC. The obtained signal is amplified and applied to an omnidirectional antenna. This constitutes the coupling of the RF signal to the RF channel. Another antenna at the receiver side is exploited to collect the message signal from the channel. The cyclic prefix is removed from the last signal, and it is then transmitted to the combining module.

The combining module is comprised of SC and MRC sub-modules. In MRC, all the branches are used as the receiving within same time intervals. Each branch signal is multiplied by a weighted gain factor that is proportional to its own SNR. The received signals constitute the summed signal which is then transmitted to the demodulator. The digital signal is decoded and sent to the data recipient. In SC only one branch is used at an interval. The combination works by selecting the signal with the highest SNR at a particular time interval.

6.3 Channel analysis of PLC and RF systems

6.3.1 Effect of the coupling circuit on the PLC channel

The PLC channel is a low-pass filter [6] which, when combined to the input CC and output CC, becomes a totally different channel. This was previously analysed and the details are presented in [9]. The structure of the channel including both input and output CCs is depicted in Fig. 6.8. It shows the two coupling circuits connected to the PLC channel. It is assumed that the CCs (input and output) are identical with a gain g_0 , and

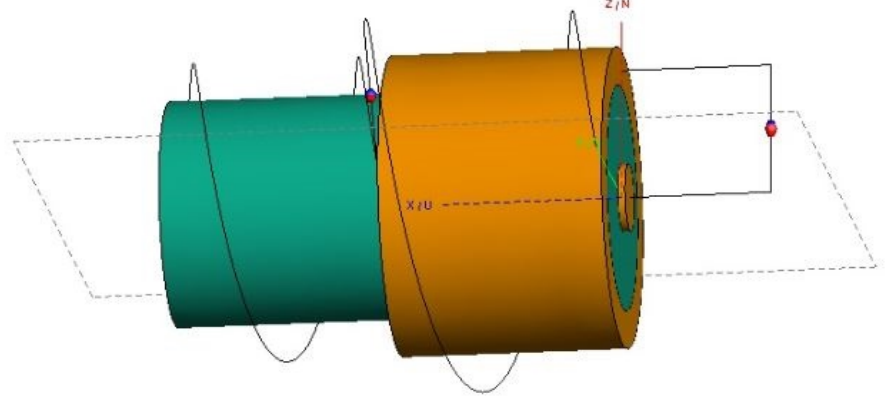


Figure 6.2: Substrate of microstrip coupling circuit front view

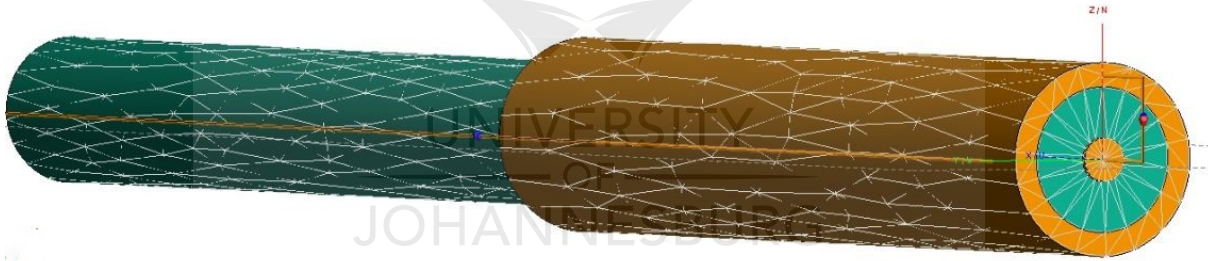


Figure 6.3: Substrate of microstrip coupling circuit side view

that they do not create any signal distortion. Consequently, the transfer function of this part of the system is given by $g_0^2 h_1$.

6.3.2 Analysis of the coupling circuit simulation

The design of the CC as depicted in Figs. 6.2 and 6.3, shows that the CC has three major components, viz. a parallel couple line, perfect conductor and substrate with dielectric material. FECO software was used for this experiment. It is user-friendly for an analysis

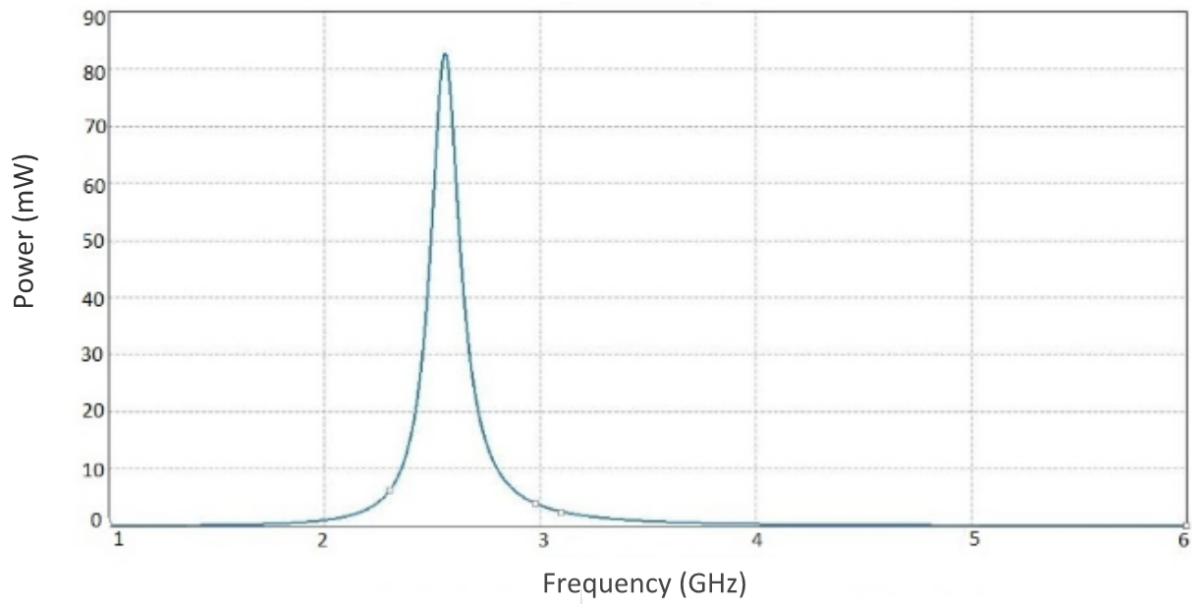


Figure 6.4: Power versus frequency CC analysis at 2.45 GHz

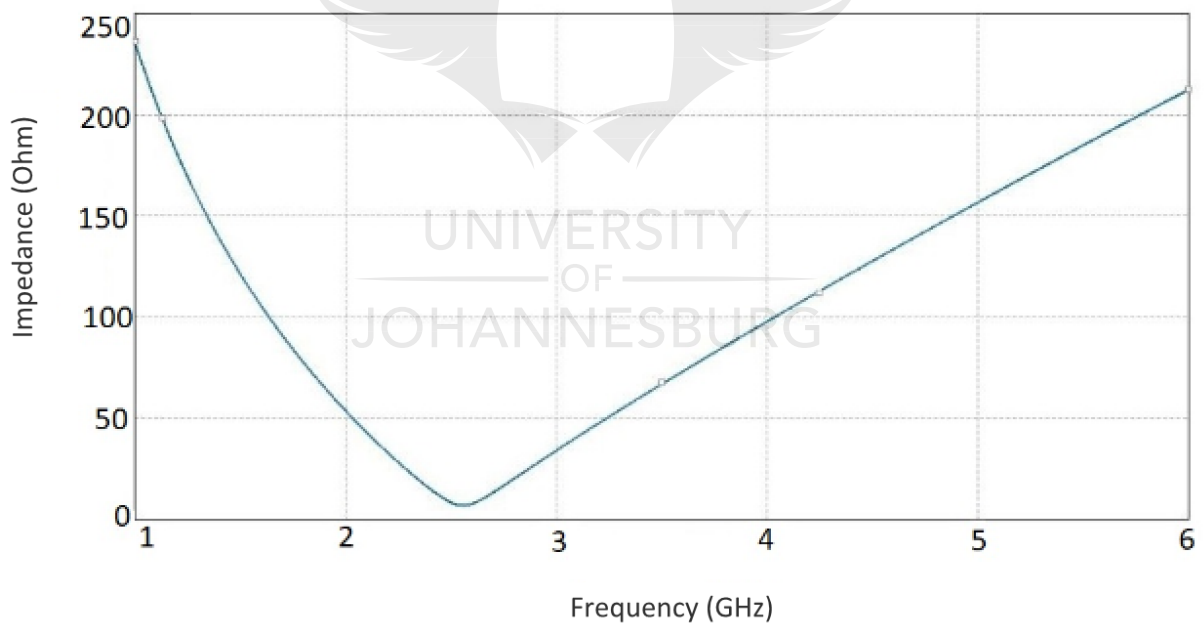


Figure 6.5: Impedance versus frequency CC analysis at 2.45 GHz

of a cable since it uses microwave circuit components for high specification performance.

The CC was designed by clicking on the menu bar of the FECO software and then select the appropriate command from the window table in the menu bar, which consists of

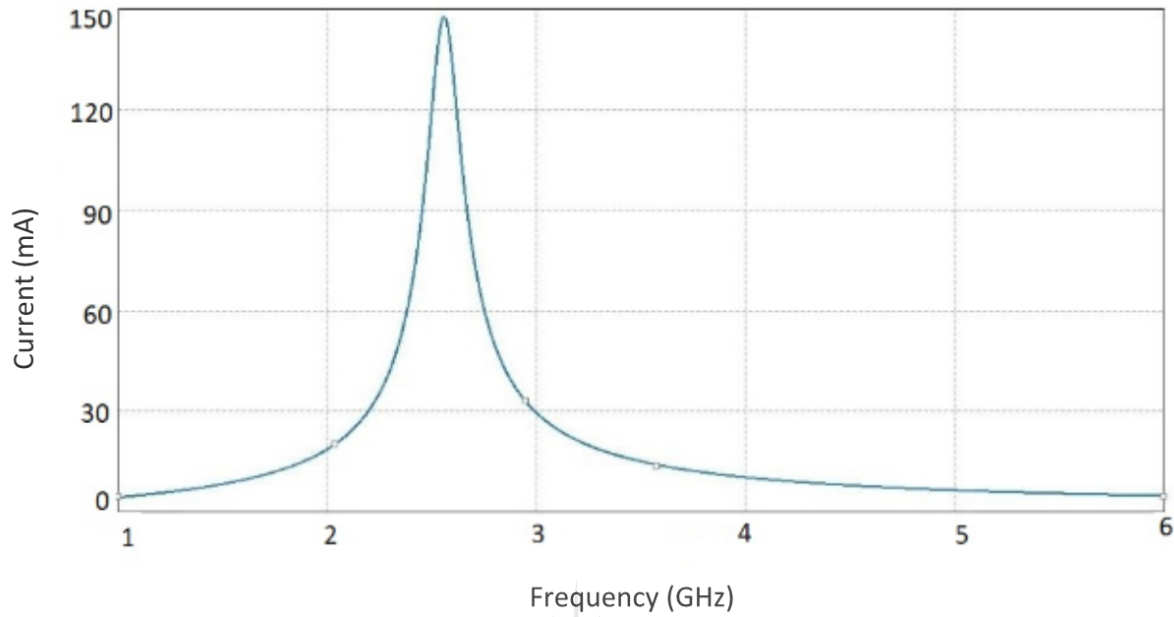


Figure 6.6: Current versus frequency CC analysis at 2.45 GHz

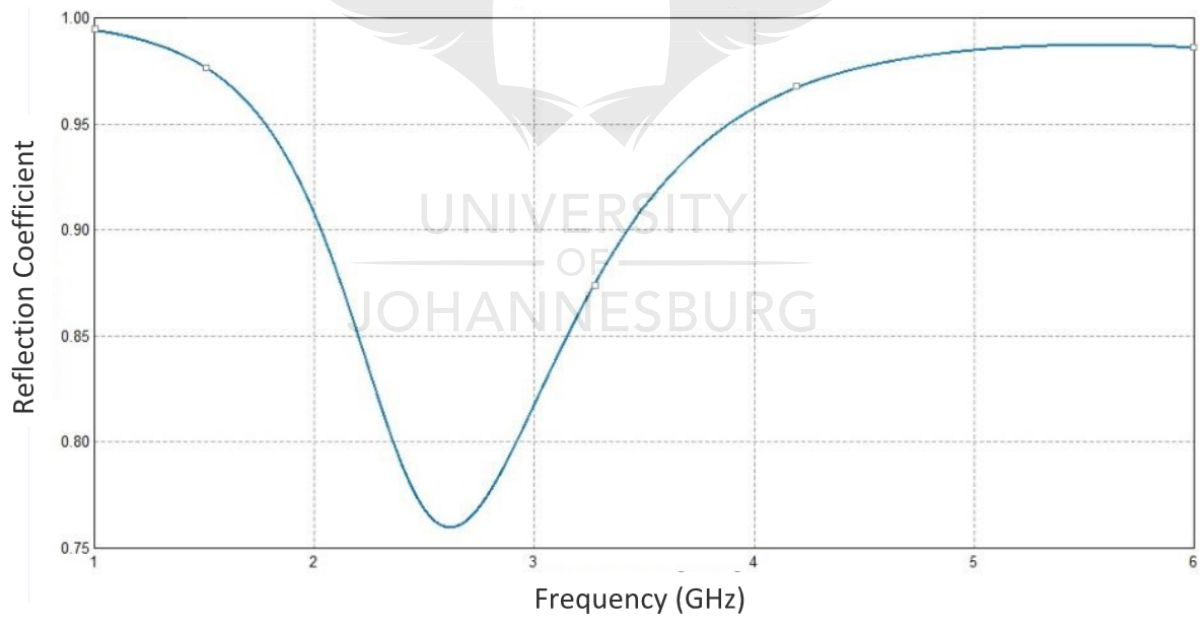


Figure 6.7: Reflection coefficient versus frequency CC analysis at 2.45 GHz

desired positions and shapes from the menu bar. The purpose of selecting the appropriate window table is to create a symmetrical coaxial CC. However, this will produce geometric components that give the option of specific dimensions with characteristics such as width,



Figure 6.8: The PLC channel highlighting the two coupling circuits

height, and radius. Ongoing editing of the specific dimension as regards its characteristics should enhance the performance of the experiment.

The design was based on the coupled lines, using two microstrip parallel-end lines for a $\frac{\lambda}{4}$ wavelength, as shown in Figs. 6.2 and 6.3. At this point, the coupled line of the CC is considered to be a perfect conductor. Figs. 6.4, 6.5, 6.6, and 6.7 summarise the frequency response characteristics of the simulated microstrip CC by FECO at 2.45 GHz Co-ax CC coil pickup 1 = 10 mm Ref00F. The performance of the coupling circuit can be presented in terms of reflection coefficient (S11), voltage source, current magnitude, impedance magnitude, and transmission power as a function of frequency. The reflection coefficient (S11) is used to calculate the return loss. The ideal design for a microstrip is expected to have a high degree of return loss; good matching electrical connecting impedance; lower insertion loss; broad bandwidth, and highly selective frequency, all of which are considered in the microstrip CC design described here. The microstrip CC is designed to operate at 2.5 GHz operation frequency in the frequency range of 1 GHz to 6 GHz.

The performance of the reflection coefficient as shown in Fig. 6.7, shows that the return loss is greater than 0.99 dB at 2.5 GHz, with approximately zero insertion loss. The optimised coupling circuit has an operating frequency of 2.5 GHz with transmission frequencies between 1 GHz and 6 GHz. The back reflection from the feeding power at the port of antenna is referred to as return loss and is due to the mismatches effect that occurs with the transmission line and the feeding point. Fig. 6.7 indicates that the coupling circuit radiates with an operating frequency selected at 2.45 GHz, and the return loss is equal to 0.99 dB.

Figure. 6.5 shows the magnitude of impedance matching, and as can be seen from Fig. 6.5 the resonance occurs at the frequency of 2.5 GHz for an impedance match of 240

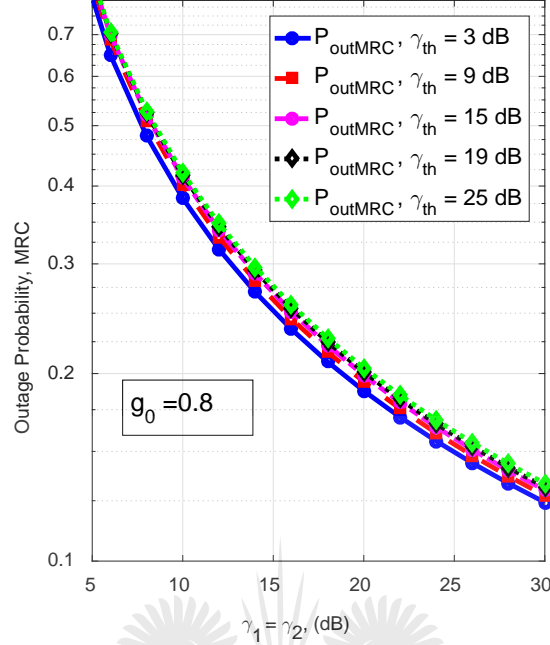


Figure 6.9: $P_{out} = f(\gamma_{th})$, MRC. Variation of the outage probability for various values of γ_{th} , 3 dB, 9 dB, 15 dB, 19 dB and 25 dB, for Fig. 6.9 MRC and Fig. 6.10 SC, $\gamma_1 = \gamma_2$.

ohms. Fig. 6.6 shows the current and resonance occurring at the frequency of 2.5 GHz for a current of 145 mA. Fig. 6.4 shows that the power and the resonance occur at the frequency of 2.5 GHz for a power of 82 mA. The bandwidth can be analysed from Fig. 6.4 referring to the return loss versus frequency at 0.9 dB. The value of the bandwidth can be captured from the return loss at 0.9 dB as 2.6 dB.

6.3.3 Introduction to receiver combining

6.3.3.1 Section combining

In SC, the combiner SNR, γ_{sc} , is the maximum of the branch SNRs [143–145].

$$\gamma_{sc} = \max[\gamma_a, \gamma_b, \dots, \gamma_N], \quad (6.1)$$

where a, b, \dots, N are the different branches.

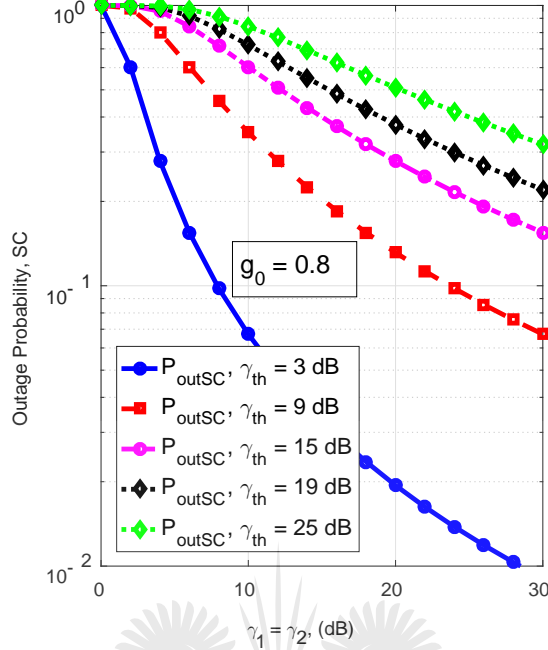


Figure 6.10: $P_{out} = f(\gamma_{th})$, SC. Variation of the outage probability for various values of γ_{th} , 3 dB, 9 dB, 15 dB, 19 dB and 25 dB, for Fig. 6.9 MRC and Fig 6.10 SC, $\gamma_1 = \gamma_2$.

6.3.3.2 Maximum ratio combining

The final SNR, γ_{mrc} is the sum of the branch SNRs [143–145].

$$\gamma_{mrc} = \sum_{i=a}^N \gamma_i, \quad (6.2)$$

where a, b, \dots, N are the different branches.

6.3.4 PLC and RF signal-to-noise ratios

The characteristics of the channels depend on the environment (PLC, RF). PLC and RF may have the same fading characteristics. They are not dependent on each other. This implies that the SNR of the PLC channel, γ_1 is totally independent of that of the RF

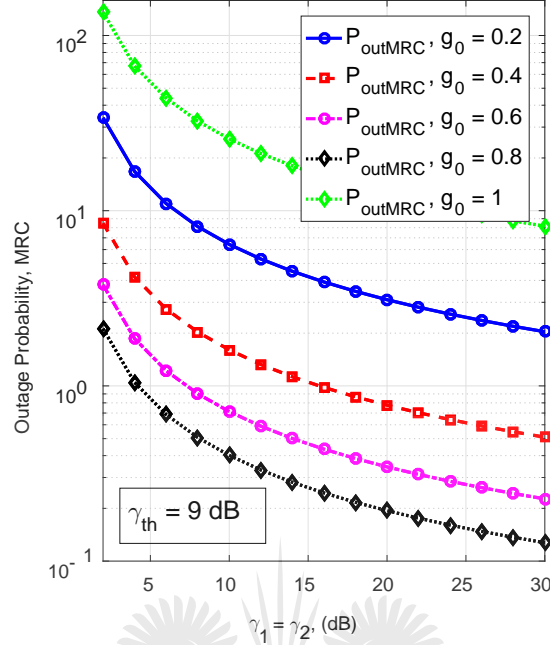


Figure 6.11: Variation of the outage probability (MRC) for various values of g_0 , 0.2, 0.4, 0.6, 0.8 and 1, for $\gamma_{th} = 9$ dB and $\gamma_1 = \gamma_2$.

link, γ_2 . They are both defined by

$$\begin{aligned}\gamma'_1 &= g_0^2 \frac{E_b}{N_{0(1)}} |h_1|^2 \\ &= g_0^2 \gamma_1\end{aligned}\tag{6.3}$$

and

$$\gamma_2 = \frac{E_b}{N_{0(2)}} |h_2|^2,\tag{6.4}$$

respectively. In Eqs. (6.3) and (6.4), the channel fading factor is defined by $|h_1|$ and $|h_2|$ for the PLC and the RF channels respectively. The power spectral density of the noise over the channels are $N_{0(1)}$ and $N_{0(2)}$, and E_b is the common bit energy as the same signal is applied to both channels. It should be noted that the average SNRs over both channels are based on Eqs. (6.3) and (6.4) and are given by $\bar{\gamma}'_1 = g_0^2 \frac{E_b}{2\sigma_1^2}$ and $\bar{\gamma}_2 = \frac{E_b}{2\sigma_2^2}$. E_b , been the common transmitted signal energy and σ_1^2 and σ_2^2 are the noise variance over PLC and RF channels respectively. Furthermore, it should also be noted that σ_1^2 involves both Gaussian variance σ_g^2 and impulsive noise variance σ_I^2 . h_1 and h_2 are given in terms of

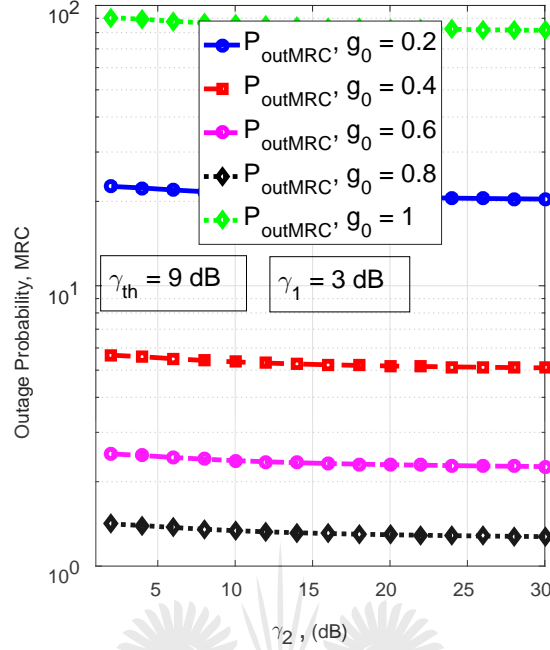


Figure 6.12: $P_{out} = f(\gamma_{th})$, $\gamma_1 = 3$ dB. Variation of the outage probability (MRC) for various values of g_0 , 0.2, 0.4, 0.6, 0.8 and 1, for $\gamma_{th} = 9$ dB and variable γ_2 .

the transmission frequency, f , by [6, 47]

$$h_1(f) = A \sum_{i=1}^N g_i(f) \exp\{-(a_0 + a_1 f^k) d_i\} \exp\left\{-j2\pi f \frac{d_i}{v}\right\}, \quad (6.5)$$

for the PLC channel, where the number of paths N and a constant coefficient A are exploited to adjust attenuation. The PLC cable characteristic are k , a_0 , and a_1 which are for the path gain $g_i(f)$ in the i^{th} path then v , f and d_i are the propagation speed of light in the cable structure, the transmission frequency and the length of the i^{th} path.

$$h_2(f) = \sum_{n=1}^M \alpha_n \exp\{-j2\pi f \tau_n\}. \quad (6.6)$$

Eq. (6.6) relates to the RF channel, where α_n and τ_n are the complex amplitude and the delay of the n^{th} wave, and, M and f are the number of waves and the transmitting frequency respectively.

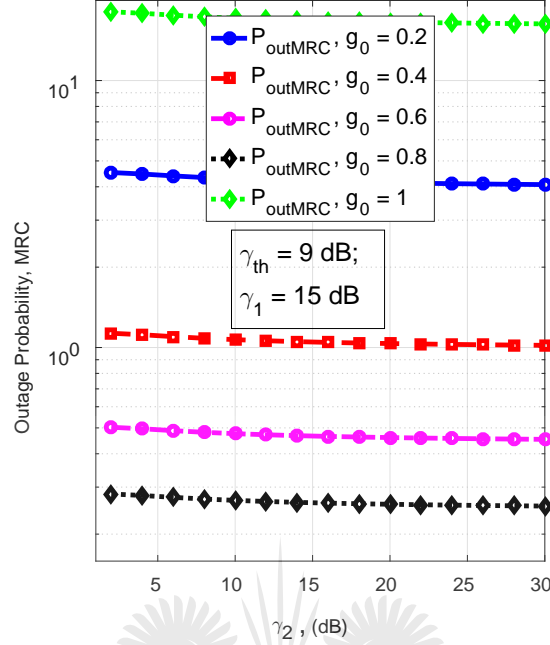


Figure 6.13: $P_{\text{out}} = f(\gamma_{th})$, $\gamma_1 = 15$ dB. Variation of the outage probability (MRC) for various values of g_0 , 0.2, 0.4, 0.6, 0.8 and 1, for $\gamma_{th} = 9$ dB and variable γ_2 .

6.3.5 Joint PLC-RF

Let ρ_1 , ρ_2 , ρ_{12} and ρ_{21} be the channel gains corresponding to the joint PLC-RF system proposed in Fig. 6.1. ρ_1 and ρ_2 are front-end PLC and RF sub-channels and ρ_{12} and ρ_{21} are cross-talk gain RF-PLC and PLC-RF respectively. The overall channel frequency response is given by

$$\mathbf{H} = \begin{bmatrix} \rho_1 & \rho_{12} \\ \rho_{21} & \rho_2 \end{bmatrix}. \quad (6.7)$$

The general transmission system with a filtered channel and additive noise is governed by [6, 43]

$$\mathbf{y}_i = \mathbf{H}\mathbf{x}_i + \mathbf{n}_i, \quad (6.8)$$

where \mathbf{y}_i and \mathbf{x}_i are the received and transmitted vectors, \mathbf{H} the channel frequency response and \mathbf{n}_i the additive noise vector. Based on (6.8), the transmission in the proposed

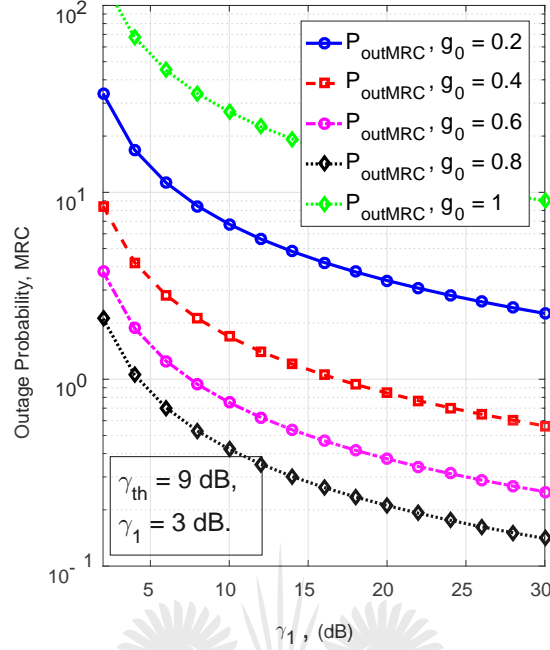


Figure 6.14: $P_{out} = f(\gamma_{th})$, $\gamma_2 = 3$ dB. Variation of the outage probability (MRC) for various values of g_0 , 0.2, 0.4, 0.6, 0.8 and 1, for $\gamma_{th} = 9$ dB and variable γ_1 .

joint PLC-RF is given by

$$\begin{bmatrix} \mathbf{y}_1 \\ \mathbf{y}_2 \end{bmatrix} = \begin{bmatrix} \mathbf{x} \end{bmatrix} \begin{bmatrix} \rho_1 & \rho_{12} \\ \rho_{21} & \rho_2 \end{bmatrix} + \begin{bmatrix} \mathbf{n}_1 \\ \mathbf{n}_2 \end{bmatrix}, \quad (6.9)$$

where \mathbf{y}_1 and \mathbf{y}_2 are the signal at PLC and RF receiving antenna respectively, \mathbf{x} is the transmitted signal and, \mathbf{n}_1 and \mathbf{n}_2 are noise at the receiving PLC and RF ports, respectively. \mathbf{n}_1 and \mathbf{n}_2 are giving by

$$\begin{cases} \mathbf{n}_1 = \sum \text{PLC noises,} \\ \mathbf{n}_2 = \sum \text{RF noises.} \end{cases} \quad (6.10)$$

Note that, various additive noise sources are present over both channel, the total noise in each channel is the sum of all these noise together. The channel is Rayleigh fading corresponding to the a chi-square distribution with two degrees of freedom. The Rayleigh distribution fits well in both PLC and RF channels here because there is no line of sight link between transmitter and receiver when the message is sent through channels. The

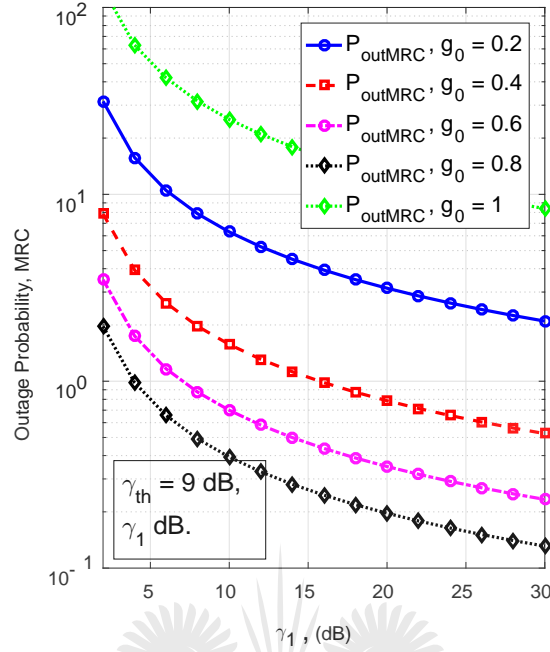


Figure 6.15: $P_{out} = f(\gamma_{th})$, $\gamma_2 = 15$ dB. Variation of the outage probability (MRC) for various values of g_0 , 0.2, 0.4, 0.6, 0.8 and 1, for $\gamma_{th} = 9$ dB and variable γ_1 .

PDF of the SNR over the i^{th} channel is given by

$$f_{\gamma_i}(\gamma_i) = \frac{1}{\bar{\gamma}_i} \exp\left\{-\frac{\gamma_i}{\bar{\gamma}_i}\right\}. \quad (6.11)$$

The corresponding cumulative distributed function (CDF), $F(\gamma_i)$, is expressed as

$$F_{\gamma_i}(\gamma_i) = 1 - \exp\left\{-\frac{\gamma_i}{\bar{\gamma}_i}\right\}, \quad (6.12)$$

where $\bar{\gamma}_i$ is the link average SNR.

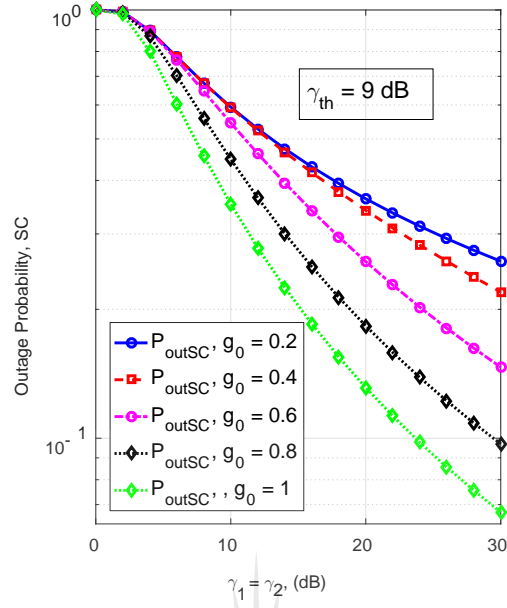


Figure 6.16: Variation of the outage probability (SC) for various values of g_0 , 0.2, 0.4, 0.6, 0.8 and 1, for $\gamma_{th} = 9$ dB and $\gamma_1 = \gamma_2$.

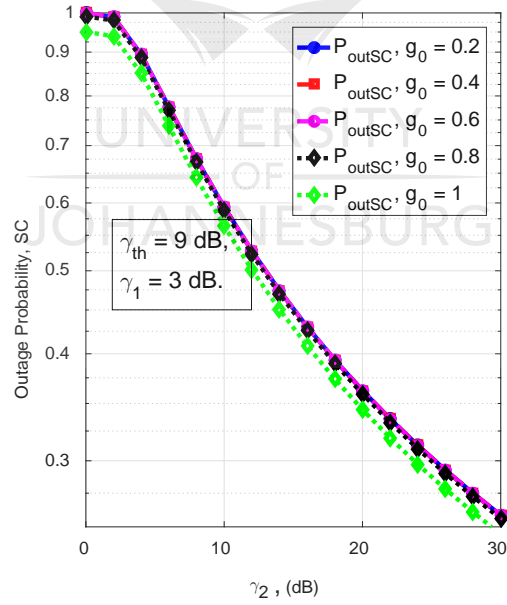


Figure 6.17: $P_{out} = f(\gamma_{th})$, $\gamma_2 = 3$ dB. Variation of the outage probability (SC) for various values of g_0 , 0.2, 0.4, 0.6, 0.8 and 1, for $\gamma_{th} = 9$ dB and variable γ_2 .

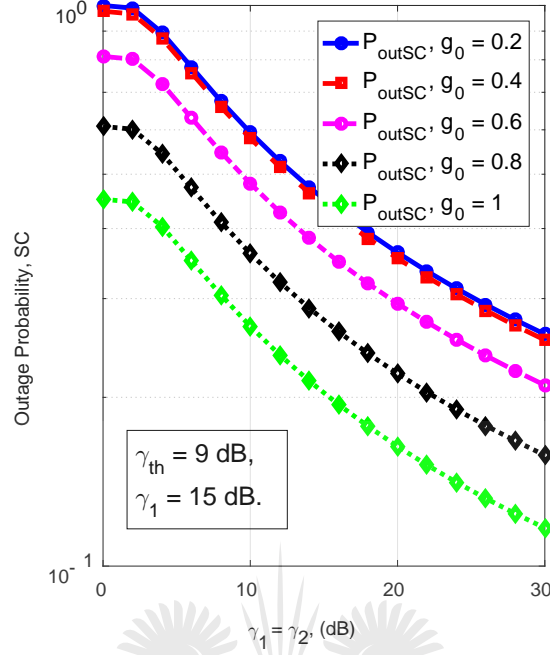


Figure 6.18: $P_{out} = f(\gamma_{th})$, $\gamma_2 = 15$ dB. Variation of the outage probability (SC) for various values of g_0 , 0.2, 0.4, 0.6, 0.8 and 1, for $\gamma_{th} = 9$ dB and variable γ_2 .

6.3.6 Selection combining

The outage probability is the probability that the SNR, γ , falls under a threshold value, γ_{th} [114]. At the output port of an SC combiner, it is given by

$$P_o = \int_0^{\gamma_{th}} f_{\gamma_1 \gamma_2}[\max(g_0^2 \gamma_1, \gamma_2)] d\gamma_1 d\gamma_2, \quad (6.13)$$

where $f(\cdot)$ denotes PDF of the received signal's SNRs. The instantaneous SNR in SC scenario is given by

$$\begin{aligned} \gamma_{sc} &= \max[g_0^2 \gamma_1, \gamma_2] \\ &= \begin{cases} g_0^2 \gamma_1, & g_0^2 \gamma_1 > \gamma_2, \\ \gamma_2, & \gamma_2 > g_0^2 \gamma_1. \end{cases} \end{aligned} \quad (6.14)$$

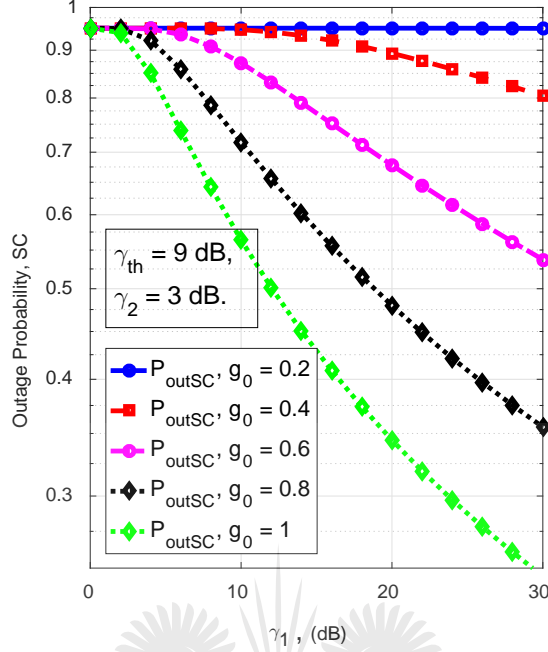


Figure 6.19: $P_{out} = f(\gamma_{th})$, $\gamma_2 = 3$ dB. Variation of the outage probability (SC) for various values of g_0 , 0.2, 0.4, 0.6, 0.8 and 1, for $\gamma_{th} = 9$ dB and variable γ_1 .

The corresponding CDF can be expressed as

$$\begin{aligned}
 F(\gamma_{sc}) &= p_r[\max(g_0^2\gamma_1, \gamma_2) \leq \gamma_{th}] \\
 &= p_r[(g_0^2\gamma_1 \leq \gamma_{th}, g_0^2\gamma_1 > \gamma_2) \cup (\gamma_2 \leq \gamma_{th}, g_0^2\gamma_1 < \gamma_2)] \\
 &= p_r(g_0^2\gamma_1 \leq \gamma_{th}, g_0^2\gamma_1 > \gamma_2) + p_r(\gamma_2 \leq \gamma_{th}, g_0^2\gamma_1 < \gamma_2),
 \end{aligned} \tag{6.15}$$

where $p_r[\cdot]$ denotes the probability operator. The above CDF can result to

$$\begin{aligned}
 F_{\gamma_{sc}}(\gamma_{sc}) &= p_r(g_0^2\gamma_1 \leq \gamma_{th}, \gamma_2 \leq \gamma_{th}) \\
 &= F_{\gamma_{th}}(g_0^2\gamma_1, \gamma_2).
 \end{aligned} \tag{6.16}$$

Due to the independence of γ_1 and γ_2 , this probability can be written as

$$F_{\gamma_{sc}}(\gamma_{sc}) = F_{\gamma_1}(\gamma_1)F_{\gamma_2}(\gamma_2), \tag{6.17}$$

where

$$F_{\gamma_1}(\gamma_{th}) = 1 - \exp\left\{-\frac{\gamma_{th}}{g_0^2\gamma_1}\right\} \tag{6.18}$$

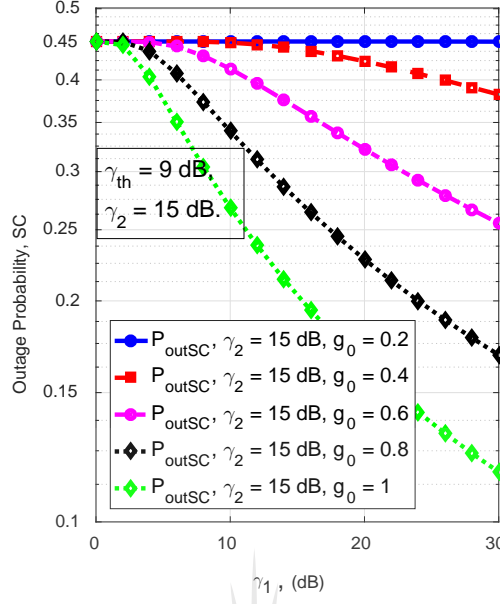


Figure 6.20: $P_{out} = f(\gamma_{th})$, $\gamma_2 = 15$ dB. Variation of the outage probability (SC) for various values of g_0 , 0.2, 0.4, 0.6, 0.8 and 1, for $\gamma_{th} = 9$ dB and variable γ_1 .

and

$$F_{\gamma_2}(\gamma_{th}) = 1 - \exp\left\{-\frac{\gamma_{th}}{\bar{\gamma}_2}\right\}. \quad (6.19)$$

By substituting equation (15), (16) into (14), then equation (17) can be written as

$$\begin{aligned} F_{\gamma_{sc}}(\gamma_{sc}) &= \left(1 - \exp\left\{-\frac{\gamma_{th}}{g_0^2 \bar{\gamma}_1}\right\}\right) \left(1 - \exp\left\{-\frac{\gamma_{th}}{\bar{\gamma}_2}\right\}\right) \\ &= 1 - \exp\left\{-\frac{\gamma_{th}}{\bar{\gamma}_2}\right\} - \exp\left\{-\frac{\gamma_{th}}{g_0^2 \bar{\gamma}_1}\right\} + \exp\left\{-\left(\frac{\gamma_{th}}{g_0^2 \bar{\gamma}_1} + \frac{\gamma_{th}}{\bar{\gamma}_2}\right)\right\}. \end{aligned} \quad (6.20)$$

6.3.7 Maximum ratio combining

In MRC, the output SNR is the sum of SNRs per branch. In the PLC-RF combining, it is given by

$$\gamma_{mrc} = g_0^2 \gamma_1 + \gamma_2, \quad (6.21)$$

and the corresponding outage probability is defined by

$$P_o = p_r(g_0^2 \gamma_1 + \gamma_2 \leq \gamma_{th}). \quad (6.22)$$

In terms of integrals, this can be written as

$$p_r(g_0^2\gamma_1 + \gamma_2 \leq \gamma_{th}) = \int_0^{\gamma_{th}} \int_0^{\gamma_{th}-\gamma_1} f_{\gamma_1\gamma_2}(\gamma_1, \gamma_2) d\gamma_1 d\gamma_2, \quad (6.23)$$

where the quantity $\int_0^{\gamma_{th}-\gamma_1} f_{\gamma_1\gamma_2}(\gamma_1, \gamma_2) d\gamma_2$ is the joint PDF related to γ_1 and γ_2 . This quantity represents the PDF of the combiner SNR, $f_{\gamma_{mrc}}(\gamma_{mrc})$. The SNRs $g_0^2\gamma_1$ and γ_2 been independent, the joint PDF, $f_{\gamma_{mrc}}(\gamma_{mrc})$, is the product of single PDFs, $f_{\gamma_1}(\gamma_1)$ and $f_{\gamma_2}(\gamma_{th} - g_0^2\gamma_1)$, and given by

$$\begin{aligned} f_{\gamma_{mrc}}(\gamma_{mrc}) &= f_{\gamma_1}(\gamma_1) f_{\gamma_2}(\gamma_{th} - g_0^2\gamma_1) \\ &= \left[\frac{1}{g_0^2\bar{\gamma}_1} \exp\left\{ -\frac{g_0^2\gamma_1}{g_0^2\bar{\gamma}_1} \right\} \right] \left[\frac{1}{\bar{\gamma}_2} \exp\left\{ -\frac{(\gamma_{th} - g_0^2\gamma_1)}{\bar{\gamma}_2} \right\} \right] \\ &= \frac{1}{g_0^2\bar{\gamma}_1\bar{\gamma}_2} \exp\left\{ -\frac{g_0^2\gamma_1\bar{\gamma}_2 + g_0^2\bar{\gamma}_1(\gamma_{th} - g_0^2\gamma_1)}{g_0^2\bar{\gamma}_1\bar{\gamma}_2} \right\}. \end{aligned} \quad (6.24)$$

Finally, the outage probability is calculated as

$$\begin{aligned} P_o &= \int_0^{\gamma_{th}} f(\gamma_{mrc}) d\gamma_{mrc} \\ &= \int_0^{\gamma_{th}} f(\gamma_1) f(\gamma_{th} - g_0^2\gamma_1) d\gamma_1 \\ &= \int_0^{\gamma_{th}} \frac{1}{g_0^2\bar{\gamma}_1\bar{\gamma}_2} \exp\left\{ -\frac{g_0^2\gamma_1\bar{\gamma}_2 + g_0^2\bar{\gamma}_1(\gamma_{th} - g_0^2\gamma_1)}{g_0^2\bar{\gamma}_1\bar{\gamma}_2} \right\} d\gamma_1. \end{aligned} \quad (6.25)$$

After integration, the final MRC outage probability is expressed as

$$P_o = \frac{1}{g_0^2\bar{\gamma}_1} \left[\exp\left\{ \frac{\gamma_{th}}{\bar{\gamma}_2} - \left(\frac{\gamma_{th}}{\bar{\gamma}_2} + 1 \right) \right\} - \exp\left\{ -\left(\frac{\gamma_{th}}{\bar{\gamma}_2} + 1 \right) \right\} \right]. \quad (6.26)$$

6.4 Results of the analysis

The numerical results of this analysis are depicted in Figs. 6.9 to 6.20. They show the plots of Eqs. (6.20) and (6.26) for a few values of the threshold SNR, γ_{th} , for $g_0 = \{0.2, 0.4, 0.6, 0.8, 1\}$ and several combinations between γ_1 and γ_2 . The total noise that was exploited includes cross-talk and other types of additive noise in the environment as, shown in Eq. (6.10).

The outage probability of both MRC and SC are given in Figs. 6.9 and 6.10. The values used for the analyses are such as: $\gamma_{th} = \{3, 9, 15, 19, 25\}$ dB, a coupling circuit gain, $g_0 = 0.8$ and $\gamma_1 = \gamma_2$. The results show that γ_{th} does not play a major role in the probability of outage for an MRC situation in the system. This is shown in Fig. 6.9. On the contrary, the chosen value of γ_{th} plays an important role in the probability of error in the SC situation. In Fig. 6.10, several values of threshold were selected at $\gamma_{th} = 3$ dB. For MRC, shown in Fig. 6.9, changes in the graph are not noticeable. In Fig. 6.10 the best results of the SNR for SC were obtained at $\gamma_{th} = 3$ dB. This means that there is less noise in the channel and at that point the probability that the system will fail is 0.3. On the other hand, when $\gamma_{th} = 25$ dB, the outage probability is 0.6, which is higher and thus resulting in more noise in the channel. Noise in the channel is poorest when the SNR is lower than the threshold.

Results of the MRC situation for $g_0 = \{0.2, 0.4, 0.6, 0.8, 1\}$, for a fixed value of $\gamma_{th} = 9$ dB and $\gamma_1 = \gamma_2$, are depicted in Fig. 6.11. They show that the value of the coupling circuit gain clearly affects the probability of error in the MRC situation. Fig. 6.11 shows an error in the system because from 0 to 9 dB, the values of the SNR are below $\gamma_{th} = 9$ dB. This confirms that at high SNR, the system performs better. At $g_0 = 1$, the poorest noise occurs in the channel, and the best noise happens at $g_0 = 0.2$. This implies that for MRC, the higher the g_0 , the higher the noise in the channel. The opposite is also true. The reason for this concerns the filtering capacities of the coupling circuit. The same situation applies in Figs. 6.12, 6.13, 6.14 and 6.15.

The results of the MRC situation for $g_0 = \{0.2, 0.4, 0.6, 0.8, 1\}$, $\gamma_{th} = 9$ dB and $\gamma_1 = 3$ dB in Fig. 6.12 and $\gamma_1 = 15$ dB in Fig. 6.13. Both sub-figures confirm that the results of an MRC situation vary with g_0 . However, the performance at $\gamma_1 = 3$ dB will be better than in the case of $\gamma_1 = 15$ dB.

Figures 6.14 and 6.15 shows the variation of the outage probability in an MRC situation. Fig. 6.14 shows the various values of g_0 , when $\gamma_{th} = 9$ dB and $\gamma_2 = 3$ dB, while Fig. 6.15 shows the various values of g_0 , when $\gamma_{th} = 9$ dB and $\gamma_2 = 15$ dB. In addition to the confirmation of the effects of the coupling circuits on the probability of outage and errors, it is also clear that at $\gamma_2 = 15$ dB, the system performance will be deficient when compared to the case where $\gamma_2 = 3$ dB.

To show the probability of error in the proposed hybrid system in an SC situation, the results depicted in Fig. 6.16 are proposed. They show the variation of the outage

probability of the system for $g_0 = \{0.2, 0.4, 0.6, 0.8, 1\}$, $\gamma_{th} = 9$ dB and $\gamma_1 = \gamma_2$. It is clear that, as shown in Fig. 6.16, for $g_0 = 1$, the system performs better than in any other case and when $g_0 = 0.2$, the worse performance occurs. However, it can be stated that at $g_0 = 0.2$ there is more noise in the channel, and at $g_0 = 1$, there is less noise in the channel. It implies that the lower the g_0 , the higher the noise, and the higher the g_0 , the lower the noise in the channel. In the outage probability of SC depicted in Figs. 6.17, when the threshold (γ_{th}) is set at 9 dB, an error occurs in the SNR from 0 to 9 dB, which is below the threshold. However, from 10 to 30 dB, the noise situation is better. The same situation applies in Figs. 6.17, 6.18, 6.19 and 6.20.

The results of the SC situation for $g_0 = \{0.2, 0.4, 0.6, 0.8, 1\}$, $\gamma_{th} = 9$ dB, $\gamma_1 = 3$ dB in Fig. 6.17 and $\gamma_1 = 15$ dB in Fig. 6.18. Fig. 6.17 shows that g_0 does not play an important role in the error probability when $\gamma_1 = 3$ dB, this is not the case when $\gamma_1 = 15$ dB as depicted in Fig. 6.18.

Finally, a variation of the outage probability is shown for a selection combining situation of variable values of g_0 , $\gamma_{th} = 9$ dB and fixed values of γ_2 . For $\gamma_2 = 3$ dB in Fig. 6.19 and $\gamma_2 = 15$ dB in Fig. 6.20. Both figures show that the system performance is better when $\gamma_2 = 3$ dB when compared to the case where $\gamma_2 = 15$ dB.

Information in Figs. 6.11 and 6.16 is compared for MRC and SC. Figs. 6.11 gives the results of PLC-RF combining where the maximum ratio combining technique was used, while Figs. 6.16 provides the results for the same system based on selection combining. It should be borne in mind that the analysis of SC and MRC is given under the consideration that PLC and RF are asymmetric channels that operate with Rayleigh distributed. This explains the non-existence of the line of sight between the transmitter and the receiver. Both the SNRs, γ_{th} at MRC and SC are equal to 9 dB, where $\gamma_1 = \gamma_2$ at this point both are equal. The outage probability of the proposed system in this case, is analysed for five randomly selected values of coupling circuit gain $g_0 = \{0.2, 0.4, 0.6, 0.8, 1\}$. Fig. 6.11 shows that as the value of the selected g_0 increases, the value $\gamma_1 = \gamma_2$ should increase to the same outage probability. For example, to obtain an outage error of 1.0, about 4 dB of $\gamma_1 = \gamma_2$ is required when the needed quality of service (QoS) requires $g_0 = 0.8$. This confirms that the results of a MRC situation vary with g_0 , and furthermore, that the system performs better as g_0 increases as expected, with the best results being obtained when $g_0 = 1$. Fig. 6.16 shows that, as in the case in Fig. 6.11, high values of $\gamma_1 = \gamma_2$ are required to ensure the same outage probability when g_0 increases.

TABLE 6.1: HYBRID TECHNOLOGY ESTIMATED IMPLEMENTATION COST.

| | Circuitry | Cost |
|--------------------------------|-------------------------------|-----------------|
| PLC Circuitry | Power Supply | \$15.6 |
| | Modern Chip Set | \$18.20 |
| | Level Converter | \$15.00 |
| | Coupling Circuit | \$7.40 |
| | Miscellaneous | \$38.00 |
| | Total | \$94.20 |
| RF Circuitry | Power Supply | \$2.64 |
| | Chip Set | \$11.15 |
| | Sensor | \$5.67 |
| | Antenna | \$0.66 |
| | Crystal-Passive-Miscellaneous | \$8.98 |
| | Total | \$29.10 |
| Hybrid PLC/RF Circuitry | Power Supply | \$15.60 |
| | Modern Chip Set | \$29.35 |
| | Level Converter/Sensor | \$20.67 |
| | Coupling Circuit/Antenna | \$8.06 |
| | Crystal-Passive-Miscellaneous | \$46.98 |
| | Total | \$120.66 |

6.5 Hybrid technology estimated implementation cost

To analyse the costs of implementing hybrid technology, it is important to consider the cost of the electronic component for the PLC and RF in general since this has a significant influence on the price of the modem. In Table 6.1, the estimated cost of the RF components is \$ 29.10, which is cheaper than the estimated cost of the PLC components, viz. \$ 94.20. This can be linked to the fact the RF technology is more mature in comparison with the PLC technology, while PLC also requires a coupling circuit which may include a transformer. Both the PLC and RF will be controlled by a microcontroller, which will synchronise the communication modules of the two technologies. The combination of the PLC and RF components into a single module using a microcontroller will help to reduce the cost of the components. The estimated cost of a hybrid PLC/RF is \$ 120.66, which is high, but considering the quality of the signal achieved with a hybrid system, which shows better performance than a single RF and PLC, the additional cost can be justified.

6.6 Conclusion

This chapter aimed to analyse the outage probability of PLC-RF diversity combining. Two different techniques were exploited to analyse the probability of failure, namely selection combining and maximum ratio combining. In each cases, the expression of the system SNR was proposed, and the channel system was analyse using outage probability in terms of its PDF and its CDF, it should be noted that high values of E_b/N_0 are required in SC to achieve the same outage probability as is the case with MRC for a selected γ_{th} which corresponds to a specific QoS. However, in both cases, it is clear that since the quality of service requires high values of g_0 , the values of γ_1 and γ_2 should be increased because the system performs better as g_0 gradually increases from 0.2 to 1.



7

Conclusion

7.1 Employment of broadband communication technology in indoor environments: problems, procedures, and proposals for their solution

WiFi technology enjoys widespread popularity as a means of providing broadband connectivity to users in indoor environments. However, its application is not without difficulties, one of which is signal degradation in such settings. Furthermore and more generally, the restrained coverage provided by existing wireless hotspots indicates that there is a need to implement a new system by using a new approach, one that will facilitate development of the continuous-connectivity technology that the future will demand. In response to this and other problems, this thesis discusses hybrid power-line and radio frequency communication systems as alternative solutions to problems associated with PLC or RF. An approach has been developed to address the problem of low data rate performance in response to the need to meet future challenges that the Internet of Things will impose. Such solutions will also contribute to improving the efficiency and cost effectiveness of recent developments in broadband technological communication systems.

In addition to the foregoing, this thesis investigated various technologies and their enhancement, and described a variety of tools and methods in an effort to address the problems mentioned above. These include the following:

- A hybrid PLC-RF system was designed, and its performance investigated at a frequency of 2.45 GHz. This was undertaken with a view to its potential usefulness in

overcoming obstructions in indoor environments that RF penetrates with difficulty due to LOS issues.

- The effect of a coupling circuit in PLC-RF diversity at 2.45 GHz. was investigated. The resulting diversity of a PLC-RF modem when a coupling circuit was added at the PLC side, contributed to the achievement of a high data rate performance. Thus, a coupling circuit greatly influences system performance.
- PLC and RF for a parallel transmission at 2.45 GHz was analysed. The study showed that there is improved performance in data transmission in the indoor environment of multi-storey buildings.
- The outage probability of PLC-RF diversity combining was analysed. Two different techniques were exploited to analyse this probability of outage, viz. selection combining and maximum ratio combining. In each case, the expression of the system SNR was proposed, as well as its probability density function and its cumulative distribution function which lead to the probability of system outage. For both techniques, the expression of the system SNR was proposed. From this analysis, it could be determined that high values of E_b/N_0 are required for SC to achieve the same outage probability as is the case with MRC for a selected γ_{th} which corresponds to a specific QoS. In both cases, it was clear that because quality service requires high values of γ_{th} , the values of γ_1 and γ_2 should be increased.
- A channel model for PLC-RF diversity that operates at 2.45 GHz was proposed, and its transmission system was analysed with due regard for the effects of the couplers used in the PLC link. The proposed system and the incoming data were coded and modulated. The same signal was sent to both PLC and RF links but with different cyclic prefixes. On the PLC side, a coupling circuit was exploited to couple the message signal to the channel. The input and output CCs were connected to the PLC channel. In this study, it was assumed that the CCs (input and output) have the same gain. Various values of the gain achieved by the CC were selected for the simulation analysis.
- Initially, a basic introduction (see Chapters 1 and 2) to both power-line and radio frequency communication technologies was presented. The channel model for both PLC and RF that has been described in the literature was reviewed. The cascaded PLC-RF channels were investigated. The proposed model measurements

and frequency responses of the channels were presented. An outline was given of both PLC and RF channels. The three channels of the cascade system, together with the values of coefficient a_0 , a_1 and voltage 1st path RF were studied to predict the behaviour of the system. The imposed coefficient values of a_0 , a_1 and voltage 1st path RF for the PLC channel model influenced the simulation results and were recorded for the cascaded PLC-RF channel, with t . The corresponding values of $a_0 = 0.01$, 0.0001 , $a_1 = 20 \times 10^{-10}$ and 10×10^{-10} , and voltage 1st path RF = 0.05, 0.25, 0.55 and 0.85, over frequencies of up to 3 GHz were also given. Finally, the costing impact of a PLC-RF diversity system that operates at 2.45 GHz was discussed.

- This research was also undertaken to prove that the power-line conductively carries and re-radiates 2.45 GHz WiFi signals over a distance. Commercial WiFi modems (IEEE 802.11g protocol) were used to transfer data on a power line for up to 65 m (non-energised), and for up to 20 m in a typical industrial energised situation. One modem was coupled to a power line which was used as a traveling-wave antenna. The second modem was used in normal RF mode. This was compared to a direct RF link where both modems are used in RF mode. The industrial indoor measurements (energised power line) show that the RF link has higher data transfer rates than the contactless PLC. This might differ in situations where there are more severe obstructions, a matter for further investigation because of the difficulty experienced by WiFi in penetrating obstructing items in multi-storey buildings. Such an investigation should also be conducted because this study showed that in an ideal situation, power-line communications at 2.45 GHz are not only possible, but comparable with direct-link RF communications.
- To introduce the experimental exercise, the speed of the data transfer rate using a control contactless cable power line for transmission and reception at 2.45 GHz in a residential building was discussed. The actual exercise was based on a simple transfer rate in an Mbps vs. floor relationship. The experiment has been shown to be more accurate when the different floors and dissimilar areas within a residential building are considered separately. The results indicated that a change in the speed of the data transfer rate depends on the position of the receiver. It was also demonstrated that the nearer the transmitter to the receiver, the faster the transfer speed, and vice versa, which implies that a power-line cable can be used as a long-wire antenna. From the results it was possible to prove that a power-line cable can radiate in the high levels of radio frequency energy at 2.45 GHz.

7.2 Contributions and applications of the study to developments in broadband communication technology

A PLC-RF system in which the end-user is mobile because of the contactless aspect of the system at 2.45 GHz, was proposed. The system was subsequently analysed, and a channel model together with its frequency response were thereafter proposed. The transmission medium was analysed on the PLC side and the transmission capability defined with regard to the types of wire used. The system was implemented practically and the radiated signal strength and feasible data rates for both RF and PLC were measured separately. It was possible to prove that a power line can be used to conductively carry and re-radiate 2.45 GHz WiFi signals over a distance. This led to the conclusion that in an indoor environment where PLC or RF are used, the effect of signal degradation occurs at any point in time because the signals are unable to penetrate the walls for RF and the effect of noise for PLC. This is likely to be useful in projects where a conventional RF line of sight operation at 2.45 GHz is obscured, for example in multi-storey buildings where WiFi has difficulty penetrating various obstacles.

This study showed that the quality of a communication service in an indoor environment was improved with the application of a diversity system. This was achieved by using two different technologies (PLC and RF) for end-to-end communication. This configuration is likely to be very useful in situations where line of sight is obscured, and direct-link RF communication is impaired, as well as in situations of PLC obstruction resulting from noise, for example inside buildings with thick walls or between floors, in Internet broadcasting, and from noise associated with mobile connectivity.

It should be noted that the work proposed in this thesis is part of a pilot project consisting of a number of steps. The first step is the proposition of the system and its analysis. The second step concerns validation of the results with practical implementation, and the third step will consist of prototyping. The prototypes can then be introduced to manufacturing companies to consider the possibility of large-scale commercial production.

7.3 Suggestions for future research

One of the aims of this study was to determine realistic outage probability and to implement an adaptive modulation scheme for PLC and RF systems, using MRC and SC diversity systems. A matter for future research would be to use the same procedure for MIMO systems, using MIMO PLC and RF systems because this will increase signal options, and thus improve signal performance. Based on the findings of this thesis, it is likely to be easier to perform a simulation of a multiple-input system. The channel frequency response results given in Chapters 4 suggest that there is also a need to investigate the channel capacity of both PLC and RF systems using the same terminology. Such an investigation might help to provide greater insight into channel performance. A statistical model such as that used in this study could form the motivation for developing a special hybrid PLC-RF which will contribute to an analysis of channel bandwidth and its operating frequency.

In Chapter 5, measurements of PLC and RF were taken in a laboratory setting and in a residential building. In future research, extensive measuring using the same approach as in the aforementioned settings could be conducted in similar areas, such as other types of residential buildings, different offices, and in workshop areas. This might constitute a feasible topic for investigation.

The outage probability of the PLC-RF system proposed in this study was verified in Chapter 6. However, the measurements described in Chapter 6 have not been practically verified, and there is therefore a need to perform practical measurements which will help to predict the outage probability of both the PLC/RF and the SC/MRC diversity systems. This matter too could receive attention in future.

In addition, the analytical curves are presented in the work from the derived expressions. However, in future Monte Carlo simulations will be carry out and the result will be compare against the analytical ones in order to verify the accuracy of the proposed mathematical framework.

More experiments should be conducted to investigate the limitation in radiation at 2.45 GHz frequency for both the LOS and NLOS environments. There is also a need to investigate the exiting transmitting power and to check the radiation distance for a power-line cable at 2.45 GHz.

References

- [1] K.-L. Du and M. N. Swamy, *Wireless communication systems: from RF subsystems to 4G enabling technologies*. Cambridge University Press, 2010.
- [2] S. Güzelgöz, H. Arslan, A. Islam, and A. Domijan, “A review of wireless and PLC propagation channel characteristics for smart grid environments,” *J. Elect. Comput. Eng.*, vol. 2011, p. 15, 2011.
- [3] S. Güzelgöz, H. B. Celebi, and H. Arsian, “Analysis of a multi-channel receiver: Wireless and PLC reception,” in *Proc. 18th IEEE Sig. Process. Conf.*, Aalborg, Denmark., Aug. 2010, pp. 1106–1110.
- [4] T. R. Oliveira, C. A. Marques, M. S. Pereira, S. L. Netto, and M. V. Ribeiro, “The characterization of hybrid PLC-wireless channels: A preliminary analysis,” in *Proc. 17th IEEE ISPLC Conf.*, Johannesburg, South Africa., Apr. 2–4 2013, pp. 98–102.
- [5] L. de MBA Dib, V. Fernandes, M. d. L. Filomeno, and M. V. Ribeiro, “Hybrid PLC/wireless communication for smart grids and internet of things applications,” *IEEE Internet Things J.*, vol. 5, no. 2, pp. 655–667, 2018.
- [6] A. R. Ndjiongue, H. C. Ferreira, J. Song, F. Yang, and L. Cheng, “Hybrid PLC-VLC channel model and spectral estimation using a nonparametric approach,” *Wiley Trans. Emerg. Telecommun. Techn.*, vol. 28, no. 12, 2017.
- [7] A. R. Ndjiongue, T. M. Ngatched, and H. C. Ferreira, “On the indoor VLC link evaluation based on the Rician K -Factor,” *IEEE Commun. Lett.*, vol. 22, no. 11, pp. 2254–2257, 2018.
- [8] Y. Qian, J. Yan, H. Guan, J. Li, X. Zhou, S. Guo, and D. N. K. Jayakody, “Design of hybrid wireless and power line sensor networks with dual-interface relay in IoT,” *Internet Things J.*, vol. 6, no. 1, pp. 239–249, 2017.
- [9] T. Samakande, T. Shongwe, A. de Beer, and H. Ferreira, “The effect of coupling circuits on impulsive noise in power line communication,” in *Proc. 22nd IEEE ISPLC Conf.*, Manchester, UK., Apr. 8 – 11 2018, pp. 1–5.

-
- [10] A. Aragon-Zavala, *Antennas and propagation for wireless communication systems*. John Wiley & Sons, 2008.
 - [11] D. W. Browne, J. Medbo, H. Asplund, and J.-E. Berg, "A simple approach to site sensitive modeling of indoor radio propagation," in *IEEE VTC Spring 55th Vehicular Techn. Conf.*, vol. 1, 2002, pp. 384–388.
 - [12] H. K. Chung and H. L. Bertoni, "Indoor propagation characteristics at 5.2 GHz in home and office environments," *IEEE J. Commun. Net.*, vol. 4, no. 3, pp. 176–188, 2002.
 - [13] I. Cuinas and M. G. Sanchez, "Measuring, modeling, and characterizing of indoor radio channel at 5.8 GHz," *IEEE Trans. Veh. Techn.*, vol. 50, no. 2, pp. 526–535, 2001.
 - [14] W. Honcharenko, H. L. Bertoni, J. L. Dailing, J. Qian, and H. Yee, "Mechanisms governing UHF propagation on single floors in modern office buildings," *IEEE Trans. Veh. Techn.*, vol. 41, no. 4, pp. 496–504, 1992.
 - [15] S. Loredó, L. Valle, and R. P. Torres, "Accuracy analysis of GO/UTD radio-channel modeling in indoor scenarios at 1.8 and 2.5 GHz," *IEEE Antennas and Propagation Mag.*, vol. 43, no. 5, pp. 37–51, 2001.
 - [16] J. Medbo and J.-E. Berg, "Spatio-temporal channel characteristics at 5 GHz in a typical office environment," in *IEEE VTS 54th Vehicular Techn. Conf.*, vol. 3, Atlantic City, NJ, USA, Oct. 7–11 2001, pp. 1256–1260.
 - [17] D. Porrat and D. C. Cox, "UHF propagation in indoor hallways," *IEEE Trans. Wireless Commun.*, vol. 3, no. 4, pp. 1188–1198, 2004.
 - [18] S. Y. Seidel and T. S. Rappaport, "Site-specific propagation prediction for wireless in-building personal communication system design," *IEEE Trans. Veh. Techn.*, vol. 43, no. 4, pp. 879–891, 1994.
 - [19] J. Tarng, W. Chang, and B. Hsu, "Three-dimensional modeling of 900-MHz and 2.44 GHz radio propagation in corridors," *IEEE Trans. Veh. Techn.*, vol. 46, no. 2, pp. 519–527, 1997.
 - [20] T. Rappaport, "Safari books online (firme)," *Wireless commun.: principles and practice*, vol. 2.
 - [21] H. L. Bertoni, *Radio propagation for modern wireless systems*. Pearson Education, 1999.
 - [22] D. Molkdar, "Review on radio propagation into and within buildings," in *IET Proc. Microwaves, Antennas and Propagation*, vol. 138, no. 1, 1991, pp. 61–73.
 - [23] A. Aragón-Zavala, *Indoor Wireless Communications: From Theory to Implementation*. John Wiley & Sons, 2017.

-
- [24] A. Al-Samman, T. Al-Hadhrani, A. Daho, M. Hindia, M. Azmi, K. Dimyati, M. Alazab, *et al.*, “Comparative study of indoor propagation model below and above 6 GHz for 5G wireless networks,” *Electronics*, vol. 8, no. 1, p. 44, 2019.
- [25] M. Kumari, T. Yadav, P. Yadav, P. K. Sharma, and D. Sharma, “Comparative study of path loss models in different environments,” *Int. J. Eng. Sci. Tech. (IJEST)*, vol. 3, no. 4, pp. 2945–2949, 2011.
- [26] P. Kaur, D. S. Rani, and O. Singh, “High pass digital fir filter design using differential evolution,” *Int. J. of Adv. Research in Comput. Sci. Softw. Eng.*, vol. 5, no. 5, 2015.
- [27] M. K. Simon and M.-S. Alouini, *Digital communication over fading channels*. John Wiley & Sons, 2005, vol. 95.
- [28] D. J. Boomgaard, “Power line communication system,” Feb. 20 1990, US Patent 4,903,006.
- [29] W. M. Brown and R. T. Dunn, “Telephone extension system utilizing power line carrier signals,” Jan. 22 1985, US Patent 4,495,386.
- [30] J. M. Kennon, “Wireless power line communication apparatus,” Feb. 17 1987, US Patent 4,644,321.
- [31] F. Zwane, “Power line communication channel modelling.” Ph.D. dissertation, 2014.
- [32] M. S. Yousuf and M. El-Shafei, “Power line communications: An overview-part i,” in *2007 Innovations in Inf. Tech. (IIT)*. IEEE, 2007, pp. 218–222.
- [33] K. Dostert, “Telecommunications over the power distribution grid—possibilities and limitations,” *IIR-Powerline*, vol. 6, no. 97, 1997.
- [34] B. Baraboi *et al.*, “Narrow band power line communication, applications and challenges,” *Ariane Controls Inc, Québec*, 2013.
- [35] A. H. Vinck and G. Lindell, “Summary of contributions at ISPLC 1997-2001,” in *Proc. 5th IEEE ISPLC Conf.*, 2001, pp. 383–413.
- [36] Y. Ma, P. So, and E. Gunawan, “Comparison of CDMA and OFDM systems for broadband power line communications,” *IEEE Trans. power delivery*, vol. 23, no. 4, pp. 1876–1885, 2008.
- [37] H. Philips, “Modelling of powerline communication channels,” in *Proc. 3rd IEEE ISPLC Conf.*, Lancaster, UK, May. 30 1999, pp. 14–21.
- [38] M. Zimmermann and K. Dostert, “A multipath model for the powerline channel,” *IEEE Commun. Lett.*, vol. 50, no. 4, pp. 553–559, 2002.

-
- [39] T. Esmailian, F. Kschischang, and P. Gulak, "An in-building power line channel simulator," in *Proc. 6th IEEE ISPLC Conf.*, Athens, Greece, May. 27–29 2002, pp. 27–29.
- [40] A. M. Tonello and F. Versolatto, "Bottom-up statistical plc channel modeling part i: Random topology model and efficient transfer function computation," *IEEE Trans. Power Delivery*, vol. 26, no. 2, pp. 891–898, 2011.
- [41] A. M. Tonello, F. Versolatto, B. Béjar, and S. Zazo, "A fitting algorithm for random modeling the PLC channel," *IEEE Trans. Power Delivery*, vol. 27, no. 3, pp. 1477–1484, 2012.
- [42] H. C. Ferreira, L. Lampe, J. Newbury, and T. G. Swart, *Power line communications: theory and applications for narrowband and broadband communications over power lines*. John Wiley & Sons, 2011.
- [43] M. Ardakani, G. Colavolpe, K. Dostert, H. Ferreira, D. Fertoni, T. Swart, A. Tonello, D. Umehara, and A. Vinck, "Digital transmission techniques," *Power Line Communications: Theory and Applications for Narrowband and Broadband Commun. over Power Lines*, pp. 195–310, 2010.
- [44] M. Koch, "Power line communications and hybrid systems for home networks," in *Ecological Design of Smart Home Networks*. Elsevier, 2015, pp. 17–28.
- [45] J. Anatory, N. Theethayi, R. Thottappillil, M. M. Kissaka, and N. H. Mvungi, "Broadband power-line communications: The channel capacity analysis," *IEEE Trans. power delivery*, vol. 23, no. 1, pp. 164–170, 2008.
- [46] P. Meier, M. Bittner, H. Widmer, J. Bermudez, A. Vukicevic, M. Rubinstein, F. Rachidi, M. Babic, and J. S. Miravalles, "Pathloss as a function of frequency, distance and network topology for various LV and MV european powerline networks," *The OPERA Consortium, Project Deliverable, EC/IST FP6 Project*, no. 507667, p. D5v0, 2005.
- [47] *MIMO power line communications: narrow and broadband standards, EMC, and advanced processing*.
- [48] A. R. Ndjiongue, T. Shongwe, H. C. Ferreira, T. N. Ngatched, and A. H. Vinck, "Cascaded PLC-VLC channel using OFDM and CSK techniques," in *Proc. IEEE GLOBECOM Conf.*, San Diego, CA, USA, Dec. 6–10 2015, pp. 1–6.
- [49] E. Biglieri, "Coding and modulation for a horrible channel," *IEEE Commun. Mag.*, vol. 41, no. 5, pp. 92–98, 2003.
- [50] A. M. Tonello and T. Zheng, "Bottom-up transfer function generator for broadband PLC statistical channel modeling," in *Proc. 13th IEEE ISPLC Conf.*, Dresden, Germany, Mar. 29 - Apr. 1 2009, pp. 7–12.

-
- [51] M. Zimmermann and K. Dostert, "An analysis of the broadband noise scenario in powerline networks," in *Proc. 17th IEEE ISPLC Conf.*, Johannesburg, South Africa, Mar. 24–27 2013, pp. 131–138.
- [52] H. C. Ferreira, L. Lampe, J. Newbury, and T. G. Swart, *Power Line Communications: Theory and Applications for Narrowband and Broadband Communications over Power Lines*. John Wiley & Sons, Ltd, 2010.
- [53] J. Cortes, L. Diez, F. Canete, and J. Sanchez-Martinez, "Analysis of the indoor broadband power-line noise scenario," *IEEE Trans. Electromagn. Compat.*, vol. 52, no. 4, pp. 849–858, Nov. 2010.
- [54] T. Shongwe, A. Vinck, and H. C. Ferreira, "On impulse noise and its models," in *Proc. 18th IEEE ISPLC Conf.*, Glasgow, Scotland, UK, Mar. 30–Apr. 2, 2014, pp. 12–17.
- [55] —, "A study on impulse noise and its models," *SAIEE Research J.*, vol. 106, no. 3, pp. 119–131, Sep. 2015.
- [56] P. Meier, M. Bittner, H. Widmer, J. Bermudez, A. Vukicevic, M. Rubinstein, F. Rachidi, M. Babic, and J. S. Miravalles, "Pathloss as a function of frequency, distance and network topology for various LV and MV european powerline networks," *The OPERA Consortium, Project Deliverable, EC/IST FP6 Project*, no. 507667, p. D5v0, 2005.
- [57] T. Esmailian, F. Kschischang, and P. Glenn, "In-building power lines as high-speed communication channels: Channel characterization and a test channel ensemble," *Int. J. Commun. Syst.*, vol. 16, no. 5, pp. 381–400, May 2003.
- [58] L. Di Bert, P. Caldera, D. Schwingshackl, and A. Tonello, "On noise modeling for power line communications," in *Proc. 15th IEEE ISPLC Conf.*, Udine, Italy, Apr. 3–6, 2011, pp. 283–288.
- [59] A. Kawaguchi, H. Okada, T. Yamazato, and M. Katayama, "Correlations of noise waveforms at different outlets in a power-line network," in *Proc. 10th IEEE ISPLC Conf.*, Orlando, FL., USA, Mar. 26–29, 2006, pp. 92–97.
- [60] L. de MBA Dib, V. Fernandes, and M. V. Ribeiro, "A discussion about hybrid PLC-wireless communication for smart grids," *Proc. XXXIV Simpósio Brasileiro de Telecomunicações*, pp. 848–852, 2016.
- [61] M. Heggo, X. Zhu, S. Sumei, and Y. Huang, "White broadband power line communication: Exploiting the TVWS for indoor multimedia smart grid applications," *Int. J. Commun. Syst.*, vol. 30, no. 16, p. e3330, May.
- [62] M. Sayed, T. A. Tsiftsis, and N. Al-Dhahir, "On the diversity of hybrid narrowband-PLC/wireless communications for smart grids," *IEEE Trans. Wireless Commun.*, vol. 16, no. 7, pp. 4344–4360, Apr. 2017.

-
- [63] M. Hoch, "Comparison of PLC G3 and prime," in *Proc. 15th IEEE ISPLC Conf.*, Udine, Italy, Apr. 3–6 2011, pp. 165–169.
- [64] D. Schneider, A. Schwager, W. Bäschlin, and P. Pagani, "European MIMO PLC field measurements: Channel analysis," in *Proc. 16th IEEE ISPLC Conf.*, Beijing, China, Mar. 27–30 2012, pp. 304–309.
- [65] B. Nikfar and A. H. Vinck, "Combining techniques performance analysis in spatially correlated MIMO-PLC systems," in *Proc. 17th IEEE ISPLC Conf.*, Johannesburg, South Africa, Mar. 24–27 2013, pp. 1–6.
- [66] D. Schneider, A. Schwager, J. Speidel, and A. Dilly, "Implementation and results of a MIMO PLC feasibility study," in *Proc. 15th IEEE ISPLC Conf.*, Udine, Italy, Apr. 3–6 2011, pp. 54–59.
- [67] M. Ju and I.-M. Kim, "Error probabilities of noncoherent and coherent FSK in the presence of frequency and phase offsets for two-hop relay networks," *IEEE Trans. Commun.*, vol. 57, no. 8, 2009.
- [68] A. Ndjiongue, H. C. Ferreira, K. Ouahada, and A. H. Vinckz, "Low-complexity SOCPBFSK-OOK interface between PLC and VLC channels for low data rate transmission applications," in *Proc. 18th IEEE ISPLC Conf.*, Glasgow, UK, Mar. 30–Apr. 2 2014, pp. 226–231.
- [69] T. Schaub, "Spread frequency shift keying," *IEEE Trans. commun.*, vol. 42, no. 234, pp. 1056–1064, 1994.
- [70] E. Sozer, J. Proakis, R. Stojanovic, J. Rice, A. Benson, and M. Hatch, "Direct sequence spread spectrum based modem for under water acoustic communication and channel measurements," in *IEEE Riding the Crest into the 21st Century*, vol. 1, 1999, pp. 228–233.
- [71] V. Fernandes, H. V. Poor, and M. V. Ribeiro, "Analyses of the incomplete low-bit-rate hybrid PLC-Wireless single-relay channel," *IEEE Internet of Things J.*, Jan. 2018.
- [72] V. Fernandes, W. A. Finamore, H. V. Poor, and M. V. Ribeiro, "The low-bit-rate hybrid power line/wireless single-relay channel," *IEEE Syst. J.*, no. 99, pp. 1–12, Dec. 2017.
- [73] M. L. G. Salmento, A. Camponogara, L. M. de Andrade Filho, and M. V. Ribeiro, "A novel synchronization scheme for impulsive UWB-based PLC systems," *IEEE Latin America Trans.*, vol. 15, no. 11, pp. 2050–2058, Oct. 2017.
- [74] L. de MBA Dib, V. Fernandes, M. d. L. Filomeno, and M. V. Ribeiro, "Hybrid PLC/wireless communication for smart grids and internet of things applications," *IEEE Internet Things J.*, Oct. 2017.

- [75] M. L. G. Salmento, E. P. de Aguiar, Â. Camponogara, and M. V. Ribeiro, "An enhanced receiver for an impulsive UWB-based PLC system for low-bit rate applications," *Dig. Sig. Process.*, vol. 70, pp. 145–154, Nov. 2017.
- [76] A. Khreishah, S. Shao, A. Gharaibeh, M. Ayyash, H. Elgala, and N. Ansari, "A hybrid RF-VLC system for energy efficient wireless access," *IEEE Trans. Green Commun. and Netw.*, vol. 2, no. 4, pp. 932–944, 2018.
- [77] M. Z. Chowdhury, M. K. Hasan, M. Shahjalal, M. T. Hossan, and Y. M. Jang, "Optical wireless hybrid networks for 5G and beyond communications," in *Proc. Int. Conf. Inf. Commun. Techn. Convergence (ICTC)*, 2018, pp. 709–712.
- [78] S. W. Lai and G. G. Messier, "Using the wireless and PLC channels for diversity," *IEEE Trans. Commun.*, vol. 60, no. 12, pp. 3865–3875, Dec. Dec. 2012.
- [79] A. Dubey, R. K. Mallik, and R. Schober, "Performance analysis of a power line communication system employing selection combining in correlated log-normal channels and impulsive noise," *IET Commun.*, vol. 8, no. 7, pp. 1072–1082, May. 2014.
- [80] T. R. Oliveira, A. A. Picorone, C. B. Zeller, S. L. Netto, and M. V. Ribeiro, "On the statistical characterization of hybrid PLC-wireless channels," *Electr. Power Syst. Research*, vol. 163, pp. 329–337, 2018.
- [81] T. R. Oliveira, F. J. Andrade, L. G. d. S. Costa, M. S. Pereira, and M. V. Ribeiro, "Measurement of hybrid PLC-wireless channels for indoor and broadband data communication," *Proc. XXXI Simposio Brasileiro de Telecommun.*, 2013.
- [82] M. Sayed and N. Al-Dhahir, "Differential modulation diversity combining for hybrid narrowband-powerline/wireless smart grid communications," in *Proc. IEEE Global Conf. on sig. process*, 2016, pp. 876–880.
- [83] W. Gheth, K. M. Rabie, B. Adebisi, M. Ijaz, G. Harris, and A. Alfitouri, "Hybrid power-line/wireless communication systems for indoor applications," in *Proc. 11th IEEE Int. Symp. on Commun Sys., Netw. & Digital Sig. Process.*, Budapest, Hungary., Jul. 18 – 20 2018, pp. 1–6.
- [84] M. Sayed and N. Al-Dhahir, "Narrowband-PLC/wireless diversity for smart grid communications," in *Proc. IEEE GLOBECOM Conf.*, Austin, TX, USA, Dec. 8 –12 2014, pp. 2966–2971.
- [85] S. W. Lai, N. Shabehpour, G. G. Messier, and L. Lampe, "Performance of wireless/power line media diversity in the office environment," in *Proc. IEEE GLOBECOM Conf.*, Austin, TX, USA, Dec. 8 –12 2014, pp. 2972–2976.
- [86] A. De Beer, F. Igboamalu, A. Sheri, H. Ferreira, and A. H. Vinck, "Contactless power line communications at 2.45 GHz," in *Proc. 20th IEEE ISPLC Conf.*, Bottrop, Germany, Apr. 3–6 2016, pp. 42–45.

-
- [87] A. De Beer, H. Ferreira, and A. H. Vinck, "Contactless power-line communications," in *Proc. 18th IEEE ISPLC Conf.*, Glasgow, Scotland, UK., Mar. 30–Apr. 2, 2014, pp. 111–115.
- [88] Q. Pan and R. Kumar, "2.4 GHz propagation characteristics of power line cable," in *Symposium on Wireless Tech. and Applications (ISWTA)*., Langkawi, Malaysia., Sept. 2011, pp. 133–136.
- [89] Q. Pan and A. Kathnaur, "Power-line networks to extend ranges of 2.4 GHz wireless communications inside multi-storey buildings," in *Radio and Wireless Symposium (RWS)*, New Orleans, LA, USA., Jun. 2010, pp. 621–624.
- [90] H. Meng, S. Chen, Y. Guan, C. Law, P. So, E. Gunawan, and T. Lie, "A transmission line model for high-frequency power line communication channel," in *Power Sys. Tech., Proc. PowerCon. Int. Conf.*, vol. 2. IEEE, 2002, pp. 1290–1295.
- [91] J. R. Marti, "Accurate modeling of frequency-dependent transmission lines in electromagnetic transient simulations," *IEEE Trans. power apparatus and syst.*, no. 1, pp. 147–157, 1982.
- [92] O. Bilal, E. Liu, Y. Gao, and T. O. Korhonen, "Design of broadband coupling circuits for power line communication," in *Proc. 8th IEEE ISPLC Conf.*, Jan. 2004, pp. 1290–1295.
- [93] D. N. Zmood, D. G. Holmes, and G. H. Bode, "Frequency-domain analysis of three-phase linear current regulators," *IEEE Trans. Ind. Appl.*, vol. 37, no. 2, pp. 601–610, 2001.
- [94] M. Yousefbeiiki, O. N. Alrabadi, and J. Perruisseau-Carrier, "Efficient MIMO transmission of PSK signals with a single-radio reconfigurable antenna," *IEEE Trans. Commun.*, vol. 62, no. 2, pp. 567–577, 2014.
- [95] A. J. Poggio and E. K. Miller, *Integral equation solutions of three-dimensional scattering problems*. MB Assoc., 1970.
- [96] C. A. Balanis, "Antenna theory: A review," *Proc. IEEE*, vol. 80, no. 1, pp. 7–23, 1992.
- [97] D. Rutledge, S. Schwarz, and A. Adams, "Infrared and submillimetre antennas," *Infrared Physics*, vol. 18, no. 5-6, pp. 713–729, 1978.
- [98] A. Reiderman, "Method and apparatus of using magnetic material with residual magnetization in transient electromagnetic measurement," Apr. 30 2013, uS Patent 8,432,167.
- [99] R. Perez, *Handbook of electromagnetic compatibility*. Academic Press, 2013.

-
- [100] M. Philipose, J. R. Smith, B. Jiang, A. Mamishev, S. Roy, and K. Sundara-Rajan, "Battery-free wireless identification and sensing," *IEEE Pervasive comput.*, vol. 4, no. 1, pp. 37–45, 2005.
- [101] W. L. Stutzman and G. A. Thiele, *Antenna theory and design*. John Wiley & Sons, 2013.
- [102] S. Yang and H. Cha, "An empirical study of antenna characteristics toward RF-based localization for IEEE 802.15. 4 sensor nodes," in *European Conf. Wireless Sensor Net.* Springer, 2007, pp. 309–324.
- [103] W. Sörgel and W. Wiesbeck, "Influence of the antennas on the ultra-wideband transmission," *EURASIP J. Adv. Sig. Process.*, vol. 2005, no. 3, p. 843268, 2005.
- [104] Z. Jacob, L. V. Alekseyev, and E. Narimanov, "Optical hyperlens: far-field imaging beyond the diffraction limit," *Opt. express*, vol. 14, no. 18, pp. 8247–8256, 2006.
- [105] C. A. Balanis, *Advanced engineering electromagnetics*. John Wiley & Sons, 1999.
- [106] R. Sunyaev and Y. B. Zel'Dovich, "Microwave background radiation as a probe of the contemporary structure and history of the universe," *Annual Review of Astronomy and Astrophysics*, vol. 18, no. 1, pp. 537–560, 1980.
- [107] E. K. Miller and J. A. Landt, "Direct time-domain techniques for transient radiation and scattering from wires," *Proc. IEEE*, vol. 68, no. 11, pp. 1396–1423, 1980.
- [108] R. Corkish, M. Green, and T. Puzzer, "Solar energy collection by antennas," *Solar Energy*, vol. 73, no. 6, pp. 395–401, 2002.
- [109] C. A. Balanis, *Antenna theory: analysis and design*. John Wiley & Sons, 2016.
- [110] A. Orlandi, "Advanced engineering electromagnetics (balanis, ca; 2012) [book review]," *IEEE Electromagn Compatibility Mag.*, vol. 4, no. 4, pp. 47–47.
- [111] B. Sklar, "Rayleigh fading channels in mobile digital communication systems. i. characterization," *IEEE Commun. Mag.*, vol. 35, no. 7, pp. 90–100, 1997.
- [112] T. S. Rappaport, J. N. Murdock, and F. Gutierrez, "State of the art in 60-GHz integrated circuits and systems for wireless communications," *Proc. IEEE*, vol. 99, no. 8, pp. 1390–1436, 2011.
- [113] S. Dharmraj, A. Rastogi, and H. Katiyar, "Overview of diversity combining techniques & cooperative relaying in wireless communication."
- [114] N. Agrawal and P. K. Sharma, "Outage analysis of selection combining based hybrid wireless plc system," in *9th Int. Conf. on Computing, Commun. and Net. Techn. (ICCCNT)*, pp. 1–5.

-
- [115] M. S. Modabbes and S. Nasri, "Bit error rate analysis for BPSK modulation in presence of noise and two co-channel interferers," *IJCSNS*, vol. 10, no. 5, p. 152, May 2010.
- [116] M. Divya, "Bit error rate performance of BPSK modulation and OFDM-BPSK with rayleigh multipath channel," *Int. J. of Eng. Adv. Techno.*, vol. 2, no. 4, pp. 623–626, 2013.
- [117] A. Shah and A. M. Haimovich, "Performance analysis of maximal ratio combining and comparison with optimum combining for mobile radio communications with cochannel interference," *IEEE Trans. Veh. Tech.*, vol. 49, no. 4, pp. 1454–1463, 2000.
- [118] P. Z. Peebles Jr, "Digital communication systems," *Englewood Cliffs, NJ, Prentice-Hall, Inc., 1987, 445 p.*, 1987.
- [119] A. J. Paulraj, D. A. Gore, R. U. Nabar, and H. Bolcskei, "An overview of MIMO communications-a key to gigabit wireless," *Proc. IEEE*, vol. 92, no. 2, pp. 198–218, 2004.
- [120] S. Roy, J. R. Foerster, V. S. Somayazulu, and D. G. Leeper, "Ultrawideband radio design: The promise of high-speed, short-range wireless connectivity," *Proc. IEEE*, vol. 92, no. 2, pp. 295–311, 2004.
- [121] J. Mietzner, R. Schober, L. Lampe, W. H. Gerstacker, and P. A. Hoeher, "Multiple-antenna techniques for wireless communications-a comprehensive literature survey," *IEEE. Commun. Sur. & tut.*, vol. 11, no. 2, 2009.
- [122] K. Feher, *Wireless digital communications: modulation & spread spectrum applications*. Prentice-Hall, Inc., 1995.
- [123] H. Hourani, "An overview of diversity techniques in wireless communication systems," *IEEE JSAC*, pp. 1200–5, 2004.
- [124] T. S. Rappaport *et al.*, *Wireless communications: principles and practice*. prentice hall PTR New Jersey, 1996, vol. 2.
- [125] D. Mitiae, "An overview and analysis of BER for three diversity techniques in wireless communication systems," *Yugoslav J. Operations Research*, vol. 25, no. 2, 2016.
- [126] N. Kaur and G. Nanak, "SNR and BER performance analysis of MRC and EGC receivers over rayleigh fading channel," *Int. J. Comput. Appl.*, vol. 132, no. 9, pp. 12–17, 2015.
- [127] P. Patel and D. Dalwadi, "Channel estimation of various communication system with different modulation technique," *Int. J. of Adv. Research in Comput. Sci. Softw. Eng.*, vol. 4, no. 1, 2014.

-
- [128] D. A. Zogas, G. K. Karagiannidis, and S. A. Kotsopoulos, "Equal gain combining over Nakagami-n (Rice) and Nakagami-q (Hoyt) generalized fading channels," *IEEE Trans. Wireless Commun.*, vol. 4, no. 2, pp. 374–379, 2005.
- [129] T. Eng, N. Kong, and L. B. Milstein, "Comparison of diversity combining techniques for Rayleigh-fading channels," *IEEE Trans. commun.*, vol. 44, no. 9, pp. 1117–1129, 1996.
- [130] A. S. de Beer, A. Sheri, H. C. Ferreira, and A. H. Vinck, "Channel frequency response for a low voltage indoor cable up to 1 GHz," in *Proc. 22nd IEEE ISPLC Conf.*, Manchester, UK., Apr. 2018, pp. 1–6.
- [131] L. G. da Silva Costa, A. C. M. de Queiroz, B. Adebisi, V. L. R. da Costa, and M. V. Ribeiro, "Coupling for power line communications: A survey," *J. Commun. Inf. Sys.*, vol. 32, no. 1, 2017.
- [132] H. Ferreira, L. Lampe, J. Newbury, and T. Swart, "Broadband plc: Theory and applications for narrowband and broadband communications over power lines," 2010.
- [133] M. A. Panjwani, A. L. Abbott, and T. S. Rappaport, "Interactive computation of coverage regions for wireless communication in multifloored indoor environments," *IEEE J. Sel. Areas Commun.*, vol. 14, no. 3, pp. 420–430, 1996.
- [134] L. Dossi, G. Tartara, and F. Tallone, "Statistical analysis of measured impulse response functions of 2.0 GHz indoor radio channels," *IEEE J. Sel. Areas Commun.*, vol. 14, no. 3, pp. 405–410, 1996.
- [135] H. C. Ferreira, H. M. Grové, O. Hooijen, and A. Han Vinck, *Power line communication*. Wiley Online Library, 2010.
- [136] D. Tse and P. Viswanath, *Fundamentals of wireless communication*. Cambridge university press, 2005.
- [137] M. A. Youssefi, N. Bounouader, Z. Guennoun, and J. El Abbadi, "Adaptive switching between space-time and space-frequency block coded OFDM systems in rayleigh fading channel," *Int. J. of Commun., Netw. and Syst. Sci.*, vol. 6, no. 06, p. 316, Jan.
- [138] J. Song, W. Ding, F. Yang, H. Yang, B. Yu, and H. Zhang, "An indoor broadband broadcasting system based on PLC and VLC," *IEEE Trans. Broadcast.*, vol. 61, no. 2, pp. 299–308, Mar. 2015.
- [139] L. Atzori, A. Iera, and G. Morabito, "The internet of things: A survey," *Comp. Net.*, vol. 54, no. 15, pp. 2787–2805, 2010.
- [140] H. Farhangi, "The path of the smart grid," *IEEE Power Energy Mag.*, vol. 8, no. 1, pp. 18–28, 2010.

- [141] S. Jordaan, P. A. J. van Rensburg, A. S. De Beer, H. C. Ferreira, and A. H. Vinck, "A preliminary investigation of the UHF properties of LV cable for WiFi over power line communications," in *Proc. 19th IEEE ISPLC Conf.*, Austin, TX, USA, Apr. 2015, pp. 35–40.
- [142] G. Santucci *et al.*, "From internet of data to internet of things," in *Proc. Int. Conf. Future Trends the Int.*, vol. 28, 2009, pp. 1–19.
- [143] M.-S. Alouini and A. J. Goldsmith, "Capacity of rayleigh fading channels under different adaptive transmission and diversity-combining techniques," *Trans. Veh. Tech.*, vol. 48, no. 4, pp. 1165–1181, 1999.
- [144] W. C. Lee, *Mobile communications design fundamentals*. John Wiley & Sons, 2010, vol. 25.
- [145] J. H. Winters, "Optimum combining in digital mobile radio with cochannel interference," *IEEE Trans. Veh. Tech.*, vol. 33, no. 3, pp. 144–155, 1984.

